The Role of Chemoreceptors in the Axonal Guidance of Olfactory Sensory Neurons

Lulu I Tsai

B.S., University of Rochester, 2007

A dissertation submitted in partial fulfillment of the requirements for the degree of Doctor of Philosophy in the Department of Molecular Biology, Cell Biology, and Biochemistry at Brown University

Providence, Rhode Island

May 2013

I dedicate my dissertation work to Ryan Y. Korsak. Your sense of humor, forbearance, and empathy have been my constant bastion.

ACKNOWLEDGEMENTS

It is my great pleasure to thank to those who made this thesis possible, including my mentor Gilad Barnea; Brown University; the faculty, students, and staff in the Neuroscience and Molecular biology, Cell biology, and Biochemistry departments; my collaborators; my committee members; and my funding sources. I am indebted to past and present lab members who have support me scientifically and emotionally. I owe my deepest gratitude to my friends and family, human and non-human, for contributing to my development during my critical periods.

– Lulu I Tsai

SIGNATURE PAGE

This dissertation by Lulu I Tsai is accepted in its present form by the Department of Molecular Biology, Cell Biology, and Biochemistry as satisfying the dissertation requirement for the degree of Doctor of Philosophy

Date _____ _____
Gilad Barnea, Ph.D., Advisor

Recommended to the Graduate Council

Date _____ _____
Justin Fallon, Ph.D., Reader

Date _____ _____
Kristi Wharton, Ph.D., Reader

Date _____ _____
Mark Zervas, Ph.D., Reader

Date _____ _____
Mark Albers, Ph.D., Reader

Approved by the Graduate Council

Date _____ _____
Peter Weber, Ph.D.
Dean of the Graduate School

CURRICULUM VITAE

LULU TSAI
Department of Molecular Biology, Cell Biology and Biochemistry
Brown University, Providence, RI 02912

I was born 蔡易璐 in Taiwan on April 15, 1985. I lived there with my parents 蔡恒山 and 陳慧芳 and my brother Benny (蔡易樵) until we moved to Tacoma, Washington on August 13, 1990. I attended school in University Place, Washington.

EDUCATION

Ph.D., Molecular Biology, Cell Biology, Biochemistry
Brown University, Providence, RI (anticipated 2013)

M.A., Molecular Biology, Cell Biology, Biochemistry
Brown University, Providence, RI (2010)

B.S. *magna cum laude*, Biochemistry
University of Rochester, Rochester, NY (2007)
Minors: Chemistry and Chinese

SELECTED RESEARCH EXPERIENCE

Graduate student research assistant to Dr. Gilad Barnea
Brown University (2008-2013)
For my dissertation I investigated the role of chemoreceptors in the axonal guidance of olfactory sensory neurons. These neurons each express one odorant receptor, the identity of which directs the neurons' axons to specific structures called glomeruli. Since these neurons naturally regenerate throughout adulthood, I examined how the mechanisms guiding these axons to their targets changed over the lifetime of an animal. I found that during an early critical period, glomeruli become irreversibly marked for input from neurons expressing specific odorant receptors. My results indicate that early development dictates later neuronal circuitry, regardless of neuronal turnover.

Graduate student research assistant to Dr. Mark Zervas
Brown University (2007-08)
Characterized the midbrain dopaminergic neuron progenitors in mice by embryonic fate mapping, immunohistochemical staining, and FACS.

Graduate student research assistant to Dr. Mark Johnson
Brown University (2008)
Screened for specific fertilization mutants in the plant *Arabidopsis thaliana* with techniques common to molecular studies in the plant field.

Graduate student research assistant to Dr. Alexander Brodsky
Brown University (2007)
Optimized an ELISA assay for studying the effects of Vitamin D on breast cancer cells.

PUBLICATIONS

Johnson, M.A.*, Tsai, L.*, Roy, D.S., Valenzuela, D.H., Mosley, C., Magklara, A., Lomvardas, S., Liberles, S.D., and Barnea, G. (2012). Neurons expressing trace amine-associated receptors project to discrete glomeruli and constitute an olfactory subsystem. Proc Natl Acad Sci U S A 109, 13410-13415.

*These authors contributed equally to this work.

Lyons, D.B., Allen, W.E., Goh, T., Tsai, L., Barnea, G., and Lomvardas, S. (2013). An epigenetic trap stabilizes singular olfactory receptor expression. Cell. In review.

Tsai, L. and Barnea, G. (2013). A critical period for imprinting glomerular identity in the olfactory system. In preparation.

PRESENTATIONS AND ABSTRACTS

Tsai, L.I., Barnea, G. "Different roles for homotypic attraction between olfactory neurons in the development and maintenance of the glomerular map." Abstract for poster presentation. Society for Neuroscience, New Orleans, LA (October, 2012).

Tsai, L.I., Barnea, G. "Evidence for homophilic attraction but not heterotypic repulsion in olfactory sensory neurons." Abstract for poster presentation. Society for Neuroscience, San Diego, CA (November, 2010).

HONORS AND AWARDS

Best poster award, graduate program annual retreat
Brown University (2012)

Oliver Cromwell Gorton Arnold Biological Pre-doctoral Fellowship
Brown University (2010-2011)

Best poster award, graduate program annual retreat
Brown University (2010)

NIH Training Grant
Brown University (2008-2010)

Bausch and Lomb Scholarship for Excellence in Science
University of Rochester (2003-2007)

Rush Rhees Scholarship for Academic Achievement
University of Rochester (2003-2007)

Seymour J. & Ruth H. Gray Endowed Scholarship for Outstanding Academic and Personal Achievement
University of Rochester (2003-2007)

MEMBERSHIPS IN PROFESSIONAL SOCIETIES

- International Society for Transgenic Technologies (2012-present)

- Sigma Xi Scientific Research Society (2010-present)
- American Association for the Advancement of Science (2010-present)
- Society for Neuroscience (2009-present)
- National Society of Collegiate Scholars (2004-2007)
- American Association of University Women (2000-present)

TEACHING EXPERIENCE

Teaching consultant, Sheridan Center for Teaching & Learning
Brown University (2012-2013)

Guest lecturer, Analysis of Development lab
Brown University (2010-2012)

Scientific advisor, Advancing Rhode Island Science Education program
Brown University (2008-2010)

Teaching assistant, Analysis of Development course and lab
Brown University (2008)

Language and cultural tutor, Families with Children from China
Rochester, NY (2005-2007)

Teaching assistant, Quest Organic Chemistry lab
University of Rochester (2004)

TABLE OF CONTENTS

LIST OF ILLUSTRATIONS

Chapter 1

Chapter 2

Chapter 3

ABSTRACT

To truly understand the function of a system, one must understand the system's structure and how individual parts interact with one another. The structure of the nervous system arises from the connections between the component neurons. The connections, in turn, arise from the axons of one population of neurons being guided to the dendrites of another population of neurons in a process called axonal guidance. This thesis studies the axonal guidance of olfactory sensory neurons in order to understand the principles that dictate structure and function. Olfactory sensory neurons each express a single odorant receptor gene. These neurons project axons to innervate neuropil structures in the olfactory bulb called glomeruli. All of the neurons expressing a given odorant receptor converge on the same set of glomeruli, the locations of which are spatially conserved between the members of a species. The odorant receptor protein has an established role in the axonal guidance of olfactory sensory neurons but previous studies concerning the mechanisms involved have primarily focused on early development. Since these neurons regenerate throughout adulthood, we studied the axonal guidance of olfactory sensory neurons born after early development. We induced the expression of a transgenic copy of a normally-occurring odorant receptor called MOR28. This caused neighboring neurons expressing only endogenous MOR28 to form supernumerary glomeruli. We then determined that the transgene must be expressed within a critical period, or developmental time window, in order to cause the formation of supernumerary glomeruli. This provides the first evidence for a critical period in the olfactory system. We also determined that after supernumerary glomeruli are formed, they will persist without continuous transgene expression. This provides novel evidence that a transient

perturbation in gene expression can cause permanent changes in neuronal circuitry. We conclude that, even though olfactory sensory neurons constantly regenerate, the development of the early neuronal circuits dictates the conformation of later neuronal circuits. This implies that consistency within the structure of the olfactory system is critical for olfactory function.

Chapter 1

Introduction

If you want to understand function, study structure.

– Francis Crick

The elucidation of the structure of DNA marked a revolution in the understanding of genetics and molecular biology. Understanding the relationships between function and structure currently drives the entire field of structural biology. What Francis Crick said was true in the 1950s and it continues to be true today because in order to understand how something works, one must know how the parts fit and work together. This thesis addresses a question of structure, the question of how neurons connect with one another to generate functional neural networks. Specifically, we will be looking at the mechanisms that guide the axons of olfactory sensory neurons to their appropriate glomerular targets. We will begin by reviewing common mechanisms that mediate axonal guidance throughout the nervous system. Then we will review one of the most well-studied models of axonal guidance, the development of the retinotopic map. Finally we will delve into what is currently known about the axonal guidance in another model, the olfactory sensory neurons. In vertebrates, these neurons are unique in their ability to regenerate throughout adulthood. The the work described in this thesis will address how the axonal guidance of the developing olfactory system differs from the axonal guidance that maintains the same system in adulthood.

Part I: **Axonal guidance – general mechanisms**

I.1. A historical perspective of the understanding of axonal guidance

As early as 1892, Ramón y Cajal proposed long-range chemoattractants as a method by which axons can be guided across long distances to properly innervate their correct targets (Translated by Swanson and Swanson, 1995). However, during the first half of the 20th century, Cajal's proposal was overshadowed by Paul Weiss's proposal that nonspecific mechanical guidance was the driving force behind neuronal connectivity (Weiss, 1945). It took Weiss's student Roger Sperry to re-ignite interest in a deterministic mechanism for guidance with his seminal experiment involving the rotation of frogs' eyes (Sperry, 1963). He clearly demonstrated that axons pass over empty, inappropriate targets to innervate the correct targets, strongly indicating that some sort of cue guides these axons to specific locations (Fig. 1). As a result, he proposed the famous chemoaffinity model that neurons express molecular tags which interact with the short-range attractants near the target for specifying synaptic connections (Sperry 1963).

The human brain contains an estimated 10^{12} neurons which make roughly 10^{15} connections, and since the genome encodes an estimated 3×10^{4} genes, it was apparent even in the 1960s that there were no unique tags for each synapse (Hattori et al., 2008). Sperry later elaborated on a model where a few chemical guidance cues could be expressed in orthogonal gradients that together give "latitude" and "longitude" coordinates for each point in a two dimensional epithelium. Each neuron would display a chemoaffinity for each chemical combination. Reminiscent of the process of chemotaxis whereby whole cells navigate via graded guidance cues, axons may navigate by relative

rather than absolute concentrations. In this way, both cells and axons can easily navigate the entire length of a gradient by adapting their sensitivity to the cues. Whether they are on the edges of the gradient where concentrations are low or near the source of the gradient where all concentrations are high, cells and axons could simply compare the concentrations between the current location and a potential future location. This expands the dynamic range of the cell, allowing a single mechanism to mediate responses to the entire gradient. In support of this idea, cells are capable of differentiating minute differences in relative concentration. Leukocytes can even distinguish a 2% difference in the protein concentrations on the front and back of a single cell (Wang, 2009). Mechanisms based on relative differences rather than absolute concentration would also be much more amenable to evolutionary change or subtle distortions in gradient expression during embryogenesis.

I.2. Heterotypic and homotypic interactions

After Sperry proposed his chemoaffinity model, many molecules were indeed identified to be expressed in gradients. Some are deposited on the surface of other cells, others are secreted as soluble molecules that diffuse from a source. One of the first identified molecule classes was cloned out of an erythropoietin-producing hepatocellular carcinoma cell line and thus called Ephs. These receptor tyrosine kinase proteins classically mediate heterotypic repulsion when a member of the EphA receptor subfamily interacts with an ephrinA ligand or the EphB receptor subfamily interacts with ephrinB ligands. However, exceptions abound. For example, at low levels, these receptor-ligand interactions can switch from heterotypic repulsion to heterotypic attraction (Hansen et al.,

2004). Some Eph receptors from one subfamily are activated by ephrin ligands from the other subfamily (Himanen et al., 2004). Furthermore, ephrin ligands can act as the receptors in a mechanism termed "reverse signaling." This has been proposed to sharpen the Eph and ephrin gradients within a population of cells (Lemke and Reber, 2005).

The bifunctionality of a given molecule is a common theme observed throughout the nervous system. Netrins, a group of laminin-related proteins named after the Sanskrit word for "one who guides," are canonical axonal guidance molecules that can also act as both chemoattractants and chemorepellants. (Huber et al., 2003). Semaphorins, named after the flag semaphore system used for long distance maritime signaling, are a class of secreted and membrane-associated proteins that bind the neuropilin and plexin receptor proteins to mediate both attraction and repulsion as well (Huber et al., 2003).

How do these signals guide axons anywhere if a given signal can result in opposite outcomes? The switch from attraction to repulsion is sometimes temporally and/or spatially segregated. For example, axons that cross the midline are initially attracted toward floorplate cells through the interaction of the Robo receptor and its Slit ligand. After crossing, the interaction switches to mediate repulsion so that the axons can successfully reach and extend past the commissure (Raper and Mason, 2010). Furthermore, not all cases of heterotypic binding necessarily cause both attraction and repulsion. For example, the novel heterotypic pair of immunoglobulin superfamily members Beat and Sidestep are currently only known to cause heterotypic attraction (Siebert et al., 2009).

In contrast to heterotypic interactions, identical molecules on different neurons can mediate a class of mechanisms termed homotypic interactions. In the fly and mouse, proteins like Dscams (Down syndrome cell adhesion molecule) and Protocadherins mediate homotypic repulsion (Hattori et al., 2008). When this occurs between different axons, neurons of the same class are prevented from converging on the same area in the target tissue. When homotypic repulsion occurs between dendrites of the same neuron, the neurites can spread across a wider area and receive inputs from more axons. Additional homotypic repulsion between neighboring dendrites also causes tiling such that dendritic arbors are closely apposed but not overlapping (Fig. 2). However, in an increasingly common example of multifunctional molecules, Dscams in the chick visual system actually promote homotypic attraction rather than homotypic repulsion during the layer-specific targeting in the visual system.

Homotypic attraction may be a general property of axons. When the sensory neurons of insects are transected, they preferentially grow back on themselves rather than on a provided substrate (Wigglesworth, 1953). Similarly, when the optic tracts of amphibians are transected, the regenerating axons preferentially grow along the route of intact axonal fibers (Gaze and Fawcett, 1983; Taylor and Gaze, 1985), indicating that axon-axon interactions promote regrowth.

I.3. Non-canonical cell types and molecules in axonal guidance

The receptor-ligand pairs described above are usually expressed on the surface of neurons. Electron microscope examination of the interaction between axons and the extracellular matrix (ECM) suggested that the ECM also plays an active role in guidance.

Although axons preferentially travel through channels and holes in the ECM, they were not observed to "swim" through the empty spaces but rather climbed along the inner surfaces of the channels (Nordlander and Singer, 1982). No follow-up experiments were performed to characterize the molecules involved in these general interactions, but perineuronal nets of chondroitin sulfate proteoglycans from the ECM are known to inhibit the axonal growth of retinal ganglion cells (Pizzorusso et al., 2002). Glia can also play a role in guiding neurite outgrowth. These cells have been observed to physically enfold young outgrowing axons (Raper and Mason, 2010), and glia are required for dendrite patterning of motor neurons in the spinal cord (Vrieseling and Arber, 2006).

In addition to non-canonical cell types, non-canonical molecules are also involved in axonal guidance. Morphogens are normally associated with specifying cell type. However, classic morphogens, including members of the Hedgehog, Wnt, and TGFβ/BMP gene families, have also been shown to guide axons. For example, Shh is a chemoattractant for commissural axons and can inhibit the growth of retinal ganglion cells. Additionally, BMPs and Wnt5 can act as chemorepellants for commissural axons (Charron and Tessier-Lavigne, 2005). Classic transcription factors like Engrailed and Otx2 can be added as soluble proteins in *in vitro* assays to cause axons to turn (Flanagan, 2006; Nguyen Ba-Charvet et al., 1998). Even neurotransmitters can affect axonal guidance. Serotonin modulates the bifunctionality of Netrin signals to switch from attraction to repulsion (Bonnin et al., 2007). Endocannabinoids cause growth cones to collapse, resulting in repulsion (Berghuis et al., 2007). Finally, Acetylcholine has been identified as an attractant in the Xenopus spinal cord (Zheng et al., 1994).

I.4. Guidepost cells and pioneer neurons

It is relatively simple to explain how gradients of any of these molecules can guide axons for short distances and in generally straight paths. However, some axonal trajectories are long, tortuous, and involve sharp turns. These paths can be explained by the use of guidepost cells, which may not necessarily be neurons themselves (Colón-Ramos et al., 2007; Shen and Bargmann, 2003). They were originally identified in the development of the grasshopper hindlimb (Bate, 1976) where guideposts serve as intermediate targets, allowing axons to employ a connect-the-dots strategy for navigation (Fig. 3). Floorplate cells also act as intermediate targets for commissural axons (Chao et al., 2009). Moreover, LOT1-staining cells that line the lateral olfactory tract act as intermediate targets as well as scaffolds that allow the elongation of mitral cells (Sato et al., 1998).

The connecting of the dots is sometimes initiated by pioneer neurons (Ho and Goodman, 1982). In invertebrates, pioneers are often distinct cell types with more complex growth cone morphologies and slower actin dynamics than the neurons that will follow their paths (Bak and Fraser, 2003). Early in development, these transient cells generate poorly-fasciculated ribbons of axons that increase in size as the follower axons are added. If the trajectory of pioneer axons is altered mechanically or genetically, the targets of the follower axons will also be altered, even if they are unmodified (Raper and Mason, 2010). This has been considered a hallmark of the effect of pioneer axons. However, pioneer cells are not always necessary for the proper guidance of all of their followers (Whitlock and Westerfield, 1998). They may act as a redundant mechanism to

protect the system against errors in axonal guidance, facilitate the ability of the follower neurons to respond to guidance cues themselves, or merely increase the efficiency of later axonal guidance. Indeed, follower neurons tend to pass guidepost cells more quickly than pioneer neurons (Bak and Fraser, 2003).

I.5. Refining axonal projections

The final configuration of axons seen in the adult is often achieved through sequential mechanisms. In the first stage, the pioneers blaze the path. In the second stage, the followers extend along this path. In the final stage, any mistakes are corrected and the map is refined. Once a follower neuron has arrived in the vicinity of the final target, the growth cone must choose between highly similar synaptic partners, sometimes even between the cellular subcompartments of a single post-synaptic neuron (Chédotal and Richards, 2010). At this point, the post-synaptic cells can influence this choice. For example, the projection neurons in the fly express specific variants of the protein teneurin such that it will form a synapse with only the odorant receptor neuron expressing the same variant (Hong et al., 2012). Besides pruning the "incorrect" axons, the "correct" axons can also be reinforced by trophic factors released from the post-synaptic neuron. These factors have been shown to promote cell survival, synaptogenesis, and additional neurite outgrowth and arborization (Zweifel et al., 2005). However, trophic factors are not necessarily required for the survival of all pre-synaptic neurons. For example, in some nicotinic synapses in the autonomic nervous system, synapses are maintained in the absence of activity; a post-synaptic response is only required to develop the ability to sustain high-frequency transmission (Krishnaswamy and Cooper, 2009)

Refinement of the axonal projections can also occur through activity-dependent mechanisms. Waves of spontaneous electrical activity propagate across the retina before the eye opens such that the firing of neighboring neurons is temporally related. Inhibiting these waves genetically or chemically disrupts the formation of eye-specific layers in the lateral geniculate nucleus (Penn et al., 1998). Electrical activity continues to shape the visual circuits shortly after the eyes open. In Wiesel and Hubel's famous experiment, kittens whose eyes had been sutured only during early development never gained normal vision. The axons originating from the second eye expanded to innervate the areas normally targeted by the first eye, but only if the second eye was left open (Wiesel and Hubel, 1963). These results indicated that there was a critical period during which experience-dependent neuronal activity is required to develop connectivity and function. If both eyes were sutured, the critical period could be extended, indicating that refinement truly depends on experience-dependent neural activity.

Critical period was originally defined as a developmental time window during which experience-dependent neural activity affected the formation of specific neuronal connections. More recently the definition of critical period has been extended to include the effect of experience on general behaviors that involve many neuronal circuits with different mechanisms of guidance and development. Examples of systemic critical periods include the imprinting of parental figures in newly-hatched birds (Lorenz, 1958) or the acquisition of a second language in humans (Hensch, 2004). This expansion of the meaning of critical period further emphasizes the connection between structure and function in the nervous system.

Part II: **Axonal guidance – the visual system as a paradigm**

II.1. The major mechanisms governing the retinotopic map

One of the most well-studied models of axonal guidance is the projection of retinal ganglion cells (RGCs) to the visual cortex. Although this area is called the superior colliculus (SC) in vertebrates, it is called the optic tectum in invertebrates and so this system is often referred to as the retinotectal map. It is also known as the retinotopic map since the connections here are topographic, i.e. the spatial relationships of the input neurons are reflected in the spatial relationships of the synapses. Topographic organization is conserved in most of the sensory systems and so the axonal guidance of RGCs has been a paradigm that has informed the studies of axonal guidance in many other populations of neurons.

The Eph receptors and their ephrin ligands described above appear to be the dominant guidance cues in the axonal guidance of RGCs. When multiple Ephs and ephrins are genetically knocked out, few RGC axons exhibit any topographical organization. The rare neurons that still target the visual cortex suggest that there are some redundant mechanisms, but the most efficient map formation appears to be mediated by Ephs and ephrins (Feldheim and O'Leary, 2010). Many guidance molecules that have been identified to affect the projection pattern of RGCs merely act as effectors for ephrinA, which localizes to the membrane via a glycophosphatidylinositol (GPI) linkage and cannot signal to the cytoplasm on its own.

In vertebrates, the projections of RGC axons occur in distinct sequential stages (Fig. 4). Initially, all axons extend through the visual cortex and terminate in the caudal

SC. In the RGCs, the EphA receptors are generally expressed in a low to high gradient along the nasotemporal axis. In the SC, the ephrinAs are generally expressed in a high to low gradient along the anteroposterior axis. The interaction of EphAs and ephrinAs result in chemorepulsion, which interacts with gradients of other molecules promoting axonal branch formation such that collateral branches are sent out from a specific position on each RGC. The main branch is then pruned back through a process akin to Wallerian degeneration and mature synapses are formed (McLaughlin and O'Leary, 2005; Nakamura and O'Leary, 1989).

An independent set of mechanisms seems to determine axonal guidance on the orthogonal mediolateral axis. Instead of identical initial projections with topographic order arising later, the dorsoventral organization of the RGCs is continuously preserved and can be seen along the length of the axons in the optic tract. Final refinement of the axonal projections is generally mediated by ephB gradients that run low to high on the dorsoventral axis in the RGCs and ephrinB gradients that run high to low on the mediolateral axis in the SC (Lemke and Reber, 2005).

II.2.Generating the final retinotopic projection pattern

Refinement of the retinotopic map also depends on competition and axon-axon interactions. Ablating the nasal half of the retina allows projections from the temporal half to expand across the visual cortex (Fig. 5). The topographic order of the remaining axons is preserved; the map merely increases in size (Schmidt and Easter, 1978). This suggests that the nasal and temporal axons normally compete for a limited number of targets. Furthermore, axon-axon interactions seem to increase the levels and slopes of

EphA/ephrinA gradients, allowing for greater distinction between signals and a more robust retinotopic map (Yates et al., 2004).

However, there appears to be a hierarchy between the axonal competition mechanism and other mechanisms such as the readout of molecular gradients. Mice were generated where a subpopulation of RGCs expressed more EphA than wildtype RGCs. The presence of these mutant RGCs shifted the wildtype RGCs caudally, even though the chemorepulsion between the wildtype RGCs and the ephrinA gradients in the SC was not affected (Brown et al., 2000). These results suggest that the guidance cues from axon-axon interactions override the cues from cell-autonomous Eph/ephrin signaling and that final projection patterns are determined by the interplay of multiple guidance mechanisms.

Part III: **Axonal guidance – the olfactory system**

III.1. The olfactory system

In contrast with the visual system, olfactory sensory neurons (OSNs) do not maintain strict topographical organization within their axonal projections. Yet the molecular and anatomical organization of the olfactory system makes these neurons also well-suited for studying axonal guidance, so perhaps OSNs would serve well as a paradigm for non-topographical axonal guidance. Furthermore, OSNs are one of the few neuronal populations that constantly regenerate throughout life so it would also serve well as a system for studying axonal guidance in the adult.

The olfactory system in rodents consists of multiple subsystems (Fig. 6) (Breer et al., 2006; Fleischer et al., 2009). Within each subsystem, sensory neurons expressing olfactory chemoreceptors extend axons into neuropil structures called glomeruli. Within the glomeruli, the sensory neurons synapse on projection neurons that in turn extend axons into the olfactory cortex. Progressing from the anterior to the posterior, the first subsystem is the Grüneberg ganglion (GG) located near the tip of the nose. OSNs here express various chemosensors and possibly even thermosensors. Their axonal projections target the interconnected necklace glomeruli within the dorsocaudal olfactory bulb (OB). The second subsystem is the vomeronasal organ (VNO) located just above the palate. The sensory neurons here are called vomeronasal sensory neurons and express members of the vomeronasal receptor (V1R and V2R), formyl peptide receptor (FPR), and odorant receptor (OR) families of G protein-coupled receptors (GPCRs). Their axonal projections target the accessory olfactory bulb (AOB) located at the dorsocaudal extreme of the OB, behind the necklace glomeruli. The third subsystem is the septal organ (SO) located just above the opening of the nasopalatine duct that connects the mouth with the nasal cavity. OSNs here express a subset of ORs which are also expressed in the main olfactory epithelium (MOE). Their axonal projections target glomeruli in both the dorsal and ventral OB. The last few subsystems are located in the MOE, which lies just anterior to the cribriform plate that separates it from the OB. Most of the OSNs here express ORs and project to glomeruli throughout the OB. A subset of the OSNs in the MOE expresses guanylyl cyclase D (GC-D) and project to the necklace glomeruli along with the GG neurons. A last subset of OSNs in the MOE expresses trace amine-associated receptors (TAARs). This last subsystem was only recently identified (Liberles and Buck, 2006) and

very little is known about them, including where the TAAR-expressing OSNs project their axons.

III.2.The wiring of the OR-expressing OSNs

Classically, olfaction has been associated with the OR-expressing OSNs in the MOE. The OR proteins are the largest subset of GPCRs and comprise 1.4-4% of the average mammalian genome (Mombaerts, 2004). They were first identified by Richard Axel and Linda Buck when she used degenerate primers to amplify many GPCRs from the MOE. By cutting with a distinct set of restriction enzymes, she was able to show that the fragments add up to more than the length of a single GPCR so she must have amplified numerous closely-related GPCRs (Buck and Axel, 1991).

In mice, there are ~900 functional OR genes and ~300 pseudogenes that do not encode for a full-length OR protein (Young et al., 2003). The coding sequences can be divided into the class I type that most resembles the ORs expressed by fish, and the class II type that seems to have evolved when amphibians first moved to land. Many of the mammalian ORs became pseudogenes when primates began to rely heavily on visual rather than olfactory stimuli (Mori and Sakano, 2011). As a family of genes, ORs vary in about 37% of their amino acid sequences though some differ by as much as 72% (Mombaerts, 2006).

The ORs are expressed from only one allele per OSN in a phenomenon called monoallelic exclusion, or the “one receptor per neuron” rule (Chess A, 1994; Lewcock and Reed, 2004; Malnic et al., 1999; Serizawa et al., 2003; Shykind et al., 2004; Shykind, 2005). This mode of expression is also seen for other olfactory subsystems and proposed

to apply to the TAARs based on expression frequency and distribution (Liberles and Buck, 2006). Mechanistically, monoallelic exclusion is thought to occur through the epigenetic silencing of all but one OR locus (Magklara et al., 2011). The population of OSNs expressing a given OR is located in stereotypical zones that are generally organized in stripes along the dorsomedial-ventrolateral axis of the MOE (Astic et al., 1987; Miyamichi et al., 2005; Ressler et al., 1994; Vassar et al., 1994). Roughly 0.1% of the total OSNs in the MOE express any given OR (Young et al., 2003).

A single unbranched axon extends from each OSN, passes through openings in the cribriform plate, streams along the surface of the OB, and finally converges on a single glomerulus within the glomerular layer of the OB (Klenoff and Greer, 1998). There are roughly 1600-1800 total glomeruli, with size varying slightly on the dorsoventral axis (Royet et al., 1988; Taniguchi et al., 2003). In the adult OB, all of the OSNs that express a given OR usually form two glomeruli per OB (Mombaerts et al., 1996; Ressler et al., 1994; Strotmann et al., 2000; Vassar et al., 1994). Since each glomerulus will only receive input from OSNs expressing one specific OR (Treloar et al., 2002), this is called the "one receptor per glomerulus" rule. The positions of the glomeruli dedicated to a given OR are generally conserved between the members of a given species (Potter et al., 2001; Ressler et al., 1994; Vassar et al., 1994). There are some local permutations in exact locations (Schaefer et al., 2001; Strotmann et al., 2000). However, between individuals the position of a given glomerulus seems to vary by only one glomerular diameter (Soucy et al., 2009). Since the identity of ORs is thus "mapped" onto the OB, the distribution of glomeruli is sometimes called the glomerular map (Fig. 7). The ORs that bind ligands with similar structural and chemical properties form

glomeruli that are coarsely clustered (Johnson and Leon, 2007; Johnson et al., 2009; Mori et al., 2006; Takahashi et al., 2004) but odorant responses in neighboring glomeruli are nearly as variable as that in distant glomeruli, so glomerular organization is not generally chemotopic (Soucy et al., 2009).

Within the glomerulus, OSNs interact with at least three other cell types. The periglomerular cells are a class of interneurons. The mitral cells are the projection neurons that pass information to the olfactory cortex. Interestingly, when glomeruli were genetically ablated in the dorsal OB, the dorsal mitral cells still sent dendrites into the dorsal glomerular layer and did not synapse with ventral glomeruli (Kobayakawa et al., 2007). This suggests that the wiring of mitral cells is determined genetically rather than established through competition or activity-dependent mechanisms. OSNs also interact with tufted cells which serve to link the two glomeruli that are dedicated to a given OR (Belluscio et al., 2002; Liu and Shipley, 1994; Lodovichi et al., 2003; Mori et al., 1999; Shepherd et al., 2004). One of these glomeruli is located in the medial half of the OB and the other in the lateral half, creating two mirror-symmetrical maps within each OB (Fig. 8). The functional relevance of having two maps is unclear. Perhaps each mediates separate aspects of the olfactory percept. One map could process the immediate, rapidly-habituated perception of an odor while the other processes the long-term, slowly-adapting perception (Zhou and Belluscio, 2008). Alternatively, one map could process orthonasal odorants that enter the nasal cavity from the front of the nose while the other processes the retronasal odorants that travel up from the mouth (Mori and Sakano, 2011). Whatever the functional relevance, it is clear that the activation of an OR is read out at the glomerulus by multiple cell types.

III.3.OR-independent mechanisms of axonal guidance in OSNs

Similar to the retinotopic map, the glomerular map is assembled in a step-wise manner. The mechanisms that are involved are sometimes independent, sometimes interdependent, and sometimes influence each other in a hierarchical manner (Key and St John, 2002). The process may begin with guidepost cells and pioneer neurons. At embryonic day E10, a molecularly distinct group of neurons called the migratory mass streams out toward the developing OB along the future trajectory of OSNs. Since this occurs before OSN axons even begin to fasciculate, they may act as guidepost cells or scaffolds for the OSNs (Miller et al., 2010). From E10-E12, mesenchymal cells lining the openings in the cribriform plate begin to express MOR256-17. A large population of OSNs also expressing this OR pushes through this mass and encircles much of the OB. Their presence peaks at E18 and then falls away as the OSNs expressing the rest of the repertoire of ORs targets the OB. MOR256-17 may be a unique OR with the ability to mediate non-specific homotypic attraction with all OSNs, allowing them to be universal pioneer neurons (Conzelmann et al., 2002; Schwarzenbacher et al., 2006; Schwarzenbacher et al., 2004).

Canonical guidance cues may also be expressed by the pioneer neurons. In zebrafish, a morphologically distinct population of pioneer neurons also precedes the OSNs. In zebrafish Robo2 mutants, these pioneers fail to innervate the OB and aggregate at the posterior end of the olfactory epithelium (Whitlock and Westerfield, 1998). In mouse Robo1/Robo2 double mutants, the OSNs also terminate before reaching the OB (Nguyen-Ba-Charvet et al., 2008), perhaps through a similar mechanism. Additionally,

other molecules may act as axonal guidance cues for the OSNs. For example, glycans deposited in the ECM are critical for OSN survival and compartmentalization into restricted channels. Furthermore, glycans may potentiate the response of OSNs to other molecules such as Slits (Cho et al., 2009).

As the OSNs begin to follow guideposts and pioneers, they may not initially require any axonal guidance cues from the OR proteins. The OSNs expressing class I and class II types of ORs normally segregate from one another within the fascicles that cross the cribriform plate. Even if OSNs are forced to express ORs from the wrong class, this segregation is not affected and the axons will proceed to innervate the same area of OB that they normally innervate (Bozza et al., 2009). Instead of OR identity, the OSN type is most likely determined by the stereotypical set of guidance cues expressed by the OSN (see below). The expression of these other molecules has been shown to be conserved when OSNs are forced to express the other class of OR (Miyamichi et al., 2005; Nakatani et al., 2003).

The OSN type seems to be determined by the position of the OSN within the MOE. In a manner analogous to the retinotopic map, the location of the OSN on the dorsomedial-ventrolateral axis in the MOE is correlated with the location of the targeted glomerulus on the dorsolateral axis in the OB. This is not considered true topographical organization since at each point on the dorsomedial-ventrolateral axis in the MOE, the OSNs expressing a given OR are randomly scattered and intermingled with OSNs expressing other ORs. However, if an OR is expressed in an abnormal zone in the MOE, the affected axons will form new glomeruli at a point on the dorsolateral axis of the OB

that is consistent with the new zone (Miyamichi et al., 2005; Vassalli et al., 2002). Also similar to the visual system, this rough topographical organization seems to be mediated by the graded expression of guidance molecules. O-MACS (a member of the medium-chain acyl-CoA synthetase family), NQO-1 [NAD(P)H dehydrogenase (quinone 1)], and OCAM (olfactory cell adhesion molecule) are all expressed in gradients along the dorsomedial-ventrolateral axis in the MOE (Gussing and Bohm, 2004; Oka et al., 2003; Yoshihara et al., 1997). These may interact with the graded expression of Msx1 (a homeobox gene), RALDH2 (a retinoic acid-synthesizing enzyme), and Alk6 (a BMP-type I receptor) in the glial support cells of the MOE (Norlin et al., 2001).

Robo2, Slit1, Sema3F (a semaphorin), and Nrp2 (a neuropilin) are also expressed in gradients and the mechanism for how these molecules affect dorsoventral patterning in the OB has been elucidated (Fig. 9). Robo2 expression is highest in the dorsomedial MOE where the OSNs mature earlier. During this time, the OB expresses a low to high gradient of Slit1 on the dorsoventral axis. Since Robo2 and Slit1 interaction results in chemorepulsion, the first OSNs to reach the OB are confined to the dorsal areas. The dorsomedial OSNs also express Sema3F, so their axons create a high to low gradient of this ligand in the OB. Nrp2 expression is expressed in a low to high gradient on the dorsomedial-ventrolateral axis in the MOE. Since Sema3F and Nrp2 interaction also results in chemorepulsion, the OSNs that arrive in the OB last are confined to the ventral areas (Takeuchi et al., 2010).

Projection along the mediolateral axis in the OB may also be determined by graded expression (Levai et al., 2003). Sema3A expression is graded in the OB and when

OSN axons lack its receptor Npn1, the lateral and medial glomeruli are both found at a new intermediate location in the OB (Schwarting et al., 2004). Expression of IGF1 and IGF2 (insulin growth factors) is also graded in the OB. The IGF receptor is expressed by all OSNs and disrupting either the ligand or the receptor affects projections on the mediolateral axis (Scolnick et al., 2008).

After reaching the OB, the convergence of OSNs into glomeruli does not seem to depend on any signals from the target tissue itself. When mice lack any OB tissue, either through bulbectomy or mutation of the Gli3 transcription factor, OSNs still form neuropil structures in whatever tissue lies posterior to the cribriform plate. The locations of the neuropils formed by OSNs expressing specific ORs are even conserved on the anteroposterior axis. Any guidance cues from the OB probably serve merely as directional cues and the relative position of glomeruli is determined solely by axon-axon interactions (Feinstein and Mombaerts, 2004; Imai et al., 2009; St John et al., 2003). Consistent with this idea, no structural elements are discernible within the glomerular layer before the OSNs axons arrive (Bailey et al., 1999; LaMantia and Purves, 1989; Treloar et al., 1999).

The number of OSNs expressing the same OR also affects the glomerular map in a mechanism termed interdependence. When only a few OSNs expressed a specific transgenic OR, the glomeruli formed by these axons were located in novel areas of the OB. These structures were transient and later eliminated. However, in founder lines where the transgenic OR was expressed in an increased population of OSNs, the ectopic glomeruli were increasingly likely to persist in the adult (Ebrahimi and Chess, 2000).

III.4. OR-dependent mechanisms of axonal guidance in OSNs

The "one receptor per glomerulus" rule strongly suggests that the ORs play a role in generating the glomerular map. Evidence that ORs are critical for axonal guidance comes from the observations that the OR proteins are axonally translated and localized to the axon tip (Fig. 10) (Barnea et al., 2004; Dubacq et al., 2009; Feinstein and Mombaerts, 2004; Strotmann et al., 2004). Additionally, OR proteins on the axonal growth cone can mediate localized cAMP (cyclic adenosine monophosphate) and calcium responses (Maritan et al., 2009). Furthermore, the location of a glomerulus can be altered by changing only the coding region of the OR being expressed in the OSNs (Cutforth et al., 2003; Wang et al., 1998). When the coding region of the odorant receptor P2 was replaced with the coding region for the odorant receptor M50, the OSNs targeted neither the P2 nor the M50 glomerulus. Instead, the new glomerulus was somewhere in between the two, suggesting that the OR is necessary but not sufficient for determining glomerular location (Fig. 11). However, the ability to mediate axonal convergence may not be specific to solely ORs. When the coding region for the odorant receptor M71 was replaced by the coding region for the β2 adrenergic receptor, these OSNs also localized this new protein to the growth cone and converged into a β2 adrenergic receptor glomerulus. While the β2 adrenergic receptor is also a GPCR, it has not been shown to be a chemosensor. In contrast, the vomeronasal receptor V1rb2 is also a GPCR but M71 OSNs that were instead forced to express V1rb2 rarely formed glomeruli (Feinstein et al., 2004). It appears that some but not all types of GPCRs can mediate the glomerular convergence of OSNs.

Some ORs are highly similar in amino acid sequence, probably due to their shared evolutionary past. For example, M71 and M72 differ by only 11 out of a total of 309 amino acids, or 4% of the protein. When a single aspartic acid residue in M71 was changed to the asparagine that was encoded in the same position in M72, the OSNs targeted a new glomerulus. Similar to the P2 to M50 swap described above, the OSNs did not target either the M71 or M72 glomeruli but formed a third novel glomerulus (Feinstein and Mombaerts, 2004). This sensitivity suggests that the mechanisms that read out OR identity must be able to distinguish very subtle changes in amino acid sequence.

One of the ways that ORs could mediate axonal guidance is by receptor activity, either in response to exogenous ligands, endogenous ligands, or its intrinsic ligand-independent activity. Some level of electrical activity seems to be required for axonal guidance because overexpression of the Kir2.1 inward-rectifying potassium channel in OSNs disrupts glomerular map formation (Yu et al., 2004). OR activity could be read out as levels of the second messenger cAMP. When the cAMP pathway was modulated by mutating the DRY (aspartic acid-arginine-tyrosine) motif on ORs or by mutating effector proteins downstream of cAMP, the affected OSNs formed glomeruli that were shifted on the anteroposterior axis (Fig. 12) (Imai et al., 2006). This is likely due to the cAMP-mediated effects on the semaphorin signaling pathway since the expression level of Npn1, Sema3A, and PlexinA1 were all affected in these experiments. These proteins are classified as type I guidance molecules and they are expressed on the axon tips of immature OSNs (Mori and Sakano, 2011). Their function may depend on intrinsic OR activity since they are not affected when exogenous ligands are blocked with naris occlusion (Imai et al., 2006; Imai et al., 2009). Mechanisms that are not dependent on

exogenous ligands are critical for OSN axon guidance because axons must be in position at the time of birth to allow newborn pups to immediately find their mothers and begin nursing (Potter et al., 2001).

Neuronal activity read out by the cAMP pathway also affects the expression of Kirrel2 and Kirrel3 (Kin of IRRE-like proteins) which have been identified to mediate homotypic attraction. These are considered type II guidance molecules and they are expressed on the axons of mature neurons (Mori and Sakano, 2011). In contrast with the type I molecules, Kirrel levels are affected by naris occlusion. This procedure also affects the pruning of transient features in the glomerular map. Early in development, some populations of OSNs express more than one OR, some OSNs expressing the same OR form more than two glomeruli, and most glomeruli are larger with less defined boundaries (Potter et al., 2001; Tian and Ma, 2008; Zou et al., 2004). These ectopic OSNs and axons persist if the mouse is naris occluded, suggesting that ligand-dependent activity plays a role in refining the glomerular map. Some ectopic glomeruli formed by the expression of transgenic ORs can also be eliminated in a similar activity-dependent manner (Nakatani et al., 2003). Furthermore, the odorant-dependent activity resulting from behavioral conditioning can accelerate the refinement of the olfactory map (Kerr and Belluscio, 2006).

In addition to cAMP, ORs also signal through the CNG (Cyclic Nucleotide-Gated) channel. Activity of this protein also affects the expression of Kirrel2 and Kirrel3 as well as EphA5 and ephrinA5. Because a critical CNG channel subunit is expressed on the X chromosome, female heterozygote mutants that undergo random X inactivation

express functional CNG channels in a mosaic population of their OSNs. The OSNs expressing a given OR were thus subdivided into one half with wildtype CNG channel activity and one half with none. Some of these OSN subpopulations segregated into two separate but neighboring glomeruli, indicating a role for CNG channel activity in glomerular convergence (Serizawa et al., 2006). Importantly, the subpopulation of OSNs without any CNG channel activity declined with age. This effect was abrogated with naris occlusion, suggesting that the loss was through activity-dependent competition from the wildtype subpopulation (Zhao and Reed, 2001). These results indicate that ligand-dependent activity results in competition that is required for the refinement of the glomerular map.

Another way that ORs could mediate axonal guidance is by homotypic attraction. When either M71 or the odorant receptor MOR23 were expressed under the control of a truncated promoter, the ORs were expressed in ectopic zones of the MOE and the OSNs formed ectopic glomeruli in novel areas of the OB. Interestingly, the OSNs that were expressing M71 or MOR23 from the wildtype, unaffected loci also began innervating these ectopic glomeruli. Since the wildtype OSNs did not express the mutant alleles, their axons seemed to be rerouted from their normal glomeruli in a cell non-autonomous fashion (Vassalli et al., 2002). Rerouting was only observed for the OSNs expressing the cognate endogenous receptor so Vassalli et al. proposed that rerouting is due to the homotypic attraction between axons expressing the same OR.

Homotypic attraction could occur via the direct interaction of OR proteins between different axons. Since the most variable residues on the OR are located in the

transmembrane domains or oriented toward the cytoplasmic side of the receptor, the extracellular surfaces may not be structurally distinct enough on their own to distinguish one OR from another. However, there are multiple candidates for adapter proteins that could interact specifically with the variable transmembrane and cytoplasmic domains of the OR and subsequently serve as the direct protein-protein binding sites. BIG-2 (a glycoprotein in the immunoglobulin superfamily) is expressed on axon tips and is involved in glomerular convergence (Kaneko-Goto et al., 2008). Members of the RTP (Receptor-Transporting Protein) and REEP (Receptor Expression Enhancing Protein) families are adapter proteins known to associate with ORs in heterologous cell culture systems (Mainland and Matsunami, 2012; Saito et al., 2004). ORs could also associate with known scaffolding proteins like OCAM. In fact, OCAM has an extensive ectodomain that lies parallel to the cell membrane, providing multiple contact sites for proteins docking, and its three dimensional shape is structurally compatible with a trans-interaction between axons (Kulahin et al., 2011). Finally, homotypic attraction could occur through an indirect method where the activity of ORs results in the differential expression of other guidance molecules that then mediate homotypic attraction. In this way ORs would act as a master regulator that merely imparts an identity to the axon. However, homotypic attraction may not be strictly required for guidance. Rare axons have been observed to take idiosyncratic trajectories, arriving at glomeruli independently of major axonal tracts (Treloar et al., 2002). Homotypic attraction may serve to increase the efficacy of other mechanisms by aggregating one population of OSNs, or they may provide a level of redundancy to ensure proper targeting.

III.5. Maintenance of the glomerular map

Like many neuronal populations in the peripheral nervous system, OSNs have an intrinsic ability to repair and regenerate. The lifespan of the average OSN is estimated to be 30-120 days (Barber, 1982; Hinds et al., 1984; Mackay-Sim and Kittel, 1991). Death and replacement are asynchronous so newly-generated OSNs usually comprise a small subpopulation of the neurons within a glomerulus. If OSNs are synchronously ablated throughout the MOE, neurogenesis increases such that olfactory function is restored within two months (Suzukawa et al., 2011). In both normal and injury-induced regeneration, the later-born OSNs expressing a given OR will continue to innervate the same glomerulus as previous early-born OSNs expressing the same OR. In this way the position of the glomerulus dedicated to a specific OR will be conserved throughout the lifetime of an animal, allowing the glomerular map to be temporally stable.

Unlike the retinotopic map, there does not seem to be a critical period for the activity-dependent mechanisms that govern the axonal guidance of OSNs. Naris occlusion can be performed at any point in the mouse's lifetime to allow the survival of OSNs with reduced CNG channel activity. The differences between the visual and olfactory systems are probably due to the fact that OSNs constantly regenerate. Some mechanisms of axonal guidance must operate in adulthood to guide the newborn OSNs to the proper glomeruli. In fact, no critical period of any kind has been identified in the olfactory system, either at the molecular or functional level (Hensch, 2004). Nevertheless, there are many differences between the developing and established glomerular maps. Later in life there are no migratory mass cells, a smaller fraction of the

total population of OSNs are actively extending axons, and glomeruli fill the entirety of the glomerular layer. It would be interesting to determine if these differences result in any changes in the mechanisms governing axonal guidance in early-born versus later-born OSNs.

RESEARCH AIMS

This thesis aims to examine the role of olfactory chemoreceptors in the axonal guidance of OSNs. ORs have an established role in mediating the convergence of OSNs into glomeruli. However, most of this work has been in the context of establishing the initial glomerular map and few studies specifically address the mechanisms of axonal guidance that maintain the map in the face of constant regeneration throughout the lifetime of the animal. In the second chapter of this thesis I describe my work in characterizing a genetic approach to manipulate OR expression and axonal guidance in adult mice. I elucidated the effects of transgenic OR expression on the OSNs that express endogenous ORs. I also described how the transgenic axons formed ectopic glomeruli throughout the OB. Most importantly, I described how endogenous ORs were recruited to rerouted glomeruli in the presence of transgenic OR expression. In the third chapter of this thesis I temporally manipulated transgenic OR expression to provide evidence that a critical period does exist for the formation of rerouted glomeruli. Furthermore, the maintenance of rerouted glomeruli is not dependent on the continuous expression of transgenic OR. These observations suggest that the olfactory system maintains the conformation of the glomerular map that is established during early development. In the fourth chapter of this thesis I compared the glomerular maps of OR- and TAAR-expressing OSNs. We identified some similarities, such as the preservation of the "one receptor per glomerulus" rule and the convergence of both types of OSNs on a small number of discrete glomeruli. However, we also identified some differences, such as the variation in the number and locations of the TAAR glomeruli. Collectively, my thesis results advance our understanding of the development of non-topographical maps by

addressing the role of chemoreceptors in the axonal guidance of OSNs. The specific aims of this thesis were the following:

I. Characterize an approach to assay the axonal guidance of regenerating OSNs.

II. Compare and contrast the axonal guidance of developing versus regenerating OSNs.

III. Compare and contrast the axonal guidance of OR-expressing and TAAR-expressing OSNs.

REFERENCES

Astic, L., Saucier, D., and Holley, A. (1987). Topographical relationships between olfactory receptor cells and glomerular foci in the rat olfactory bulb. Brain Res *424*, 144-152.

Bailey, M.S., Puche, A.C., and Shipley, M.T. (1999). Development of the olfactory bulb: evidence for glia-neuron interactions in glomerular formation. J Comp Neurol *415*, 423-448.

Bak, M., and Fraser, S. (2003). Axon fasciculation and differences in midline kinetics between pioneer and follower axons within commissural fascicles. Development *130*, 4999-5008.

Barber, P. (1982). Neurogenesis and regeneration in the primary olfactory pathway of mammals. Bibliotheca anatomica *23*, 12-25.

Barnea, G., O'Donnell, S., Mancia, F., Sun, X., Nemes, A., Mendelsohn, M., and Axel, R. (2004). Odorant receptors on axon termini in the brain. Science *304*, 1468.

Bate, C. (1976). Pioneer neurones in an insect embryo. Nature *260*, 54-56.

Belluscio, L., Lodovichi, C., Feinstein, P., Mombaerts, P., and Katz, L. (2002). Odorant receptors instruct functional circuitry in the mouse olfactory bulb. Nature *419*, 296-300.

Berghuis, P., Rajnicek, A., Morozov, Y., Ross, R., Mulder, J., Urbán, G., Monory, K., Marsicano, G., Matteoli, M., Canty, A., *et al.* (2007). Hardwiring the brain: endocannabinoids shape neuronal connectivity. Science *316*, 1212-1216.

Bonnin, A., Torii, M., Wang, L., Rakic, P., and Levitt, P. (2007). Serotonin modulates the response of embryonic thalamocortical axons to netrin-1. Nat Neurosci *10*, 588-597.

Bozza, T., Vassalli, A., Fuss, S., Zhang, J., Weiland, B., Pacifico, R., Feinstein, P., and Mombaerts, P. (2009). Mapping of class I and class II odorant receptors to glomerular domains by two distinct types of olfactory sensory neurons in the mouse. Neuron *61*, 220-233.

Breer, H., Fleischer, J., and Strotmann, J. (2006). The sense of smell: multiple olfactory subsystems. Cell Mol Life Sci *63*, 1465-1475.

Brown, A., Yates, P., Burrola, P., Ortuño, D., Vaidya, A., Jessell, T., Pfaff, S., O'Leary, D., and Lemke, G. (2000). Topographic mapping from the retina to the midbrain is controlled by relative but not absolute levels of EphA receptor signaling. Cell *102*, 77-88.

Buck, L., and Axel, R. (1991). A novel multigene family may encode odorant receptors: a molecular basis for odor recognition. Cell *65*, 175-187.

Chao, D., Ma, L., and Shen, K. (2009). Transient cell-cell interactions in neural circuit formation. Nat Rev Neurosci *10*, 262-271.

Charron, F., and Tessier-Lavigne, M. (2005). Novel brain wiring functions for classical morphogens: a role as graded positional cues in axon guidance. Development *132*, 225-262.

Chédotal, A., and Richards, L. (2010). Wiring the brain: the biology of neuronal guidance. Cold Spring Harb Perspect Biol *2*.

Chess A, S.I., Cedar H, Axel R. (1994). Allelic inactivation regulates olfactory receptor gene expression. Cell *78*, 823-834.

Cho, J., Prince, J., and Cloutier, J. (2009). Axon guidance events in the wiring of the mammalian olfactory system. Mol Neurobiol *39*, 1-9.

Colón-Ramos, D., Margeta, M., and Shen, K. (2007). Glia promote local synaptogenesis through UNC-6 (netrin) signaling in C. elegans. Science *318*, 103-106.

Conzelmann, S., Levai, O., Breer, H., and Strotmann, J. (2002). Extraepithelial cells expressing distinct olfactory receptors are associated with axons of sensory cells with the same receptor type. Cell Tissue Res *307*, 293-301.

Cutforth, T., Moring, L., Mendelsohn, M., Nemes, A., Shah, N., Kim, M., Frisen, S., and Axel, R. (2003). Axonal ephrin-As and odorant receptors: coordinate determination of the olfactory sensory map. Cell *114*, 311-322.

Dubacq, C., Jamet, S., and Trembleau, A. (2009). Evidence for developmentally regulated local translation of odorant receptor mRNAs in the axons of olfactory sensory neurons. J Neurosci *29*, 10184-10190.

Ebrahimi, F., and Chess, A. (2000). Olfactory neurons are interdependent in maintaining axonal projections. Curr Biol *10*, 219-222.

Feinstein, P., Bozza, T., Rodriguez, I., Vassalli, A., and Mombaerts, P. (2004). Axon guidance of mouse olfactory sensory neurons by odorant receptors and the beta2 adrenergic receptor. Cell *117*, 833-846.

Feinstein, P., and Mombaerts, P. (2004). A contextual model for axonal sorting into glomeruli in the mouse olfactory system. Cell *117,* 817-831.

Feldheim, D., and O'Leary, D. (2010). Visual map development: bidirectional signaling, bifunctional guidance molecules, and competition. Cold Spring Harb Perspect Biol *2*.

Flanagan, J. (2006). Neural map specification by gradients. Curr Opin Cell Biol *16,* 59-66.

Fleischer, J., Breer, H., and Strotmann, J. (2009). Mammalian olfactory receptors. Front Cell Neurosci *3*, 9.

Gaze, R., and Fawcett, J. (1983). Pathways of Xenopus optic fibres regenerating from normal and compound eyes under various conditions. J Embryol Exp Morphol *73*, 17-38.

Gussing, F., and Bohm, S. (2004). NQO1 activity in the main and the accessory olfactory systems correlates with the zonal topography of projection maps. Eur J Neurosci *19*, 2511-2518.

Hansen, M., Dallal, G., and Flanagan, J. (2004). Retinal axon response to ephrin-as shows a graded, concentration-dependent transition from growth promotion to inhibition. Neuron *42,* 717-730.

Hattori, D., Millard, S., Wojtowicz, W., and Zipursky, S. (2008). Dscam-mediated cell recognition regulates neural circuit formation. Annu Rev Cell Dev Biol *24*, 597-620.

Hensch, T. (2004). Critical period regulation. Annu Rev Neurosci *27,* 549-579.

Himanen, J., Chumley, M., Lackmann, M., Li, C., Barton, W., Jeffrey, P., Vearing, C., Geleick, D., Feldheim, D., Boyd, A., *et al.* (2004). Repelling class discrimination: ephrin-A5 binds to and activates EphB2 receptor signaling. Nat Neurosci *7*, 501-509.

Hinds, J., Hinds, P., and McNelly, N. (1984). An autoradiographic study of the mouse olfactory epithelium: evidence for long-lived receptors. Anat Rec *210*, 375-383.

Ho, R., and Goodman, C. (1982). Peripheral pathways are pioneered by an array of central and peripheral neurones in grasshopper embryos. Nature *297*, 404-406.

Hong, W., Mosca, T., and Luo, L. (2012). Teneurins instruct synaptic partner matching in an olfactory map. Nature *484*, 201-207.

Huber, A., Kolodkin, A., Ginty, D., and Cloutier, J. (2003). SIGNALING AT THE GROWTH CONE: Ligand-Receptor Complexes and the Control of Axon Growth and Guidance. Annu Rev Neurosci *26*, 509-563.

Imai , T., Suzuki, M., and Sakano, H. (2006). Odorant receptor-derived cAMP signals direct axonal targeting. Science *314*, 657-661.

Imai, T., Yamakazi, T., Kobayakawa, R., Kobayakawa, K., Abe, T., Suzuki, M., and Sakano, H. (2009). Pre-target axon sorting establishes the neural map topography. Science.

Johnson, B.A., and Leon, M. (2007). Chemotopic odorant coding in a mammalian olfactory system. J Comp Neurol *503*, 1-34.

Johnson, B.A., Xu, Z., Ali, S.S., and Leon, M. (2009). Spatial representations of odorants in olfactory bulbs of rats and mice: similarities and differences in chemotopic organization. J Comp Neurol *514*, 658-673.

Kaneko-Goto, T., Yoshihara, S., Miyazaki, H., and Yoshihara, Y. (2008). BIG-2 mediates olfactory axon convergence to target glomeruli. Neuron *57*, 834-846.

Kerr, M.A., and Belluscio, L. (2006). Olfactory experience accelerates glomerular refinement in the mammalian olfactory bulb. Nat Neurosci *9*, 484-486.

Key, B., and St John, J. (2002). Axon navigation in the mammalian primary olfactory pathway: where to next? Chem Senses *27*, 245-260.

Klenoff, J.R., and Greer, C.A. (1998). Postnatal development of olfactory receptor cell axonal arbors. J Comp Neurol *390*, 256-267.

Kobayakawa, K., Kobayakawa, R., Matsumoto, H., Oka, Y., Imai, T., Ikawa, M., Okabe, M., Ikeda, T., Itohara, S., Kikusui, T., *et al.* (2007). Innate versus learned odour processing in the mouse olfactory bulb. Nature *450*, 503-508.

Krishnaswamy, A., and Cooper, E. (2009). An activity-dependent retrograde signal induces the expression of the high-affinity choline transporter in cholinergic neurons. Neuron *61*, 272-286.

Kulahin, N., Kristensen, O., Rasmussen, K., Olsen, L., Rydberg, P., Vestergaard, B., Kastrup, J., Berezin, V., Bock, E., Walmod, P., *et al.* (2011). Structural model and trans-interaction of the entire ectodomain of the olfactory cell adhesion molecule. Structure *19*, 203-211.

LaMantia, A.S., and Purves, D. (1989). Development of glomerular pattern visualized in the olfactory bulbs of living mice. Nature *341*, 646-649.

Lemke, G., and Reber, M. (2005). Retinotectal Mapping: New Insights from Molecular Genetics. Annu Rev Cell Dev Biol *21*, 551-580.

Levai, O., Breer, H., and Strotmann, J. (2003). Subzonal organization of olfactory sensory neurons projecting to distinct glomeruli within the mouse olfactory bulb. J Comp Neurol *458*, 209-220.

Lewcock, J., and Reed, R. (2004). A feedback mechanism regulates monoallelic odorant receptor expression. PNAS *101*, 1069-1074.

Liberles, S., and Buck, L. (2006). A second class of chemosensory receptors in the olfactory epithelium. Nature *442*, 645-650.

Liu, W.L., and Shipley, M.T. (1994). Intrabulbar associational system in the rat olfactory bulb comprises cholecystokinin-containing tufted cells that synapse onto the dendrites of GABAergic granule cells. J Comp Neurol *346*, 541-558.

Lodovichi, C., Belluscio, L., and Katz, L.C. (2003). Functional topography of connections linking mirror-symmetric maps in the mouse olfactory bulb. Neuron *38*, 265-276.

Lorenz, K. (1958). The evolution of behavior. Sci Am *199*, 67-74.

Mackay-Sim, A., and Kittel, P. (1991). On the Life Span of Olfactory Receptor Neurons. 3 *208-215*.

Magklara, A., Yen, A., Colquitt, B., Clowney, E., Allen, W., Markenscoff-Papadimitriou, E., Evans, Z., Kheradpour, P., Mountoufaris, G., Carey, C., *et al.* (2011). An epigenetic signature for monoallelic olfactory receptor expression. Cell *145*, 555-570.

Mainland, J., and Matsunami, H. (2012). RAMP like proteins : RTP and REEP family of proteins. Adv Exp Med Biol *744*, 75-86.

Malnic, B., Hirono, J., Sato, T., and Buck, L. (1999). Combinatorial receptor codes for odors. Cell *96*, 713-723.

Maritan, M., Monaco, G., Zamparo, I., Zaccolo, M., Pozzan, T., and Lodovichi, C. (2009). Odorant receptors at the growth cone are coupled to localized cAMP and Ca2+ increases. Proc Natl Acad Sci *106*, 3537-3542.

McLaughlin, T., and O'Leary, D. (2005). Molecular gradients and development of retinotopic maps. Annu Rev Neurosci *28*, 327-355.

Miller, A., Treloar, H., and Greer, C. (2010). Composition of the migratory mass during development of the olfactory nerve. J Comp Neurol *518*, 4825-4841.

Miyamichi, K., Serizawa, S., Kimura, H., and Sakano, H. (2005). Continuous and overlapping expression domains of odorant receptor genes in the olfactory epithelium determine the dorsal/ventral positioning of glomeruli in the olfactory bulb. J Neurosci *25*, 3586-3592.

Mombaerts, P. (2004). Odorant receptor gene choice in olfactory sensory neurons: the one receptor-one neuron hypothesis revisited. Curr Opin Neurobiol *14*, 31-36.

Mombaerts, P. (2006). Axonal wiring in the mouse olfactory system. Annu Rev Cell Dev Biol *22*, 713-737.

Mombaerts, P., Wang, F., Dulac, C., Chao, S., Nemes, A., Mendelsohn, M., Edmonson, J., and Axel, R. (1996). Visualizing an olfactory sensory map. Cell *87*, 675-686.

Mori, K., Nagao, H., and Yoshihara, Y. (1999). The olfactory bulb: coding and processing of odor molecule information. Science *286*, 711-715.

Mori, K., and Sakano, H. (2011). How is the olfactory map formed and interpreted in the mammalian brain? Annu Rev Neurosci *34*, 467-499.

Mori, K., Takahashi, Y.K., Igarashi, K.M., and Yamaguchi, M. (2006). Maps of odorant molecular features in the Mammalian olfactory bulb. Physiol Rev *86*, 409-433.

Nakamura, H., and O'Leary, D. (1989). Inaccuracies in initial growth and arborization of chick retinotectal axons followed by course corrections and axon remodeling to develop topographic order. J Neurosci *9*, 3776-3795.

Nakatani, H., Serizawa, S., Nakajima, M., and Imai, T., Sakano, H (2003). Developmental elimination of ectopic projection sites for the transgenic OR gene that has lost zone specificity in the olfactory epithelium. Eur J Neurosci *18*, 2425-2432.

Nguyen-Ba-Charvet, K., Di Meglio, T., Fouquet, C., and Chédotal, A. (2008). Robos and slits control the pathfinding and targeting of mouse olfactory sensory axons. J Neurosci *28*, 4244-4249.

Nguyen Ba-Charvet, K., von Boxberg, Y., Guazzi, S., Boncinelli, E., and Godement, P. (1998). A potential role for the OTX2 homeoprotein in creating early 'highways' for axon extension in the rostral brain. Development *125*, 4273-4282.

Nordlander, R., and Singer, M. (1982). Spaces precede axons in Xenopus embryonic spinal cord. Exp Neurol *75*, 221-228.

Norlin, E., Alenius, M., Gussing, F., Hägglund, M., Vedin, V., and Bohm, S. (2001). Evidence for gradients of gene expression correlating with zonal topography of the olfactory sensory map. Mol Cell Neurosci *18*, 283-295.

Oka, Y., Kobayakawa, K., Nishizumi, H., Miyamichi, K., Hirose, S., Tsuboi, A., and Sakano, H. (2003). O-MACS, a novel member of the medium-chain acyl-coA synthetase family, specifically expressed in the olfactory epithelium in a zone-specific manner. Eur J Biochem *270*, 1995-2004.

Penn, A., Riquelme, P., Feller, M., and Shatz, C. (1998). Competition in retinogeniculate patterning driven by spontaneous activity. Science *279*, 2108-2112.

Pizzorusso, T., Medini, P., Berardi, N., Chierzi, S., Fawcett, J., and Maffei, L. (2002). Reactivation of ocular dominance plasticity in the adult visual cortex. Science *298*, 1248-1251.

Potter, S., Zheng, C., Koos, D., Feinstein, P., Fraser, S., and Mombaerts, P. (2001). Structure and emergence of specific olfactory glomeruli in the mouse. J Neurosci *21*, 9713-9723.

Raper, J., and Mason, C. (2010). Cellular strategies of axonal pathfinding. Cold Spring Harb Perspect Biol *2*.

Ressler, K., Sullivan, S., and Buck, L. (1994). Information coding in the olfactory system: evidence for a stereotyped and highly organized epitope map in the olfactory bulb. Cell *79*, 1245-1255.

Royet, J.P., Souchier, C., Jourdan, F., and Ploye, H. (1988). Morphometric study of the glomerular population in the mouse olfactory bulb: numerical density and size distribution along the rostrocaudal axis. J Comp Neurol *270*, 559-568.

Saito, H., Kubota, M., Roberts, R.W., Chi, Q., and Matsunami, H. (2004). RTP family members induce functional expression of mammalian odorant receptors. Cell *119*, 679-691.

Sato, Y., Hirata, T., Ogawa, M., and Fujisawa, H. (1998). Requirement for early-generated neurons recognized by monoclonal antibody lot1 in the formation of lateral olfactory tract. J Neurosci *18*, 7800-7810.

Schaefer, M.L., Finger, T.E., and Restrepo, D. (2001). Variability of position of the P2 glomerulus within a map of the mouse olfactory bulb. J Comp Neurol *436*, 351-362.

Schmidt, J., and Easter, S. (1978). Independent biaxial reorganization of the retinotectal projection: a reassessment. Exp Brain Res *31*, 155-162.

Schwarting, G.A., Raitcheva, D., Crandall, J.E., Burkhardt, C., and Puschel, A.W. (2004). Semaphorin 3A-mediated axon guidance regulates convergence and targeting of P2 odorant receptor axons. Eur J Neurosci *19*, 1800-1810.

Schwarzenbacher, K., Fleischer, J., and Breer, H. (2006). Odorant receptor proteins in olfactory axons and in cells of the cribriform mesenchyme may contribute to fasciculation and sorting of nerve fibers. Cell Tissue Res *323*, 211-219.

Schwarzenbacher, K., Fleischer, J., Breer, H., and Conzelmann, S. (2004). Expression of olfactory receptors in the cribriform mesenchyme during prenatal development. Gene Expr Patterns *4*, 543-552.

Scolnick, J., Cui, K., Duggan, C., Xuan, S., Yuan, X., Efstratiadis, A., and Ngai, J. (2008). Role of IGF signaling in olfactory sensory map formation and axon guidance. Neuron *57*, 847-857.

Serizawa, S., Miyamichi, K., Nakatani, H., Suzuki, M., Saito, M., Yoshihara, Y., and H, S. (2003). Negative feedback regulation ensures the one receptor-one olfactory neuron rule in mouse. Science *302*, 2088-2094.

Serizawa, S., Miyamichi, K., Takeuchi, H., Yamagishi, Y., Suzuki, M., and Sakano, H. (2006). A neuronal identity code for the odorant receptor-specific and activity-dependent axon sorting. Cell *127*, 1057-1069.

Shen, K., and Bargmann, C. (2003). The immunoglobulin superfamily protein SYG-1 determines the location of specific synapses in C. elegans. Cell *112*, 619-630.

Shepherd, G., Chen, W., and Greer, C. (2004). The Synaptic Organization of the Brain, G. Shepherd, ed. (New York, Oxford Univ Press), pp. 165-216.

Shykind, B., Rohani, S., O'Donnell, S., Nemes, A., Mendelsohn, M., Sun, Y., Axel, R., and Barnea, G. (2004). Gene switching and the stability of odorant receptor gene choice. Cell *117*, 801-815.

Shykind, B.M. (2005). Regulation of odorant receptors: one allele at a time. Hum Mol Genet *14 Spec No 1*, R33-39.

Siebert, M., Banovic, D., Goellner, B., and Aberle, H. (2009). Drosophila motor axons recognize and follow a Sidestep-labeled substrate pathway to reach their target fields. Genes Dev *23*, 1052-1062.

Soucy, E.R., Albeanu, D.F., Fantana, A.L., Murthy, V.N., and Meister, M. (2009). Precision and diversity in an odor map on the olfactory bulb. Nat Neurosci *12*, 210-220.

Sperry, R. (1963). Chemoaffinity in the orderly growth of nerve fiber patterns and connections. PNAS *50*, 703-710.

St John, J., Clarris, H., McKeown, S., Royal, S., and Key, B. (2003). Sorting and convergence of primary olfactory axons are independent of the olfactory bulb. J Comp Neurol *464*, 131-140.

Strotmann, J., Conzelmann, S., Beck, A., Feinstein, P., Breer, H., and Mombaerts, P. (2000). Local permutations in the glomerular array of the mouse olfactory bulb. J Neurosci *20*, 6927-6938.

Strotmann, J., Levai, O., Fleischer, J., Schwarzenbacher, K., and Breer, H. (2004). Olfactory receptor proteins in axonal processes of chemosensory neurons. J Neurosci *24*, 7754-7761.

Suzukawa, K., Kondo, K., Kanaya, K., Sakamoto, T., Watanabe, K., Ushio, M., Kaga, K., and Yamasoba, T. (2011). Age-related changes of the regeneration mode in the mouse peripheral olfactory system following olfactotoxic drug methimazole-induced damage. J Comp Neurol *519*, 2154-2174.

Takahashi, Y.K., Kurosaki, M., Hirono, S., and Mori, K. (2004). Topographic representation of odorant molecular features in the rat olfactory bulb. J Neurophysiol *92*, 2413-2427.

Takeuchi, H., Inokuchi, K., Aoki, M., Suto, F., Tsuboi, A., Matsuda, I., Suzuki, M., Aiba, A., Serizawa, S., Yoshihara, Y., *et al.* (2010). Sequential Arrival and Graded Secretion of Sema3F by Olfactory Neuron Axons Specify Map Topography at the Bulb. Cell *141*, 1056-1067.

Taniguchi, M., Nagao, H., Takahashi, Y.K., Yamaguchi, M., Mitsui, S., Yagi, T., Mori, K., and Shimizu, T. (2003). Distorted odor maps in the olfactory bulb of semaphorin 3A-deficient mice. J Neurosci *23*, 1390-1397.

Taylor, J., and Gaze, R. (1985). The effects of the fibre environment on the paths taken by regenerating optic nerve fibres in Xenopus. J Embryol Exp Morphol *89*, 383-401.

Tian, H., and Ma, M. (2008). Activity plays a role in eliminating olfactory sensory neurons expressing multiple odorant receptors in the mouse septal organ. Mol Cell Neurosci *38*, 484-488.

Translated by Swanson, N., and Swanson, L. (1995). Histology of the Nervous System of Man and Vertebrates. History of Neuroscience *6*.

Treloar, H., Feinstein, P., Mombaerts, P., and Greer, C. (2002). Specificity of glomerular targeting by olfactory sensory axons. J Neurosci *22*, 2469-2477.

Treloar, H.B., Purcell, A.L., and Greer, C.A. (1999). Glomerular formation in the developing rat olfactory bulb. J Comp Neurol *413*, 289-304.

Vassalli, A., Rothman, A., Feinstein, P., Zapotocky, M., and Mombaerts, P. (2002). Minigenes impart odorant receptor-specific axon guidance in the olfactory bulb. Neuron *35*, 681-696.

Vassar, R., Chao, S., Sitcheran, R., Nuñez, J., Vosshall, L., and Axel, R. (1994). Topographic organization of sensory projections to the olfactory bulb. Cell *79*, 981-991.

Vrieseling, E., and Arber, S. (2006). Target-induced transcriptional control of dendritic patterning and connectivity in motor neurons by the ETS gene Pea3. Cell *127*, 1439-1452.

Wang, F. (2009). The signaling mechanisms underlying cell polarity and chemotaxis. Cold Spring Harb Perspect Biol *1*.

Wang, F., Nemes, A., Mendelsohn, M., and Axel, R. (1998). Odorant receptors govern the formation of a precise topographic map. Cell *93*, 47-60.

Weiss, P. (1945). Experiments on cell and axon orientation in vitro; the role of colloidal exudates in tissue organization. J Exp Zool *100*, 353-386.

Whitlock, K., and Westerfield, M. (1998). A transient population of neurons pioneers the olfactory pathway in the zebrafish. J Neurosci *18*, 8919-8927.

Wiesel, T., and Hubel, D. (1963). Effects of visual deprivation on morphology and physiology of cells in the cat lateral geniculate body J Neurophysiol *26*, 978-993.

Wigglesworth, V. (1953). The origin of sensory neurones in an insect, Rhodnius prolixus (Hemiptera). Quart J Microsc Sci *94*, 93-112.

Yates, P., Holub, A., McLaughlin, T., Sejnowski, T., and O'Leary, D. (2004). Computational modeling of retinotopic map development to define contributions of EphA-ephrinA gradients, axon-axon interactions, and patterned activity. J Neurobiol *59*, 95-113.

Yoshihara, Y., Kawasaki, M., Tamada, A., Fujita, H., Hayashi, H., Kagamiyama, H., and Mori, K. (1997). OCAM: A new member of the neural cell adhesion molecule family related to zone-to-zone projection of olfactory and vomeronasal axons. J Neurosci *17*, 5830-5842.

Young, J., Shykind, B., Lane, R., Tonnes-Priddy, L., Ross, J., Walker, M., Williams, E., and Trask, B. (2003). Odorant receptor expressed sequence tags demonstrate olfactory expression of over 400 genes, extensive alternate splicing and unequal expression levels. Genome Biol *4*.

Yu, C., Power, J., Barnea, G., O'Donnell, S., Brown, H., Osborne, J., Axel, R., and Gogos, J. (2004). Spontaneous neural activity is required for the establishment and maintenance of the olfactory sensory map. Neuron *42*, 553-566.

Zhao, H., and Reed, R. (2001). X inactivation of the OCNC1 channel gene reveals a role for activity-dependent competition in the olfactory system. Cell *104*, 651-660.

Zheng, J., Felder, M., Connor, J., and Poo, M. (1994). Turning of nerve growth cones induced by neurotransmitters. Nature *1994*.

Zhou, Z., and Belluscio, L. (2008). Intrabulbar projecting external tufted cells mediate a timing-based mechanism that dynamically gates olfactory bulb output. J Neurosci *28*, 9920-9928.

Zou, D.J., Feinstein, P., Rivers, A.L., Mathews, G.A., Kim, A., Greer, C.A., Mombaerts, P., and Firestein, S. (2004). Postnatal refinement of peripheral olfactory projections. Science *304*, 1976-1979.

Zweifel, L., Kuruvilla, R., and Ginty, D. (2005). Functions and mechanisms of retrograde neurotrophin signalling. Nat Rev Neurosci *6*, 615-625.

FIGURES

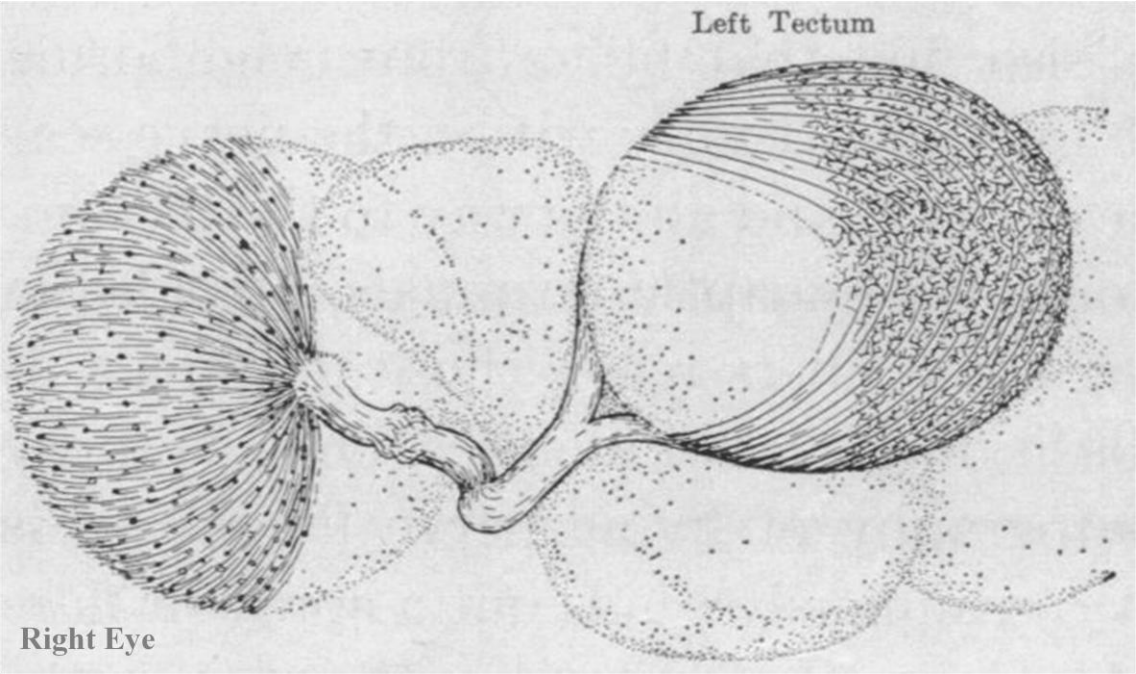

Figure 1. Axons pass potential synaptic partners to innervate correct locations

Following ablation of the temporal retina and optic nerve section, regenerating optic fibers grow through extensive stretches of the semi-denervated anterior tectum, but form synaptic layer and connections only in posterior tectum. Adapted from (Sperry, 1963).

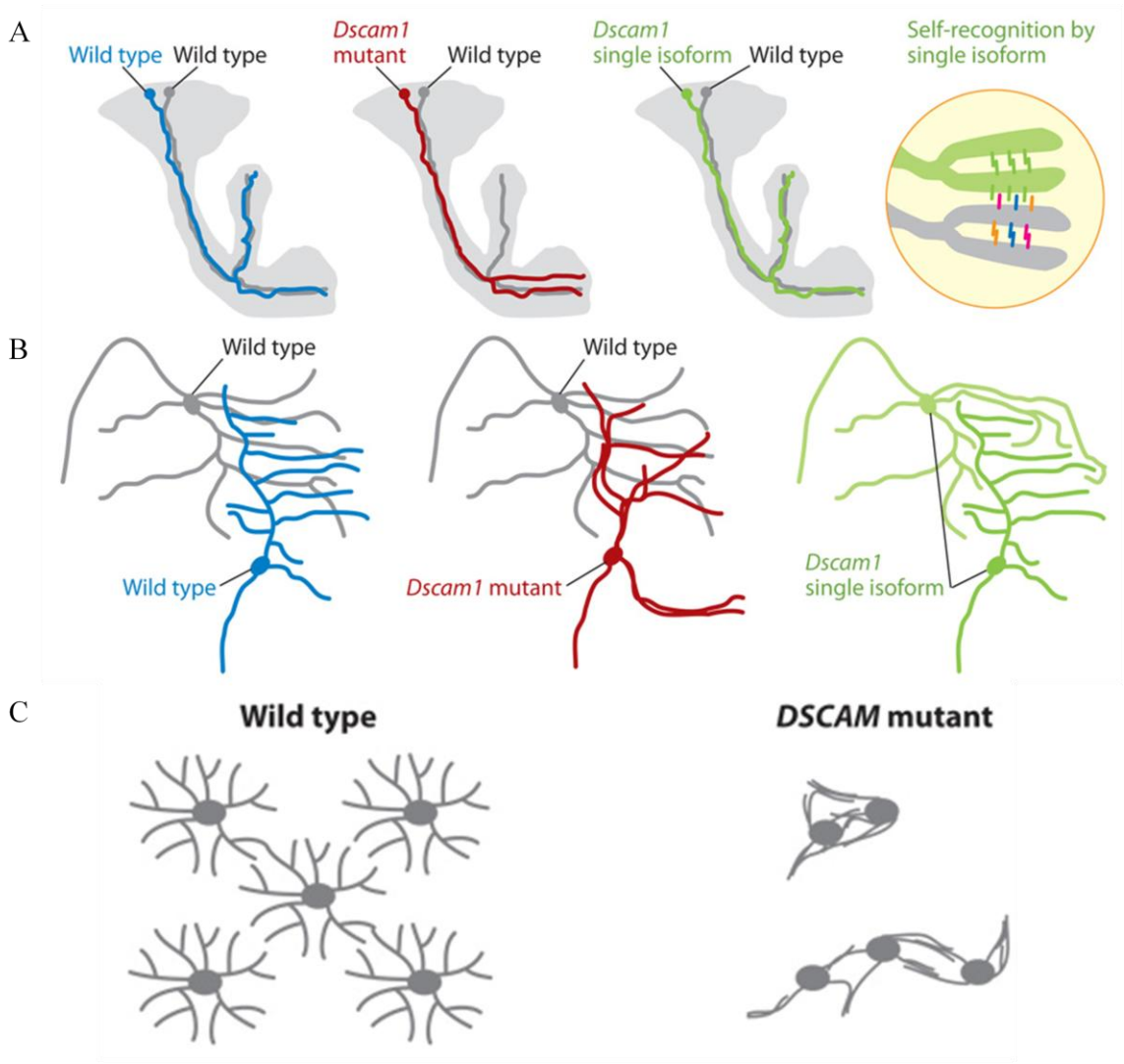

Figure 2. Dscam1 mediates homotypic repulsion.
A) Mushroom body axons normally bifurcate and extend one branch medially and the other dorsally. Each neuron expresses a unique combination of isoforms. As a consequence, sister branches recognize each other through Dscam1 matching. This signals repulsion and subsequent segregation of axons to separate pathways. **B)** (*Left*) Wild-type mushroom body axon branches segregate with high fidelity. (*Middle*) The branches of a single *Dscam* mutant neuron in a wild-type background frequently do not segregate appropriately. (*Right*) Expression of a single arbitrarily chosen isoform promotes branch segregation in a single *Dscam1* null mutant cell. These and other experiments demonstrated that it is crucial that each neuron expresses isoforms different from its neighbors. **C)** Mouse DSCAM mediates both self-avoidance and tiling. (*Left*) DSCAM-positive amacrine cells exhibit both self-avoidance and tiling properties. (*Right*) In the absence of DSCAM, both self-avoidance and tiling are lost. Branches from individual amacrine cells fasciculate with one another and with other cells of the same type. Adapted from (Hattori et al., 2008).

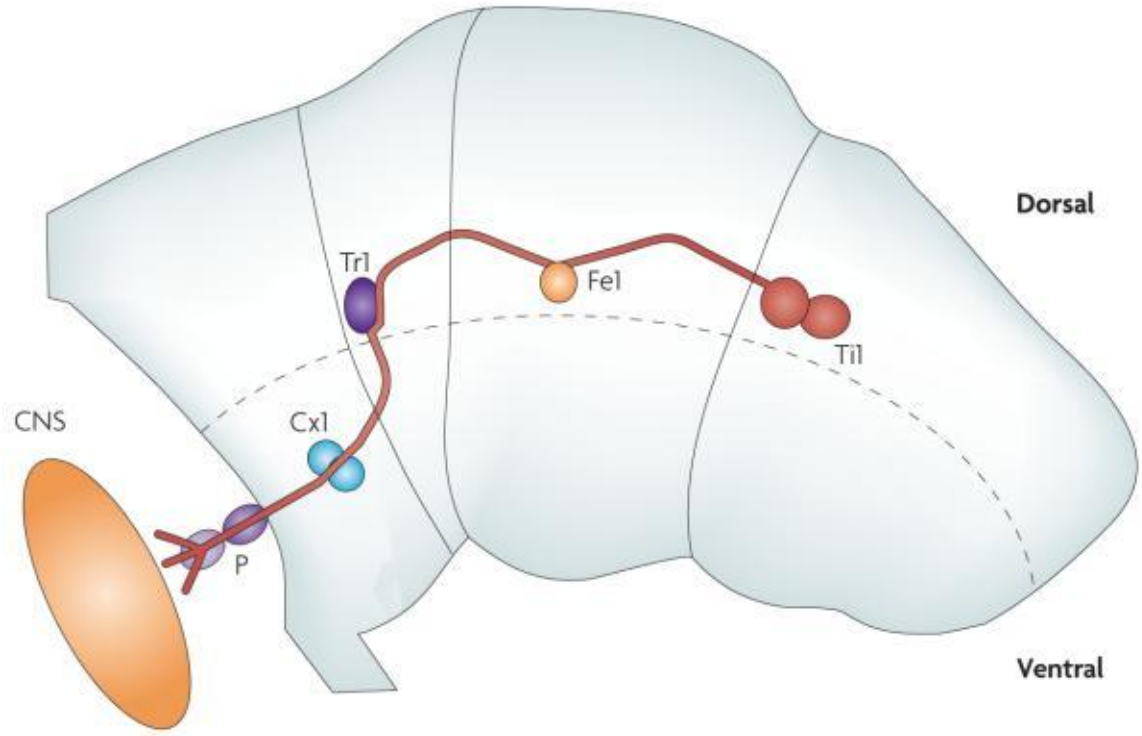

Figure 3. Guidepost cells in the axonal guidance of grasshopper pioneer neurons.

The stereotyped axonal trajectory of Ti1 neurons. Ti1 axons reorient their trajectory at points of contact with specific cell types (Fe1, Tr1, Cx1 and P). Ablation of Cx1 cells causes Ti1 axons to wander and form ectopic branches. Adapted from (Chao et al., 2009).

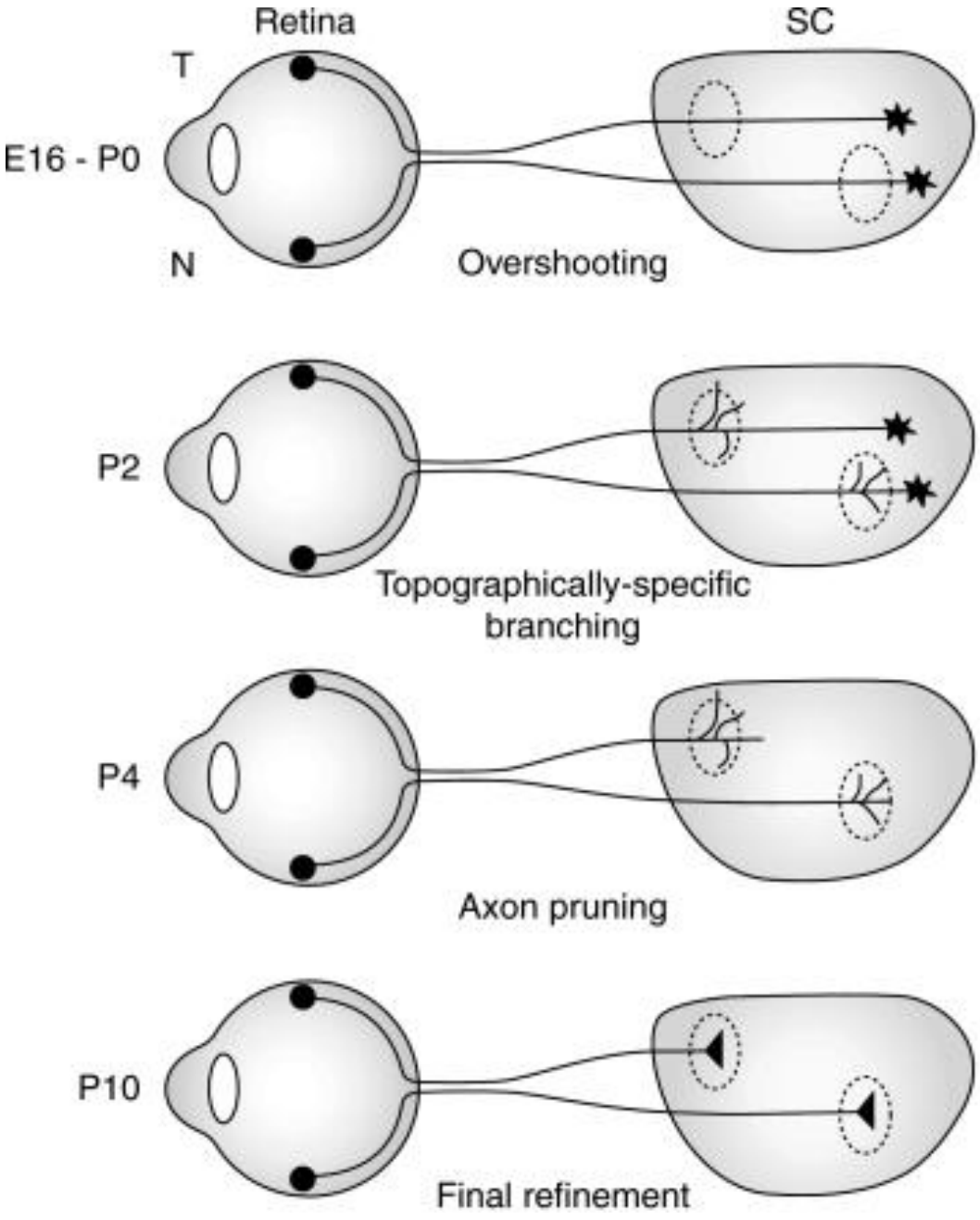

Figure 4. Developmental stages in mapping nasotemporal retinal axis on the anteroposterior axis of the colliculus/tectum in mice and chicks.

Initially RGC axons enter the SC at the anterior end and project to the posterior SC overshooting their topographically appropriate termination zone (dashed circles). Then branching occurs from the axon at the topographically specific location followed by pruning of the posterior axon. At later stages the branches are stabilized, and refined to form strong synapses. Adapted from (Feldheim and O'Leary, 2010).

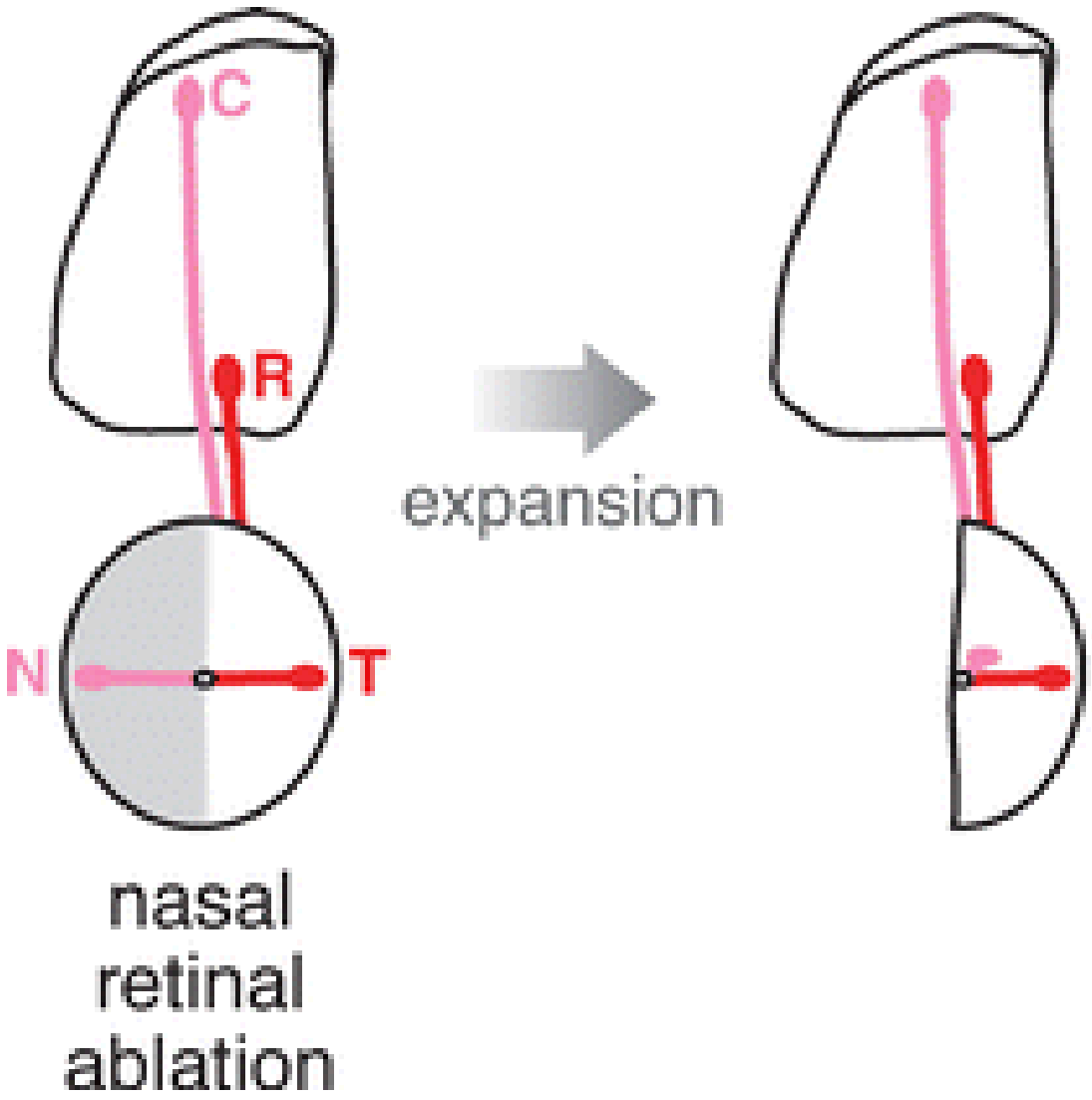

Figure 5. Plasticity of the retinotopic map.

When the nasal half of the retina is ablated in amphibians, the termination zones of the ablated nasal RGCs are lost from the caudal tectum. The vacated tectal sites are eventually occupied by the axons of the RGCs that remain, and this occupation is retinotopic. Adapted from (Lemke and Reber, 2005).

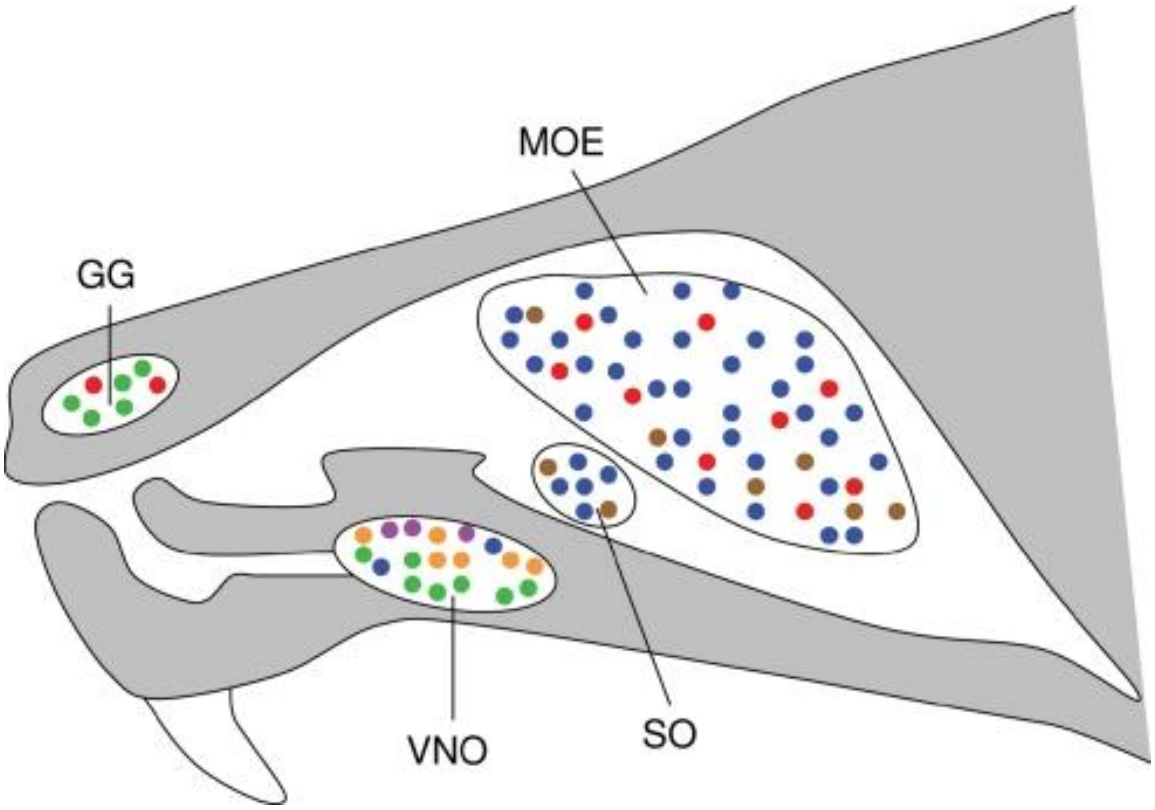

Figure 6. The subsystems of the olfactory system.

Schematic representation of the murine nose and its olfactory subsystems, including the Grüneberg ganglion (GG), the vomeronasal organ (VNO), the septal organ (SO), and the main olfactory epithelium (MOE). The olfactory receptor types expressed in each of these organs are indicated by color: ORs in blue, V1Rs in orange, V2Rs in green, TAARs in red, FPRs in purple, GC-D in brown. Adapted from (Fleischer et al., 2009).

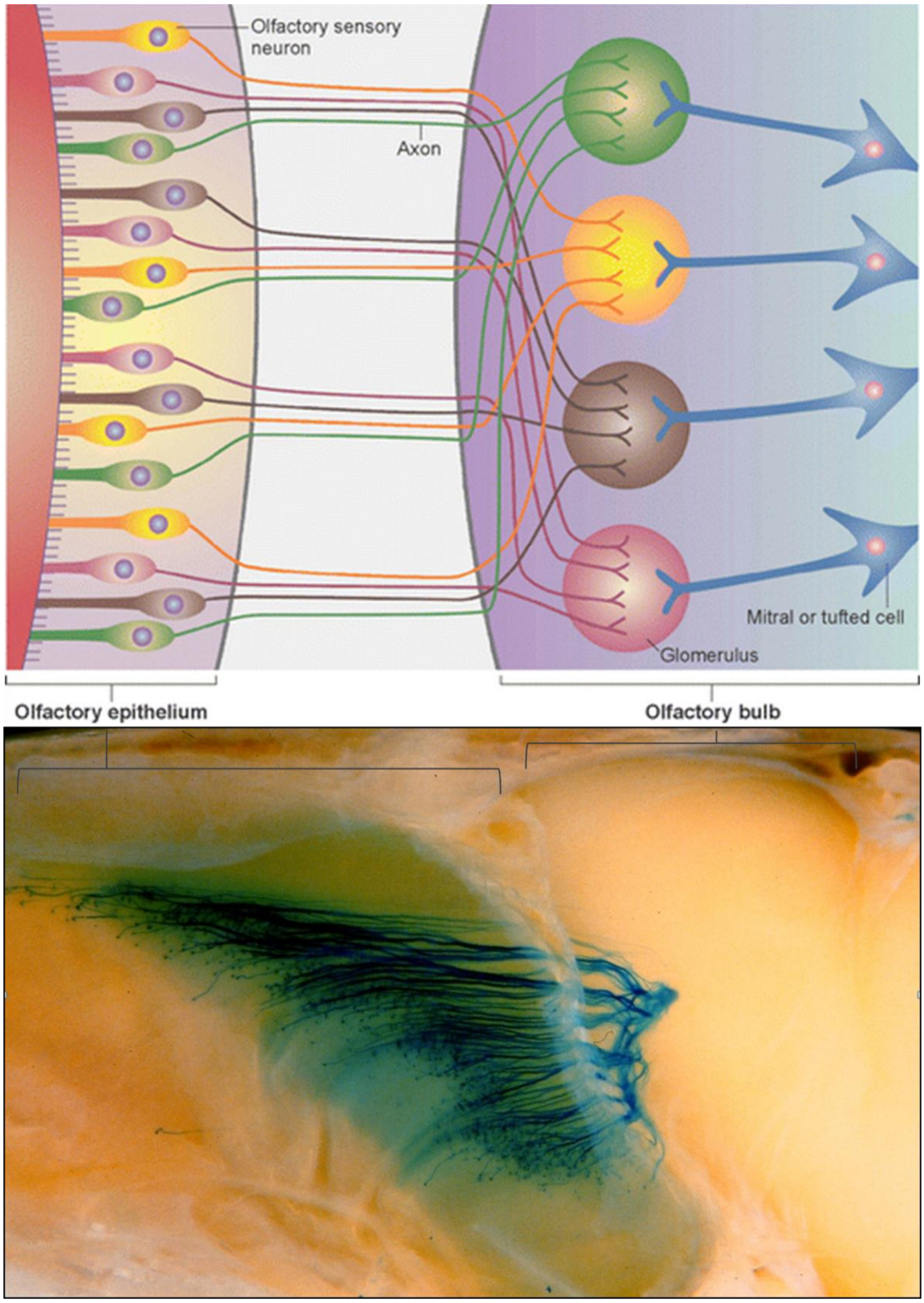

Figure 7. (legend continued on next page)

Figure 7. Wiring of the mouse olfactory system.

(*Top*) Four different populations of OSNs, each expressing a different OR, are depicted in green, orange, brown, and red. OSNs that express the same OR are scattered in a seemingly random fashion with the epithelium, but their axons coalesce into the same glomeruli in the olfactory bulb. Within a glomerulus, OSN axons synapse with the dendrites of the second-order neurons, the mitral or tufted cells. (*Bottom*) Actual projection patterns of the OSNs expressing a representative OR, P2. Whole mount of a P2-IRES-tau-lacZ mouse, stained with X-Gal. View of the nasal septum and the medial aspect of the bulb. Adapted from (Mombaerts, 2006; Mombaerts et al., 1996).

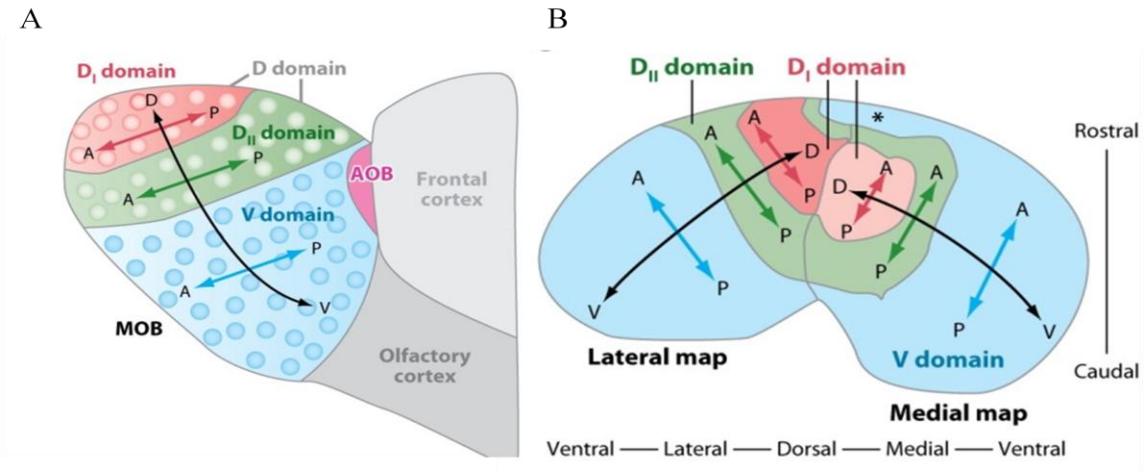

Figure 8. Structure and organization of the OB.

A) A lateral view of the domain organization of glomeruli in the lateral map of the OB. Double-headed colored arrows indicate the anterior-posterior (A-P) axis of each domain. Black arrows indicate the dorsal-ventral (D-V) axis of the lateral map. Abbreviations: AOB, accessory olfactory bulb; D_I, class I part of the D domain; D_{II}, class II part of the D domain. **B)** A dorsal centered view of an unrolled flattened map of glomerular layer of the OB. Double-headed colored arrows indicate the A-P axis of each domain of the lateral and medial maps. Black arrows indicate the D-V axis of the lateral and medial maps. In mice, an individual OR is typically represented by a pair of glomeruli: one in the lateral map and the other in the medial map. However, for a small subset of ORs, each OR is represented only by a single glomerulus. Some of these glomeruli are located in the tongue-shaped region indicated by an asterisk. Adapted from (Mori and Sakano, 2011).

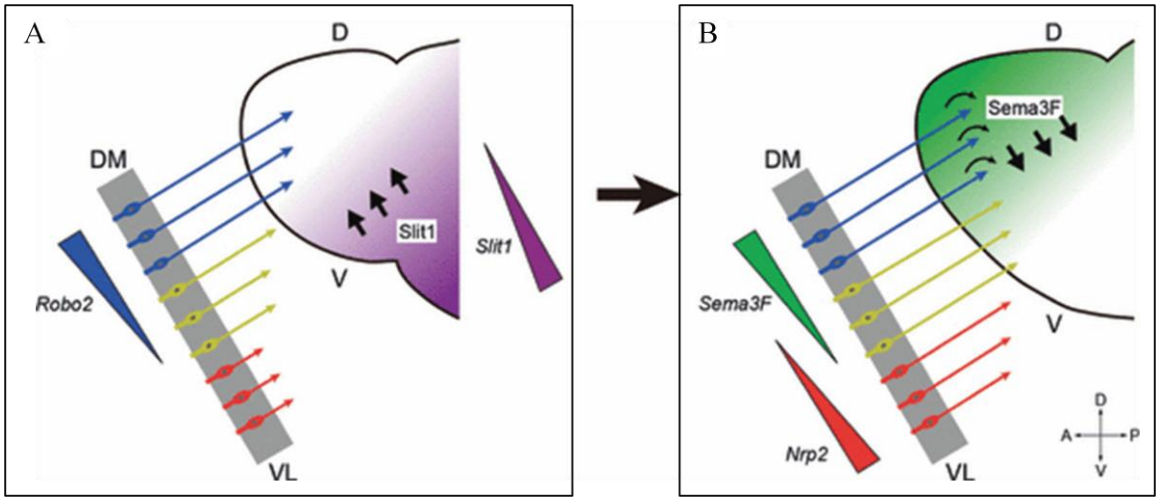

Figure 9. The sequential projection of OSN axons results in the dorsoventral axis of the map.

(A) OSNs in the dorsomedial zone of the MOE mature earlier and project axons to the OB before ventrolateral OSNs. Dorsomedial OSNs express an axon guidance receptor, Robo2. Slit1, a repulsive ligand for Robo2, is expressed in the septum and ventral OB during early development. As a result, dorsomedial OSNs project axons to the prospective dorsal domain of the embryonic OB. **(B)** Ventrolateral OSNs express an axon guidance receptor, Nrp2. Its repulsive ligand, Sema3F, is expressed in dorsomedial OSNs, but not in the OB. The axonal projection of OSNs occurs sequentially along the dorsomedial–ventrolateral axis of the MOE as the OB grows ventrally during development. Sema3F secreted by dorsomedial OSN axons in the OB prevents late-arriving Nrp2+ axons from invading the dorsal region of the OB. This may help maintain the topographic order between the MOE and OB during axonal projection. Medial sides of the OBs are schematically shown. A, anterior; D, dorsal; DM, dorsomedial; P, posterior; V, ventral; VL, ventrolateral. Adapted from (Mori and Sakano, 2011).

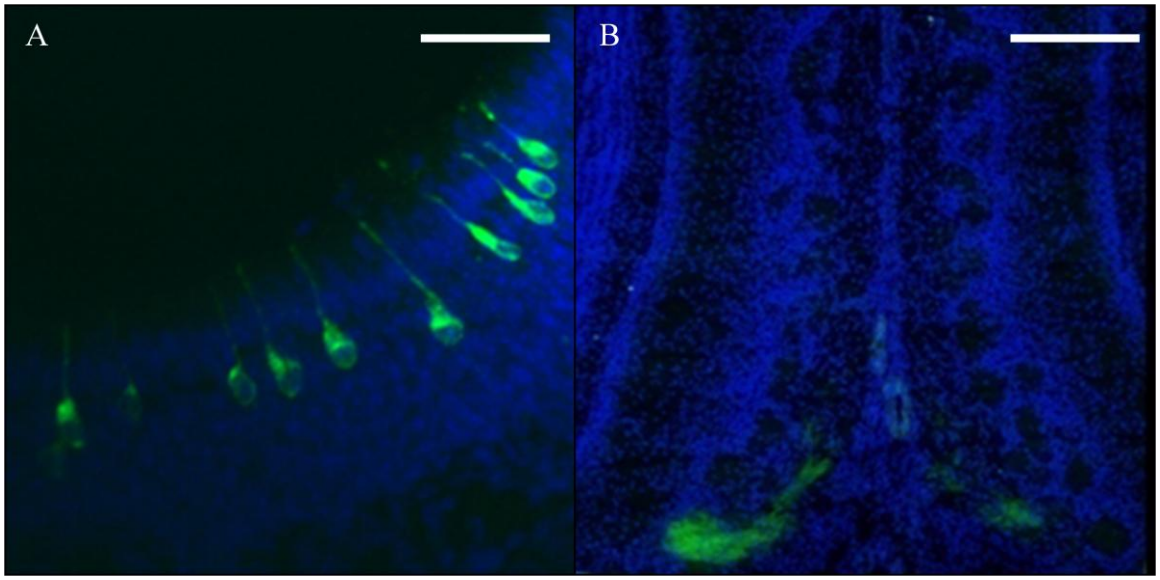

Figure 10. OR protein is expressed on both dendrites and axons of OSNs.

A,B) Coronal sections of MOE and OB, respectively, immunohistochemically stained for MOR28. The OR is localized to the cell bodies, the apical dendrites, and the axon tips within the glomeruli. Scale bars, 100 μm. Adapted from (Barnea et al., 2004).

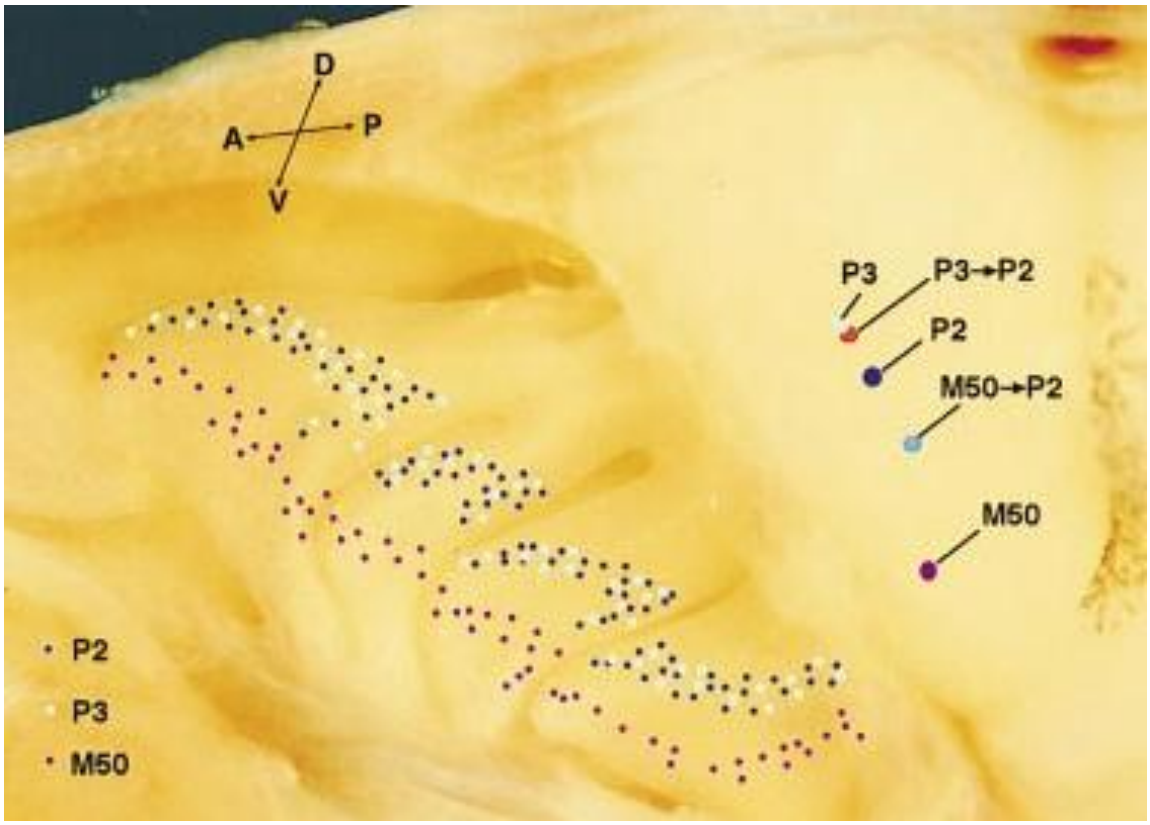

Figure 11. Altering the OR coding region affects the axonal guidance of OSNs.

A schematic representation of the pattern of expression of the wild-type P2, P3, and M50 neurons in the epithelium and the relative positions of the wild-type P2, P3, M50, and the P3→P2, M50→P2 glomeruli in the olfactory bulb. Adapted from (Wang et al., 1998).

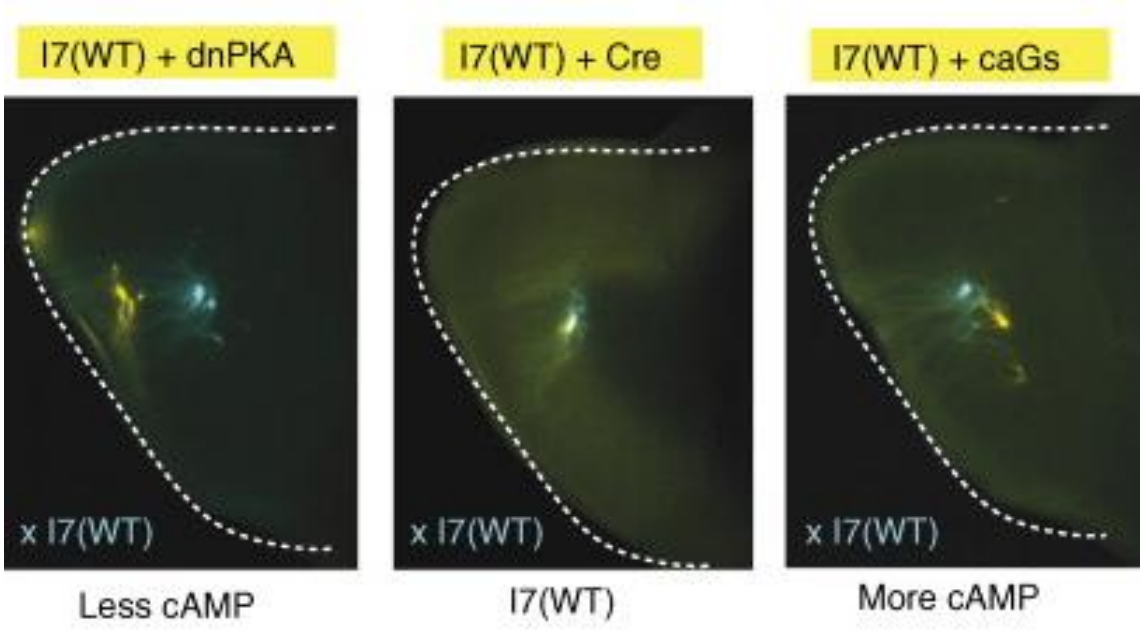

Figure 12. OR-derived cAMP signals direct axonal targeting along the A-P axis.

Axons were visualized with gap-ECFP or gap-EYFP fluorescence in the whole-mount medial OBs. (*Middle*) A wildtype odorant receptor I7 navigated axons to a specific glomerulus in the OB (eCFP). (*Left*) Co-expression of the dominant-negative mutant of PKA (dnPKA), which blocks cAMP signals, caused an anterior shift of glomeruli. (*Right*) In contrast, co-expression of a constitutively-active G_s mutant (caG_s) caused a posterior shift of the target glomeruli. We assume that each OR generates a unique level of cAMP signals, driven by its intrinsic activity at an earlier stage of OSN projection. The level of cAMP signals is converted to a relative expression level of axon guidance molecules (e.g. Neuropilin-1) via cAMP-dependent PKA and CREB. Neuropilin-1, together with other guidance molecules, navigates OSN axons along the anteroposterior axis according to its expression level. Adapted from (Imai and Sakano, 2007).

Chapter 2

Expression of transgenic odorant receptor causes the formation of rerouted glomeruli

ABSTRACT

Most neurons in the nervous system develop early and are retained for the lifetime of the animal. Accordingly, most of the studies addressing the development of neuronal circuitry and axonal guidance focus on how neural connections are initially established. However, subpopulations of neurons do regenerate during adulthood. In order to fully understand how the adult nervous system functions, we need to understand how these later-born neurons integrate into existing neuronal circuitry. The olfactory sensory neurons are well-suited for studying axonal guidance in the adult. They are generated throughout adulthood and it is known that the odorant receptor proteins expressed in these neurons impact axonal guidance. In this chapter we established an inducible transgenic approach to temporally manipulate odorant receptor expression so that we can assay specifically the mechanisms of axonal guidance that operate during adulthood. We characterized the ectopic glomeruli that are formed by the axons of olfactory sensory neurons expressing transgenic odorant receptor. Importantly, we also characterized the effect of the transgenic odorant receptor on the olfactory sensory neurons expressing only endogenous odorant receptors. These neurons are rerouted into supernumerary glomeruli in a distinct phenotype that is dependent on the expression of transgenic odorant receptor. This work establishes a foundation for interpreting the experiments in the next chapter where we will assay the effect of temporally manipulating transgenic odorant receptor expression.

INTRODUCTION

OSNs are a population of neurons that exhibit exquisite context specificity during axonal guidance. While some of the mechanisms that allow the first populations of OSNs to converge on spatially stereotyped targets have been elucidated (Mori and Sakano, 2011), less attention has been paid to the mechanisms that control the axonal guidance of later populations of OSNs and how they maintain the same projection patterns in the face of continuous regeneration. Since OSNs are one of the few populations of neurons that are generated in adulthood, they could represent an untapped source of information about adult-specific mechanisms of axonal guidance. In this chapter we set up a genetic approach to assay specifically the axonal guidance of later-born OSNs.

It is well established that OR proteins play a role in guiding the axons of OSNs, especially since the OSNs expressing a given OR all converge on the same homogenous glomeruli (Mombaerts, 2006). Therefore we generated a mouse line expressing a transgenic copy of an endogenous OR, assuming that this ectopic expression would generate an axonal guidance phenotype distinct from that seen in wildtype mice. To tailor this mouse model for assaying later-born OSNs, we placed the transgene under the control of an inducible promoter that can be reversibly silenced at any point in the mouse's life. A similar genetic strategy had been reported to successfully generate transgenic OR expression (Clowney et al., 2012; Fleischmann et al., 2008; Nguyen et al., 2010; Nguyen et al., 2007) and numerous labs have employed the inducibility of the promoter (Bertram and Hillen, 2008; Gogos et al., 2000; Yu et al., 2004) but no lab has yet used the this promoter to examine the role of ORs in axonal guidance in adults.

In this chapter we characterized the genetic strategy we used to express a transgenic OR. We generated the transgenic mice, verified its expression, explored the effects the transgene has on endogenous ORs, and quantified the axonal guidance phenotype specific to our transgene. This work provides a foundation for interpreting the experiments that will be described in Chapter 3.

MATERIALS AND METHODS

*Animals***.** We used C57/Bl6 mice purchased from Jackson Labs as the wildtype strain for all our experiments. The TO28 mice used in our experiments are on a mixed C57/BL6; 129 background. Mice were genotyped by PCR using primers that recognize TO28 (Int2 for: CTCTCCACAGGTGTCCACTCC and SP1 dA rev: AGATCTGTTGCCTCAGGG-CCACAAGG), tTA (tTA for: GCTTTGCTCGACGCCTTAGCCA and tTA rev: CCGT-AGGGGGCGGAGTCGTG) GFP (GFP for: GACCCTGAAGTTCAGCTGC and GFP rev: TGTCGCCATGATATAGACG), R26RtdTomato (TdTom3: GGCATTAAAGCAG-CGTATCC and TdTom4: CTGTTCCTGTACGGCATGG), Cre recombinase (Cre for: TAGCCGAAATTCCCAGGATCAGGG and Cre rev: TACATTGGTCCAGCCACCAG-CTTG). PCR was also used to distinguish heterozygotes and homozygotes of MOR28-IRES-C6 (SP1 WT forward: GACAGCTTCTTCTGTGATGTACC, SP1 reverse: GAAGTAGTTTGAAGTAGGGAATGC, and C6 end for: CTCTGAGGAACAAGCAG-GTG). For the mice used to address whether TO28 shut off endogenous ORs, the Cre alleles and the Cre reporter were transmitted through the mother, or only one was transmitted through the father to avoid premature reporter activation from OR expression in the sperm. Dox was administered via dox-supplemented chow (Bioserv, 200 mg/kg carrier chow) provided *ad libitum* and replaced once weekly. All animal procedures were in compliance with the guidelines of the Institutional Animal Care and Use Committee (IACUC) of Brown University.

Immunohistochemistry. The mice were anesthetized via intraperitoneal injection of 2,2,2-tribromoethanol (1.2% in 2-methyl-2-butanol and water, final dosage 240 mg/kg body

weight). For detection of β-galactosidase and tdTomato, animals were anaesthetized and transcardially perfused with 2% and 4% paraformaldehyde, respectively, in PBS. For all conditions, the MOE and OBs were dissected separately and embedded in OCT (Sakura) or M1 (Shandon) in a dry ice/ethanol bath. 14 μm coronal sections were cut on a cryostat (Leica CM3050S) and collected on SuperFrost plus slides (Fisher). The sections were post-fixed with 1% paraformaldehyde in PBS for 10 minutes at room temperature, washed three times in PBS for 5 minutes, permeabilized in 0.1% Triton X-100 in PBS (PBS-T) for 30 minutes at room temperature, blocked in 5% heat in-activated donkey serum in PBS-T (P/T/S) for 30 minutes at room temperature, incubated with primary antibody in P/T/S under parafilm (Fisher) overnight in a humidified chamber at 4˚C, washed three times in PBS-T for 5 minutes, blocked with P/T/S for 30 minutes at room temperature, incubated with a fluorescent-conjugated secondary antibody in P/T/S with TOTO-3 (Invitrogen, 1:1000) for 2 hours at room temperature, washed three times in PBS-T for 5 minutes, and coverslipped with Prolong Gold (Invitrogen). Images were taken using a Zeiss LSM 510 DuoScan confocal microscope.

Primary antibodies included goat anti-β-galactosidase (Chemicon, 1:1000), rabbit anti-Cre (Novagen, 1:1000), rabbit anti-activated caspase 3 (Cell Signaling, 1:1000), goat anti-Neuropilin 1 (R&D Systems, 1:1000) rabbit anti-GFP (Invitrogen, 1:1000), guinea pig anti-MOR28 (Barnea *et al.* 2004, 1:6000), rabbit anti-C6 (Barnea *et al.* 2004, 1:3000), guinea pig anti-M50 (Barnea *et al.* 2004, 1:3000), guinea pig anti-M71 (Barnea *et al.* 2004, 1:3000), guinea pig anti-TAAR4 (Johnson *et al.* 2012, 1:5000, pre-cleared by incubation overnight at 4°C with fixed HEK 239T cells), and guinea pig anti-TAAR5 (Johnson *et al.* 2012, 1:5000). Secondary antibodies used were donkey anti-guinea pig

Alexa Fluor® 488, donkey anti-rabbit Alexa Fluor® 488, donkey anti-goat Alexa Fluor® 555, donkey anti-rabbit Alexa Fluor® 549 and/or donkey anti-rabbit Alexa Fluor® 647 (Molecular Probes). C6 expression in the OB was amplified with the Tyramide Signal Amplification kit (Molecular Probes).

*Wholemount X-gal staining***.** MOE and OB was dissected intact, incubated 30 min at room temperature in fixative (1% formaldehyde, 0.2% gluteraldehyde, 2 mM $MgCl_2$, 5 mM EGTA, 0.02% NP-40, PBS), washed three times for 5 minutes in 0.02% NP-40 in PBS, incubated 24 hours in the dark at 37°C in staining solution (1 mg/ml X-gal, 5 mM $K_3Fe(CN)_6$, 5 mM $K_4Fe(CN)_6$, 2 mM $MgCl_2$, 0.01% sodium deoxycholate, 0.01% NP-40), washed three times in PBS for 10 minutes, and stored in 80% glycerol in PBS at 4°C. Images were taken using a Nikon SMZ1500 stereomicroscope.

*Quantification of staining frequency***.** An Olympus BX41 fluorescent microscope was used to identify the number of OSNs per section that stained positive for the proteins indicated in the text. The six consecutive sections per mouse that exhibited peak expression were averaged to generate a single mean value per mouse.

Quantification of interglomerular distances. An Olympus BX41 fluorescent microscope was used to identify the midpoint of each glomerulus (as defined by the section where the glomerulus had the largest diameter). QCapture Pro was used to image these sections and Photoshop (Adobe) was used to generate single images of each entire section. Image J (NIH) was used to identify the midpoint of each OB (as defined by the intersection of the widest and tallest lines that could be drawn per bulb). The XY coordinates (as defined by the distance from the midpoint of the glomerulus to the midpoint of the OB section) and

the Z coordinates (as the defined by the number of sections between a pair of glomeruli) were converted to microns and used to calculate the distance between two glomeruli.

RESULTS

Inducing transgenic MOR28 expression throughout the olfactory system

In order to temporally control the expression of ORs, we used the inducible tetO promoter to drive a transgenic OR. The strategy involves three alleles. The first, designated OMP-IRES-tTA (Gogos et al., 2000), drives the expression of the tetracycline transactivator (tTA) in all OSNs (Fig. 1A). The second allele, designated tetO::MOR28-IRES-tau-lacZ (TO28), allows the expression of both MOR28 and the reporter fusion protein tau-β-galactosidase (tau-lacZ) in OSNs expressing tTA (Fig. 1B). The drug doxycycline (dox) can be given to mice at any age to specifically silence only this promoter, allowing us to control transgenic expression in time. We obtained two founder lines for this transgene which differ in expression due to position effect variegation. TO28L is expressed in 1% of OSNs and TO28H is expressed in 5% of OSNs (Fig. 1D,E). These neurons expressed both MOR28 and tau-lacZ from the transgene and were found not only in the MOR28 zone but also throughout the MOE. To distinguish between endogenous MOR28 OSNs and transgenic MOR28 OSNs, we introduced the third allele, designated MOR28-IRES-GFP, which drives the expression of GFP only in endogenous MOR28 OSNs (Fig. 1C). Since lacZ and GFP are exogenous to mice, staining for each indicates the presence of transgenic or endogenous MOR28, respectively (Fig. 1F). OSNs expressing endogenous MOR28 are still found in their normal zone even when transgenic MOR28 is expressed.

When the Axel and Belluscio labs used the same OMP-IRES-tTA driver to induce the expression of similar transgenes, they saw OR expression in the VNO, presumably

because OMP is expressed throughout the olfactory system (Fleischmann et al., 2008; Nguyen et al., 2007). We also observed transgenic MOR28 in the VNO of TO28 mice, but only in the apical layer of the VNO where V1Rs are normally expressed (Fleischer et al., 2009) (Fig. 1G,H). We had expected that the basal layer of the VNO would express TO28 since the VSNs there also express OMP and the previous papers had observed transgene expression throughout the entire VNO. Additionally, we did not observe that the frequency of expression in the VNO was higher than in the MOE as reported by Nguyen et al. We hypothesize that their FVB/N wildtype background compared to our mixed C57/BL6-129 background accounts for the differences in expression pattern. LacZ-positive neurons were also observed in the GG where other olfactory chemoreceptors are expressed (Fleischer and Breer, 2010) (data not shown). These results indicate that our strategy is capable of overriding the expression of endogenous chemoreceptors to drive transgenic OR.

The transgene affects the expression of endogenous ORs

To verify that TO28 indeed overrode endogenous chemoreceptor expression, we quantified the number of OSNs expressing endogenous ORs. Originally we expected to see a 1-5% decrease, consistent with the 1-5% TO28 expression in the two founder lines. Surprisingly, we observed that the number of OSNs expressing the ORs C6, M50, and M71 actually decreased by more than 50% (Fig. 2A).

To track the inverse correlation between TO28 and endogenous OR expression, we quantified the expression of both as we temporarily silenced the transgene. Breeding pairs of mice were administered dox such that litters of pups capable of TO28 expression

were kept phenotypically wildtype throughout gestation and until P14. The dox was then removed and the expression of both TO28 and endogenous ORs was assayed at one week intervals. Low levels of TO28 were observed within the first several weeks and then sharply increased seven to nine weeks after the last administration of dox. Levels of three endogenous ORs as well as the levels of TAAR4 and TAAR5 followed an inverse trend with exactly the same time course, suggesting an immediate effect of TO28 on these other chemoreceptors (Fig. 2B,C).

OMP is thought to be expressed in mature OSNs that have already begun to express an OR and project toward the OB (Rogers et al., 1987). Since TO28 expression depends on OMP and seemed to immediately decrease the number of OSNs expressing endogenous ORs, we speculated that transgene induction was causing OSNs to either undergo apoptosis or shut off the original OR. This hypothesis was strengthened by the observation that TO28 was very rarely co-labeled the same OSNs as C6 and never with M50, M71, MOR10, TAAR4, or TAAR5 (Fig. 2D-I). The rare co-labeling with C6 may not indicate stable co-expression but rather represent OSNs that have just initiated TO28 expression. All previous experiments with ORs encoded on transgenes have failed to observe stable co-expression of two ORs (Fleischmann et al., 2008; Qasba and Reed, 1998; Serizawa et al., 2000; Serizawa et al., 2003; Vassalli et al., 2002).

To address the induction of apoptosis, we quantified the number of OSNs expressing the apoptotic marker activated caspase 3 in the MOE of TO28 and control mice. We observed significantly more apoptotic cells when TO28L or TO28H was expressed. Notably, the frequency of apoptotic OSNs for both TO28 founder lines was

only 30-50% over that of controls. Since the frequency of OSNs expressing C6, M50, and M71 was decreased by 60-90%, we had expected a greater increase in apoptosis. However, our systemic apoptosis assay encompassed all OSNs in the MOE and it is possible that different populations of OSNs are affected to different degrees.

To address whether endogenous ORs were also simply shut off by TO28 without inducing apoptosis, we employed a Cre-based system to irreversibly mark all OSNs that have ever expressed specific endogenous ORs. The strategy involves two new alleles (Fig. 3B-D). The first, either P2-IRES-Cre or MOR28-IRES-Cre, drives the expression of Cre recombinase in all OSNs that express endogenous P2 or MOR28. The second, designated as R26RtdTomato, irreversibly turns on tdTomato if co-expressed with Cre. We crossed these alleles to mice expressing OMP-IRES-tTA and TO28L. While we did observe many OSNs that had switched to express a second OR (tdTomato positive but Cre negative), few of these co-expressed TO28 (Fig. 3 Table 1). Together, these results indicate that TO28 induction causes most OSNs to undergo apoptosis instead of turning off endogenous ORs.

The transgene causes the formation of ectopic glomeruli throughout the OB

It is possible that the 1-5% of OSNs that we observed expressing TO28 were in the process of beginning to undergo apoptosis. To visualize whether these OSNs instead survived and innervated the OB, we stained whole-mount preparations for lacZ using the chromogenic substrate X-gal. MOR28-IRES-GFP and MOR28-IRES-tau-lacZ controls show that this assay exhibits no background in the OB and can clearly visualize the lateral MOR28 glomeruli (Fig. 4A,B). The TO28 OSNs do successfully target glomeruli

throughout the OB (Fig. 4C-F). Furthermore, these OSNs seem to be stably integrated since projection patterns were similar in young (1 month) and old (13 month) mice (data not shown). Following the nomenclature from Vassalli et al., we call these TO28 targets ectopic glomeruli (Vassalli et al., 2002). Notably, the distribution of ectopic glomeruli is highly variable, with asymmetries observed even between the two OBs in a given mouse (Fig. 4D,F). In coronal sections we observed lacZ and MOR28 protein in ~1% or 5% of the total glomeruli in the OBs of TO28L and TO28H mice, respectively, consistent with the 1% or 5% TO28 expression in the MOE for these two lines.

Since we were using the same driver and a similar transgene as Fleischmann et al. (Fleischmann et al., 2008), we repeated some of their analyses. Like their mice, we also saw transgenic OSNs innervating glomeruli throughout the AOB (Fig. 4H). However, where they observed their transgenic OSNs co-innervating glomeruli with OSNs expressing endogenous ORs, we did not observe any co-convergence of TO28 with C6 or M50 (Fig. 4I,J). This difference may be due to the fact that the transgene used by Fleischmann et al. was expressed in >95% of the OSNs and every glomerulus received input from transgenic axons. Similar to what Fleischmann et al. reported for their transgenic animals, the glomeruli formed by endogenous ORs stained more faintly than in controls, indicating that they contained less OR protein. This is probably due to the fewer OSNs in the MOE that we observed expressing endogenous ORs.

Besides Fleischmann et al., Nguyen et al. also assayed mice expressing the same driver and a similar transgene (Nguyen et al., 2010; Nguyen et al., 2007). Both labs reported that their transgenic glomeruli displayed normal morphologies. When we

examined the morphologies of our TO28 ectopic glomeruli, we found that they differed slightly in size but the differences fell within the normal range observed for nearby glomeruli (Fig. 5A). The intensity of MOR28 staining also varied between ectopic glomeruli but the two parameters were not correlated (Fig. 5B). Overall, TO28 axons seem to form morphologically normal ectopic glomeruli in a random pattern across the OB.

Transgene expression causes endogenous MOR28 axons to form rerouted glomeruli

Next we examined more closely the OB near the wildtype MOR28 glomeruli. Endogenous MOR28 axons normally target four glomeruli per mouse, one lateral (Fig. 6A) and one medial (not shown) in each OB. In TO28 mice, the endogenous MOR28 axons continue to form four wildtype MOR28 glomeruli that are roughly the same size and in the same location as before, though they are often co-innervated by TO28 axons (Fig. 6B). Strikingly, endogenous MOR28 axons also now form supernumerary glomeruli along with TO28 axons (Fig. 6C). We have observed 0-3 supernumerary glomeruli in the vicinity of any given wildtype MOR28 glomerulus. An average of 3-5 supernumerary glomeruli were observed in a given mouse, with no significant difference seen between TO28L and TO28H (Fig. 6D). TO28 expression seems to cause these supernumerary glomeruli in a cell non-autonomous manner since the endogenous MOR28 axons are not lacZ-positive and therefore not expressing the transgene themselves. We hypothesize that supernumerary glomeruli are the result of ectopic glomeruli located near the wildtype MOR28 glomeruli which recruit endogenous MOR28 axons from their normal target, and so we have called these rerouted glomeruli. Notably, glomeruli formed by other

endogenous ORs were not co-innervated by TO28 axons (Fig. 4I,J). Perhaps rerouted glomeruli are the result of homotypic attractions and can only be formed by axons expressing the same OR as the transgene.

If rerouted glomeruli are the result of ectopic glomeruli recruiting endogenous MOR28 axons, we would expect to see all rerouted glomeruli located closer to the wildtype MOR28 glomerulus than the nearest ectopic glomerulus. We measured the distance from each rerouted glomerulus to its wildtype glomerulus, and we compared this to the distance from the wildtype glomerulus to the closest ectopic glomerulus. In 27 out of 33 comparisons, the rerouted glomeruli were indeed closer to the wildtype MOR28 glomerulus (Fig. 6E). The remaining 6 comparisons where the ectopic glomeruli were closer may due to the fact that different intensities of MOR28 were observed in ectopic glomeruli (Fig. 5). Perhaps these ectopic glomeruli did not express enough MOR28 protein to induce homotypic attraction and rerouting. Alternatively, these ectopic glomeruli may have been located in an area of the OB that is not passed by endogenous MOR28 axons. Homotypic attraction in this case would be precluded since it is a contact-mediated mechanism. It is noteworthy that rerouted glomeruli were not always found within an absolute radius from the wildtype MOR28 glomerulus. Since the locations of ectopic glomeruli are highly variable, this observation is consistent with the hypothesis that rerouted glomeruli are a subset of ectopic glomeruli that are located near wildtype MOR28 glomeruli and not targets with predetermined locations.

Changing the identity and concentration of an OR at the axon tip does not affect axonal guidance

The recruitment of endogenous MOR28 axons to rerouted glomeruli could conceivably occur through two distinct mechanisms. As mentioned previously, homotypic attractions between the axons of transgenic and endogenous MOR28 axons could drag the endogenous MOR28 axons to nearby glomeruli. The other possible mechanism is that when transgenic MOR28 axons coalesce into a glomerulus, the glia and post-synaptic cells involved in defining the neuropil structure are indelibly imprinted or marked for innervation from MOR28 axons. These non-OSN cells could then be responsible for actively recruiting endogenous MOR28 axons to cause rerouting. Homotypic attractions are only proposed to occur between OSNs so they would not be involved in this latter mechanism.

Homotypic attraction can be broken down further into different models. First, OR proteins themselves interact between OSN axons to form adhesion complexes. Second, OR proteins could bind to adapter molecules on the cell membrane that then directly mediate adhesion. Third, the intrinsic activation or basal activity of OR proteins could affect the expression of other guidance cues that then act independently of ORs to cause homotypic attraction. All of these models predict that homotypic attractions are sensitive to the identity and/or concentration of the OR expressed by an axon. For example, if a second OR were co-expressed in an OSN, it would dilute the number of sites where the original OR interacts with another axon or adapter molecules. Similarly, if there were less of the original OR in an OSN, there would be less intrinsic activation and therefore

altered expression of the other guidance cues. This prediction is strengthened by the observation that introducing an IRES sequence to the coding region of M71 decreases OR expression by ten-fold and causes these OSNs to form glomeruli in novel locations (Feinstein and Mombaerts, 2004; Serizawa et al., 2000).

We changed both the identity and concentration of MOR28 OSNs by expression of the MOR28-IRES-C6 allele, which drives the co-expression of C6 in OSNs that normally express MOR28 (Fig. 7A). First, we verified that this knock-in approach drives OR co-expression, a strategy that had yet to be successfully implemented in the field (Nguyen et al., 2007). In a MOR28-IRES-C6 heterozygote we observed roughly 50% of the OSNs that stained positive for MOR28 also stained positive for C6 (Fig. 7B), indicating not only successful co-expression, but also that the allele was chosen at the same frequency as the unmodified wildtype MOR28 allele. Next, we examined the zonal expression of the MOR28-IRES-C6 OSNs. OSNs expressing both MOR28 and C6 were perfectly intermingled with wildtype MOR28 OSNs (Fig. 7C). In fact, the two MOR28-positive populations were identical in all parameters examined within the MOE, including the intensity of MOR28 staining. Within the C6 zone of expression we also verified that the frequency, distribution, and staining intensity of wildtype C6 OSNs were not affected by expression of the MOR28-IRES-C6 allele (Fig. 7D). Finally, we examined whether the modified allele affected the mechanisms that normally ensure OR expression from a single allele. We stained for M50, an OR that is expressed within the MOR28 zone, and never saw co-labeling in the MOR28-IRES-C6 OSNs (Fig. 7E,F).

Similar to MOR28, expression of C6 also causes OSNs to converge on four glomeruli per mouse (representative glomeruli shown in Fig. 8A,B). In the OB of MOR28-IRES-C6 homozygotes, the MOR28-IRES-C6 axons formed discrete glomeruli where the MOR28 glomeruli are normally found (Fig. 8D). Indeed, in MOR28-IRES-C6 heterozygotes the MOR28-IRES-C6 OSNs and wildtype MOR28 OSNs co-innervated the same glomerulus, strongly indicating that this is the glomerulus normally targeted by MOR28 (Fig. 8F). We noticed that within the glomerulus the MOR28-IRES-C6 axons were segregated from wildtype MOR28 axons. This appears to be caused by an altered expression of other guidance proteins such as Neuropilin 1 in the MOR28-IRES-C6 axons (Fig. 8G). However, this is also similar to the degree of separation seen between the maternal and paternal alleles of MOR28 as distinguished by expression of the reporter genes GFP and lacZ (Fig. 8H) so the separation of MOR28-IRES-C6 may also be the result of expression from a different allele. No MOR28-IRES-C6 axons were found in or around the C6 glomeruli (Fig. 8C,E). Since MOR28 and C6 OSNs are normally located in disparate zones of the MOE, the OSNs that express MOR28-IRES-C6 normally do not express C6 and so are subject to different guidance cues than wildtype C6 OSNs.

Importantly, the intensity of MOR28 staining was decreased in the MOR28-IRES-C6 axons. This is surprising, considering that the staining intensity in the MOE was the same as in wildtype MOR28 OSNs. Regardless of the mechanism underlying this phenomenon, we could now generate MOR28 OSNs that were modified in both the concentration as well as the identity of the expressed ORs. We generated mice expressing this allele as well as TO28L to see if the MOR28-IRES-C6 axons would exhibit different levels of homotypic attraction and thus be differentially recruited to rerouted glomeruli.

We observed that MOR28-IRES-C6 and wildtype MOR28 axons were equally represented in both wildtype and rerouted glomeruli (Fig. 9A-C). These results were not what we expected if homotypic attractions are involved in forming rerouted glomeruli. However, our assumption that homotypic attraction is sensitive to OR concentration and identity may have been wrong so we do not interpret this finding to conclusively indicate that homotypic attractions are not involved in forming rerouted glomeruli. Furthermore, the fact that MOR28-IRES-C6 and wildtype MOR28 axons have the same phenotype indicates that changing the OR concentration and identity can have little effect on the axonal guidance of OSNs.

DISCUSSION

In this chapter we characterized the genetic strategy that will be used in the next chapter to assay the axonal guidance of OSNs in adulthood. Using the transgene TO28 we were able to successfully express transgenic MOR28 and a lacZ reporter in both the cell bodies and axon tips of 1-5% of the OSNs in the MOE. Curiously, TO28 expression decreased the number of OSNs expressing endogenous chemoreceptors by more than 50%. This is the first evidence that relatively low transgenic OR expression can have such a drastic effect on the expression of other ORs. Although Fleischmann et al. noted a 20-fold decrease in endogenous OR expression, their transgene was expressed in >95% of OSNs and it was assumed that endogenous ORs simply shut off due to the mechanisms ensuring expression of a single OR allele (Fleischmann et al., 2008). Nguyen et al. published transgenes that were expressed in 10-30% of OSNs but they did not report the frequency of endogenous OR expression in these mice (Nguyen et al., 2010; Nguyen et al., 2007).

We discovered an increased number of apoptotic OSNs in our TO28 animals, suggesting that the drastic decrease in endogenous OR expression is due to OSNs dying when the transgene is induced. This was unexpected, given that Fleischmann et al. did not observe an increase in apoptosis in their transgenic mice (Fleischmann et al., 2008). We also saw the same trend when we repeated the TUNEL staining that Fleischmann et al. used to assay for apoptotic cells (data not shown). It is possible that the expression of different OR transgenes is not equal. The integration of our TO28 cassettes into the genome may have disrupted nearby genes in such a way that TO28 expression increases

the likelihood of cell death. The transgene used by Fleischmann et al. may have integrated into a relatively gene-sparse locus, causing less disruption and allowing it to be expressed in >95% of OSNs. The apoptosis results indicate that TO28 is initially expressed in a larger fraction of OSNs but most of these die, leaving the 1-5% that we observe actively expressing TO28 in the two founder lines.

Next we examined the axonal projections of the TO28 OSNs that did not undergo apoptosis. We found that these neurons formed ectopic glomeruli in random locations throughout the OB. They resemble the glomeruli formed by OR minigenes and other OR transgenes (Fleischmann et al., 2008; Nguyen et al., 2010; Nguyen et al., 2007; Vassalli et al., 2002). The mechanism underlying the formation of these ectopic glomeruli has not been described. Presumably OSNs begin expressing an OR and initiate axonal outgrowth based on the signals that roughly map the dorsomedial-ventrolateral axis in the MOE onto the dorsal-ventral axis in the OB. OMP begins to be expressed late in this outgrowth stage, which induces TO28 expression, which in turn causes many OSNs to undergo apoptosis. The difference between the OSNs that die versus the OSNs that survive may also be due to the timing of TO28 expression. Perhaps the OSNs that die were the ones that had already targeted a glomerulus by the time that TO28 turned on. Activity-dependent competition would identify these TO28 axons as "targeting mistakes" since they do not express the same OR as the other axons within the glomerulus. Cell death would be induced by the mechanisms that underlie the "one receptor per glomerulus" rule. In contrast, the OSNs that survive may express TO28 earlier, before synaptogenesis, which allows them to respond to guidance cues mediated by transgenic MOR28. However, they must do so from wherever the axonal growth cone was located at the time

OMP induced TO28 expression. Since the 1-5% of OSNs that stably express TO28 are scattered randomly in the MOE, the locations of the growth cones when they switch to TO28 expression are probably also random. These locations then influence the last step of axonal guidance, the convergence of OSNs that now express the same transgenic MOR28. Since these glomeruli consist only of MOR28 axons, the axons do not break the "one receptor per glomerulus" rule and they are not induced to undergo apoptosis

Regardless of the mechanisms that determine ectopic glomeruli formation and placement, they also appear to cause the endogenous MOR28 axons to be recruited into rerouted glomeruli. Vassalli et al. also reported that expression of M71 and MOR23 from their minigenes caused axons expressing endogenous M71 and MOR23 to form supernumerary glomeruli (Vassalli et al., 2002). These observations suggest the involvement of homotypic attractions between axons expressing the same OR, so we attempted to provide definitive evidence for homotypic attraction by assaying the axonal guidance of OSNs expressing MOR28-IRES-C6. We designed this experiment assuming that OR identity and concentration would affect the strength of homotypic attractions between OSNs. While MOR28-IRES-C6 axons successfully co-expressed C6 and decreased MOR28 protein concentration, they were not differentially recruited to rerouted glomeruli. We do not interpret these results to exclude the contribution of homotypic attractions in the formation of rerouted glomeruli. We could have been wrong in our assumption that adding C6 or changing MOR28 concentration at the axon tip would alter homotypic attraction. Perhaps the presence of any MOR28 on an axon is sufficient to mediate homotypic attraction. The expression of C6 may also have compensated for the decrease in MOR28. Alternatively, the equal representation of

MOR28-IRES-C6 within rerouted glomeruli could truly indicate that homotypic attractions do not cause rerouting. In this case, recruitment to the rerouted glomeruli could be mediated by the glia and post-synaptic neurons that interact with OSNs within the neuropil. Innervation from OSNs expressing a specific OR could mark these cells to recruit only the same type of OSNs in the future.

One of the mouse lines currently being developed by our lab could be used to distinguish between these two possibilities. The lox-MOR28-lox-M71-IRES-mCherry allele (Cre-out MOR28 or CO28) normally should not affect endogenous MOR28 expression (Fig. 10A). However, activation of Cre recombinase will cause these axons to turn off MOR28 and express the odorant receptor M71 as well as the reporter mCherry. Our experiment would consist of generating mice expressing TO28, an olfactory-specific CreER (OMP-IRES-CreER, Cre recombinase fused to the estrogen receptor expressed in all OSNs, Fig. 10B), and also homozygous for CO28. These mice would be allowed to form rerouted glomeruli and reach adulthood. Then we would begin the mice on a dox regimen to silence current and future TO28 expression. Simultaneously we would administer tamoxifen such that CreER would be activated in all CO28 axons, causing them to switch to express M71. Since OMP is only expressed by mature OSNs, this would activate Cre recombinase in only the axons that have already innervated the OB. In this way we would remove all MOR28 protein from the rerouted glomeruli, either by turning off TO28 or switching CO28. These would now be M71 glomeruli that were once innervated by MOR28 axons. We could examine these glomeruli with electron microscopy to ensure that MOR28 protein was completely removed from the axon tips. New CO28 axons born after tamoxifen administration would distinguish whether the

OSNs or the glia and post-synaptic cells were responsible for forming rerouted glomeruli. These OSNs would have arisen from precursor cells that did not express OMP at the time of tamoxifen expression, so they would express MOR28 from the CO28 allele. If homotypic attractions from OSNs are involved, the MOR28-expressing CO28 axons would not be recruited to the rerouted glomeruli since there would be no homotypic attractions between them and the M71-expressing CO28 axons there (Fig. 10Ca). Alternatively, if the glia and post-synaptic cells were marked for MOR28-expressing axons, the MOR28-expressing CO28 axons would continue to be recruited to rerouted glomeruli (Fig. 10Cb).

We do not predict that the glia and post-synaptic cells are responsible for forming rerouted glomeruli. The current model of axonal guidance in OSNs posits that axon-axon interactions are the major determinant of glomerular formation. In fact, normal guidance occurs in the absence of post-synaptic cells (Bulfone et al., 1998). Furthermore, reconstitution of the glomerular map after a massive lesion requires the preservation of at least a small population of OSNs. For example, normal axonal guidance was restored when 95% of OSNs were genetically ablated (Gogos et al., 2000) but not when 100% of the OSNs were ablated by dichlobenil (St John and Key, 2003). The glomerular map is also not restored after 100% of OSNs are ablated via axotomy but these results may be confounded by the scarring caused by nerve transection (Christensen et al., 2001; Costanzo, 2000). Moreover, some glomeruli are transiently heterogeneous during early development, being co-innervated by OSNs expressing different ORs (Zou et al., 2004). If glia and post-synaptic cells were marked during this time, they would recruit more than one population of OSNs later in life.

Although we have not fully addressed the question of how rerouted glomeruli are formed, we do know that they are the consequence of a cell non-autonomous effect on axonal guidance that is caused by TO28 expression. We will use them in the next chapter as an assay for addressing adult-specific mechanisms of axonal guidance.

However, the experiments described in this chapter can also serve as a foundation for studying other aspects of axonal guidance. No studies have been able to directly address the involvement of OR-mediated heterotypic repulsion between the axons of OSNs. Transgenic ORs were never reported to be co-expressed with endogenous ORs so when transgenic axons targeted new glomeruli, mechanisms such as homotypic attraction from the transgenic OR could easily explain this phenotype. However, our MOR28-IRES-C6 allele successfully causes MOR28 axons to also express C6. These axons coalesce into discrete glomeruli, suggesting that heterotypic repulsions between MOR28 and C6 are negligible, at least in comparison with any homotypic attractions mediated by MOR28 or C6. We are currently developing mice expressing C6-IRES-MOR28 from the MOR28 locus to ensure that the phenotype of MOR28-IRES-C6 OSNs is not due to decreased expression of the OR downstream of IRES. We expect to observe that C6-IRES-MOR28 and MOR28-IRES-C6 will have the same phenotype since decreasing MOR28 concentration did not affect axonal guidance. Heterotypic repulsions are known to be involved in the dorsoventral positioning of glomeruli but perhaps there is no role for heterotypic repulsion between different ORs.

We are also developing mice expressing C6-IRES-MOR28 from the C6 locus. Endogenous C6 OSNs are normally located in a zone distant from the MOR28 zone,

suggesting that C6 OSNs are a different subtype than MOR28 OSNs. Accordingly, C6 glomeruli are normally located in an area of the OB distant from the MOR28 glomeruli. We will cross these mice to TO28 mice. If C6-IRES-MOR28 OSNs also form rerouted glomeruli near the C6 glomeruli, this would be strong evidence that rerouted glomeruli are formed through homotypic interaction mediated by the MOR28 protein.

We observed that the MOR28-IRES-C6 axons in our experiment expressed less Neuropilin 1 than the wildtype MOR28 axons. Neuropilin 1 is classified as a type I guidance molecule that has been proposed to function in the global axonal guidance cues that determine the position of a glomerulus on the anteroposterior and mediolateral axes in the OB (Imai et al., 2006; Schwarting et al., 2004). However, the decreased expression of Neuropilin 1 did not prevent the MOR28-IRES-C6 axons from co-innervating the MOR28 glomerulus with the wildtype MOR28 axons. It appears that the mechanisms governing the convergence of axons into glomeruli may override some of the guidance cues that determine the location of the glomerulus. Similar to the retinotopic map where axon-axon interactions override the cues from cell-autonomous Eph/ephrin signaling, there may be hierarchies within the mechanisms governing the formation of the glomerular map.

The MOR28-IRES-C6 allele could also inform on aspects of the olfactory system that are not directly related to axonal guidance. Remarkably, MOR28-IRES-C6 axons displayed a decreased staining intensity for both MOR28 and C6 when compared to the axons expressing the cognate wildtype ORs. This decrease was specific to the axons since the staining of the cell bodies of these same neurons was indistinguishable from wildtype

OSNs. Perhaps a limited amount of OR protein is allowed to be transported, locally translated, or packed into the membrane of axon tips. To distinguish limited mRNA transport from other possible explanations, we plan to perform laser capture microscopy on MOR28-IRES-C6 heterozygotes and compare the amount of OR mRNA in MOR28-IRES-C6 versus wildtype MOR28 axons.

The TO28 transgene can also be used to examine the mechanisms that ensure monoallelic expression of ORs because we and other labs have observed that expression of transgenic ORs is almost always mutually exclusive with the expression of endogenous ORs (Fleischmann et al., 2008; Nguyen et al., 2007; Serizawa et al., 2000). In a paper currently under review, our collaborators have shown that TO28 can ectopically induce a gene in the pathway that transcriptionally silences other OR alleles (Lyons et al., in review). These results indicate that the OR protein is a signal that feeds into the monoallelic regulation of ORs, even when it is encoded on a transgene.

Finally, the multiple MOR28 glomeruli that we observed in our TO28 mice could be used in behavior studies to study how glomerular number impacts olfactory processing. Fleischmann et al. found that mice expressing M71 in >95% of OSNs were less able to detect the M71 odorant acetophenone, perhaps because such high expression over-saturates the system (Fleischmann et al., 2008). The ectopic glomeruli we quantified comprise only 1-5% of the total glomeruli in the OB and may therefore sensitize mice to MOR28 ligands. Another graduate student in the lab is currently searching for the MOR28 ligand to facilitate these behavior studies. In conclusion, the work described in

this chapter not only enables work for the rest of my thesis but also serves as a starting point for studying other exciting aspects of the olfactory system.

REFERENCES

Bertram, R., and Hillen, W. (2008). The application of Tet repressor in prokaryotic gene regulation and expression. Microb Biotechnol *1*, 2-16.

Bulfone, A., Wang, F., Hevner, R., Anderson, S., Cutforth, T., Chen, S., Meneses, J., Pedersen, R., Axel, R., and Rubenstein, J. (1998). An olfactory sensory map develops in the absence of normal projection neurons or GABAergic interneurons. Neuron *21*, 1273-1282.

Christensen, M., Holbrook, E., Costanzo, R., and Schwob, J. (2001). Rhinotopy is disrupted during the re-innervation of the olfactory bulb that follows transection of the olfactory nerve. Chem Senses *26*, 359-369.

Clowney, E.J., LeGros, M.A., Mosley, C.P., Clowney, F.G., Markenskoff-Papadimitriou, E.C., Myllys, M., Barnea, G., Larabell, C.A., and Lomvardas, S. (2012). Nuclear aggregation of olfactory receptor genes governs their monogenic expression. Cell *151*, 724-737.

Costanzo, R. (2000). Rewiring the olfactory bulb: changes in odor maps following recovery from nerve transection. Chem Senses *25*, 199-205.

Feinstein, P., and Mombaerts, P. (2004). A contextual model for axonal sorting into glomeruli in the mouse olfactory system. Cell *117*, 817-831.

Fleischer, J., and Breer, H. (2010). The Grueneberg ganglion: a novel sensory system in the nose. Histol Histopathol *25*, 909-915.

Fleischer, J., Breer, H., and Strotmann, J. (2009). Mammalian olfactory receptors. Front Cell Neurosci *3*, 9.

Fleischmann, A., Shykind, B., Sosulski, D., Franks, K., Glinka, M., Mei, D., Sun, Y., Kirkland, J., Mendelsohn, M., Albers, M., *et al.* (2008). Mice with a "monoclonal nose:" perturbations in an olfactory map impair odor discrimination. Neuron *60*, 917-926.

Gogos, J., Osborne, J., Nemes, A., Mendelsohn, M., and Axel, R. (2000). Genetic ablation and restoration of the olfactory topographic map. Cell *103*, 609-620.

Imai , T., Suzuki, M., and Sakano, H. (2006). Odorant receptor-derived cAMP signals direct axonal targeting. Science *314*, 657-661.

Lyons, D., Allen, W., Goh, T., Tsai, L., Barnea, G., and Lomvardas, S. (in review). An epigenetic trap stabilizes singular olfactory receptor expression. Cell.

Mombaerts, P. (2006). Axonal wiring in the mouse olfactory system. Annu Rev Cell Dev Biol *22*, 713-737.

Mori, K., and Sakano, H. (2011). How is the olfactory map formed and interpreted in the mammalian brain? Annu Rev Neurosci *34*, 467-499.

Nguyen, M., Marks, C., Belluscio, L., and Ryba, N. (2010). Early Expression of Odorant Receptors Distorts the Olfactory Circuitry. J Neuroscei *3*-, 9271-9279.

Nguyen, M., Zhou, Z., Marks, C., Ryba, N., and Belluscio, L. (2007). Prominent roles for odorant receptor coding sequences in allelic exclusion. Cell *131*, 1009-1017.

Qasba, P., and Reed, R. (1998). Tissue and zonal-specific expression of an olfactory receptor transgene. J Neurosci *18*, 227-236.

Rogers, K., Dasgupta, P., Gubler, U., Grillo, M., Khew-Goodall, Y., and Margolis, F. (1987). Molecular cloning and sequencing of a cDNA for olfactory marker protein. Proc Natl Acad Sci *84*, 1704-1708.

Schwarting, G.A., Raitcheva, D., Crandall, J.E., Burkhardt, C., and Puschel, A.W. (2004). Semaphorin 3A-mediated axon guidance regulates convergence and targeting of P2 odorant receptor axons. Eur J Neurosci *19*, 1800-1810.

Serizawa, S., Ishii, T., Nakatani, H., Tsuboi, A., Nagawa, F., Asano, M., Sudo, K., Sakagami, J., Sakano, H., Ijiri, T., *et al.* (2000). Mutually exclusive expression of odorant receptor transgenes. Nat Neurosci *3*, 687-693.

Serizawa, S., Miyamichi, K., Nakatani, H., Suzuki, M., Saito, M., Yoshihara, Y., and H, S. (2003). Negative feedback regulation ensures the one receptor-one olfactory neuron rule in mouse. Science *302*, 2088-2094.

St John, J., and Key, B. (2003). Axon mis-targeting in the olfactory bulb during regeneration of olfactory neuroepithelium. Chem Senses *28*, 773-779.

Vassalli, A., Rothman, A., Feinstein, P., Zapotocky, M., and Mombaerts, P. (2002). Minigenes impart odorant receptor-specific axon guidance in the olfactory bulb. Neuron *35*, 681-696.

Yu, C., Power, J., Barnea, G., O'Donnell, S., Brown, H., Osborne, J., Axel, R., and Gogos, J. (2004). Spontaneous neural activity is required for the establishment and maintenance of the olfactory sensory map. Neuron *42*, 553-566.

Zou, D.J., Feinstein, P., Rivers, A.L., Mathews, G.A., Kim, A., Greer, C.A., Mombaerts, P., and Firestein, S. (2004). Postnatal refinement of peripheral olfactory projections. Science *304*, 1976-1979.

FIGURES

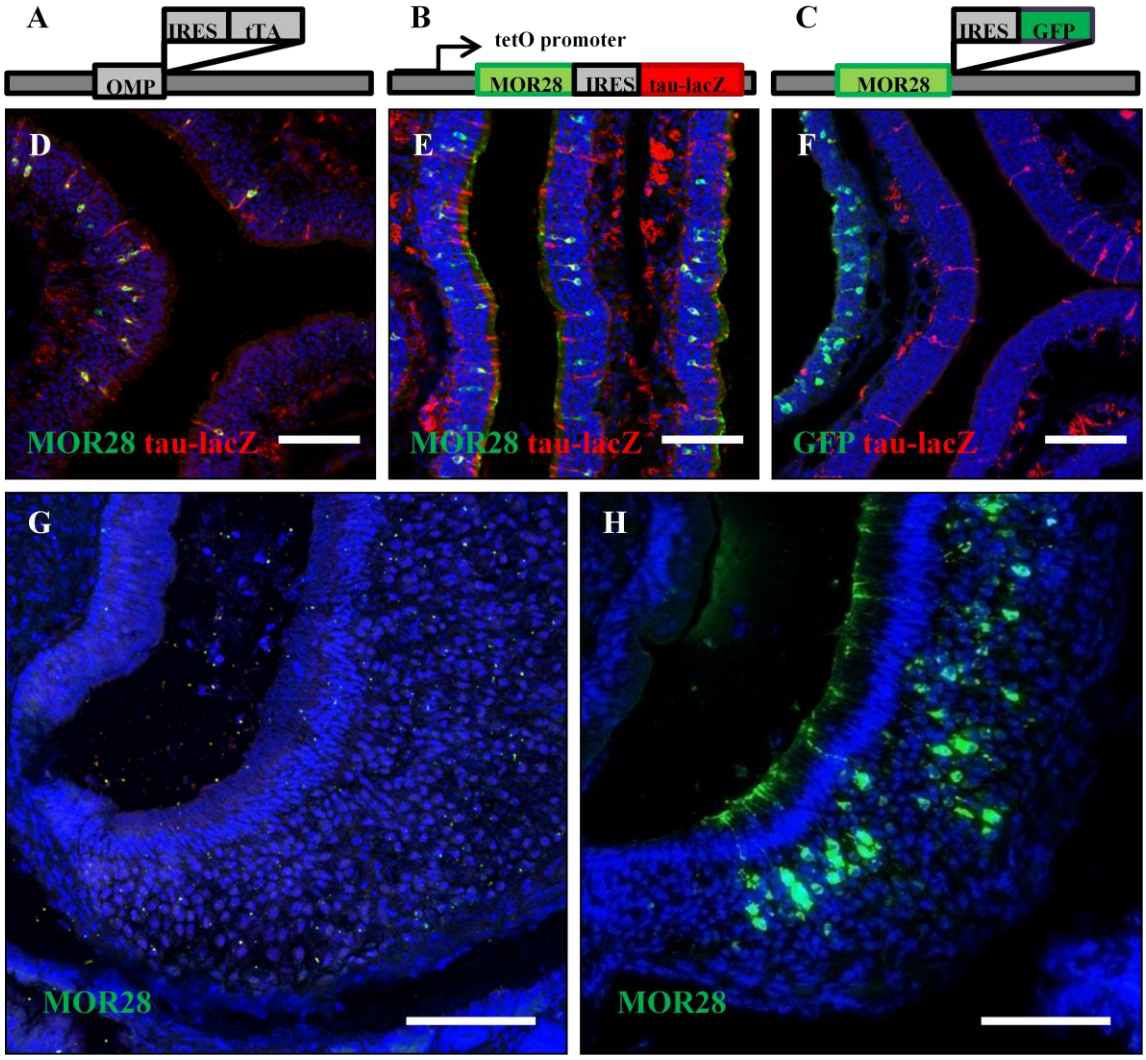

Figure 1. Transgenic MOR28 is expressed throughout the olfactory system.

A-C) The alleles used to drive and distinguish transgenic MOR28. **A)** OMP-IRES-tTA, drives synthetic transcriptional activator expression in all OSNs. **B)** tetO::MOR28-IRES-tau-lacZ (TO28), drives transgenic MOR28 and tau-lacZ expression in the presence of tTA. **C)** MOR28-IRES-GFP, drives GFP in all neurons expressing endogenous MOR28. **D-H)** Coronal sections of MOE and VNO immunohistochemically stained for the proteins indicated. **D,E)** Mice expressing TO28L and TO28H, respectively, express both MOR28 and lacZ at different frequencies in non-MOR28 zones of the MOE. **F)** Mouse bearing the three alleles described in A-C expresses transgenic MOR28 ubiquitously without affecting the zonal expression of endogenous MOR28. **G)** MOR28 protein is not normally expressed in the VNO of a wildtype mouse. **H)** Transgenic MOR28 is expressed in the apical layer of the VNO in mice expressing TO28L. Scale bars, 100 μm.

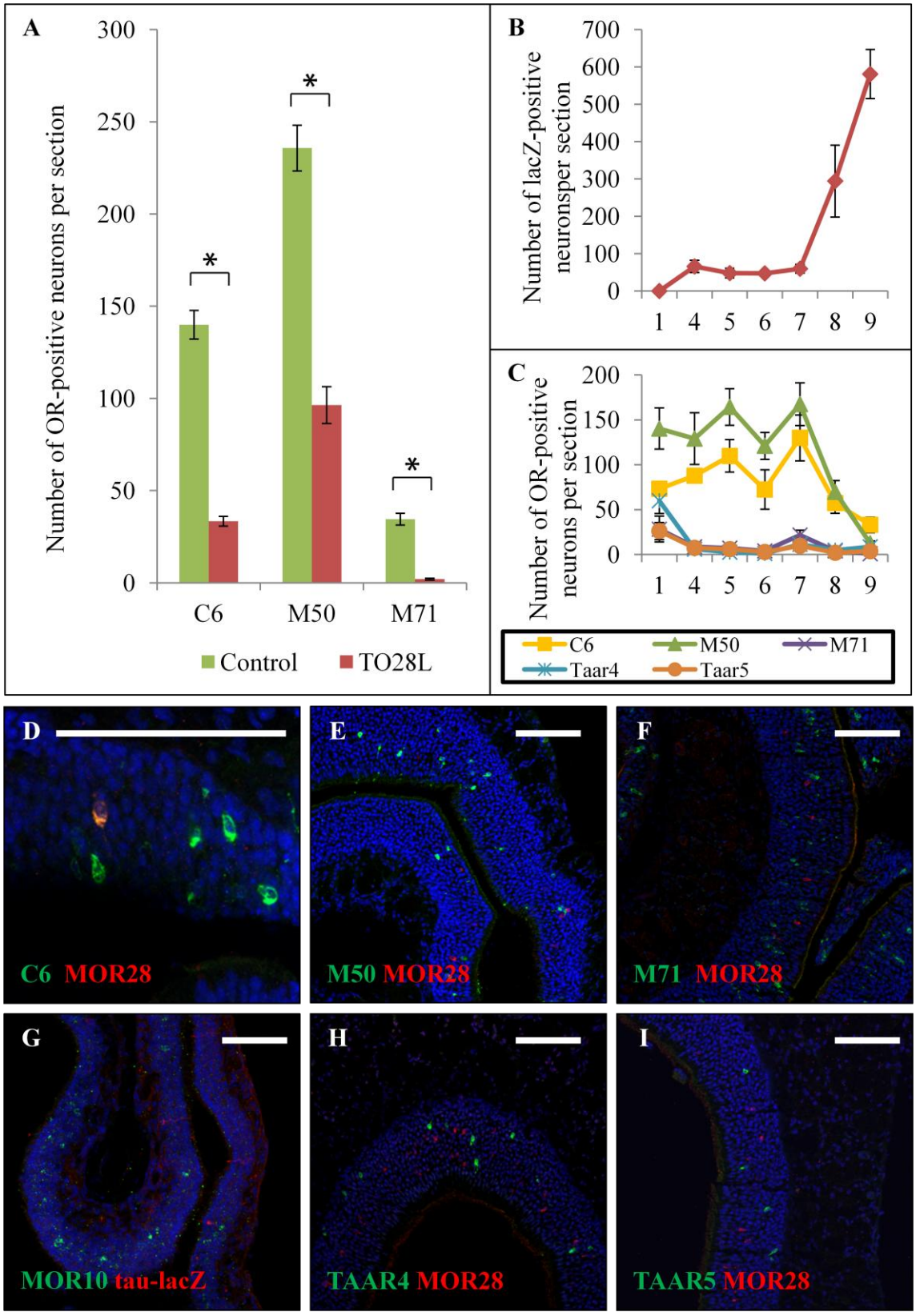

Figure 2. (legend continued on next page)

Figure 2. TO28 affects the expression of other endogenous ORs.

A) The number of OSNs expressing endogenous ORs is decreased by more than 50% when TO28 is expressed. ($p < 0.050$. Error bars show standard error.) **B,C)** TO28 expression increases several weeks after being silenced with dox. The x-axis is the number of weeks after the last dose of dox, error bars show standard deviation. The number OSNs expressing endogenous ORs is always inversely related to the number of OSNs expressing lacZ. **D-I)** Coronal sections of MOE immunohistochemically stained for the proteins indicated, with the exception of MOR10, which was visualized with *in situ* hybridization. TO28 is rarely co-expressed with endogenous ORs or TAARs (C6: 3/614; M50: 0/2395; M71: 0/37; M10: 0/360; TAAR4: 0/1022; TAAR5: 0/350). The transgenic animals used for these experiments came from the TO28L founder line. Scale bars, 100 μm.

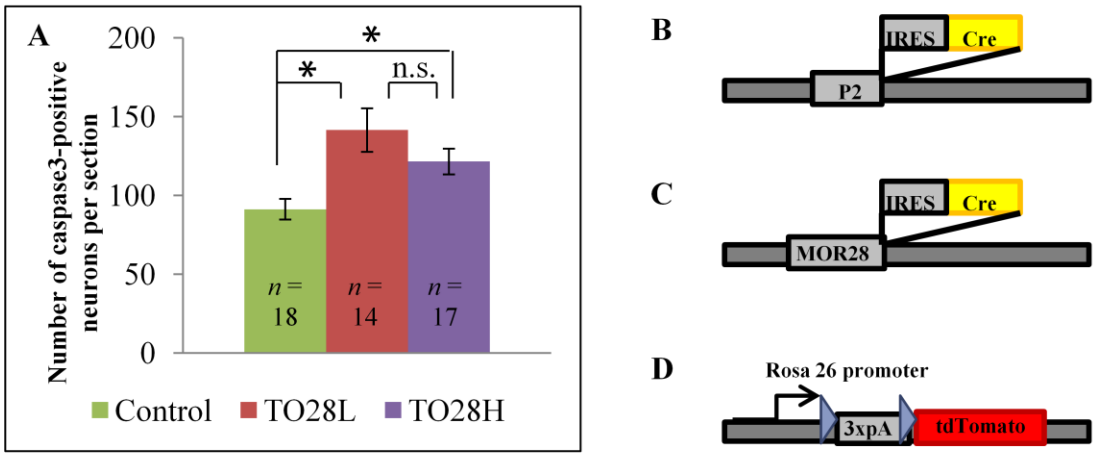

Table 1	**OSNs actively expressing Cre** (Cre+,tdTomato+)	**OSNs that have switched** (Cre-,tdTomato+, lacZ-)	**TO28 OSNs that have switched** (Cre-, tdTomato+, lacZ+)
tdTomato; P2iCre; OMPitTA TO28L	43	906	8
tdTomato; MOR28iCre; OMPitTA TO28L	834	9739	9

Figure 3. TO28 causes OSNs to undergo apoptosis instead of shutting off endogenous ORs.

A) The number of apoptotic OSNs is significantly increased in TO28 mice. ($p < 0.050$. Error bars show standard error.) **B,C)** P2-IRES-Cre and MOR28-IRES-Cre, drives Cre recombinase in all neurons expressing endogenous P2 or MOR28, respectively. **D)** R26RtdTomato, a Cre reporter that will irreversibly express tdTomato if co-expressed with Cre recombinase. **Table 1)** Quantification of OSNs immunohistochemically stained for the proteins indicated. Many OSNs switch off endogenous P2 or MOR28 but few of these co-express TO28. (n = 2 mice for tdtomato; P2iCre; OMPitTA; TO28L; n = 1 mouse for tdtomato; MOR28iCre; OMPitTA; TO28L)

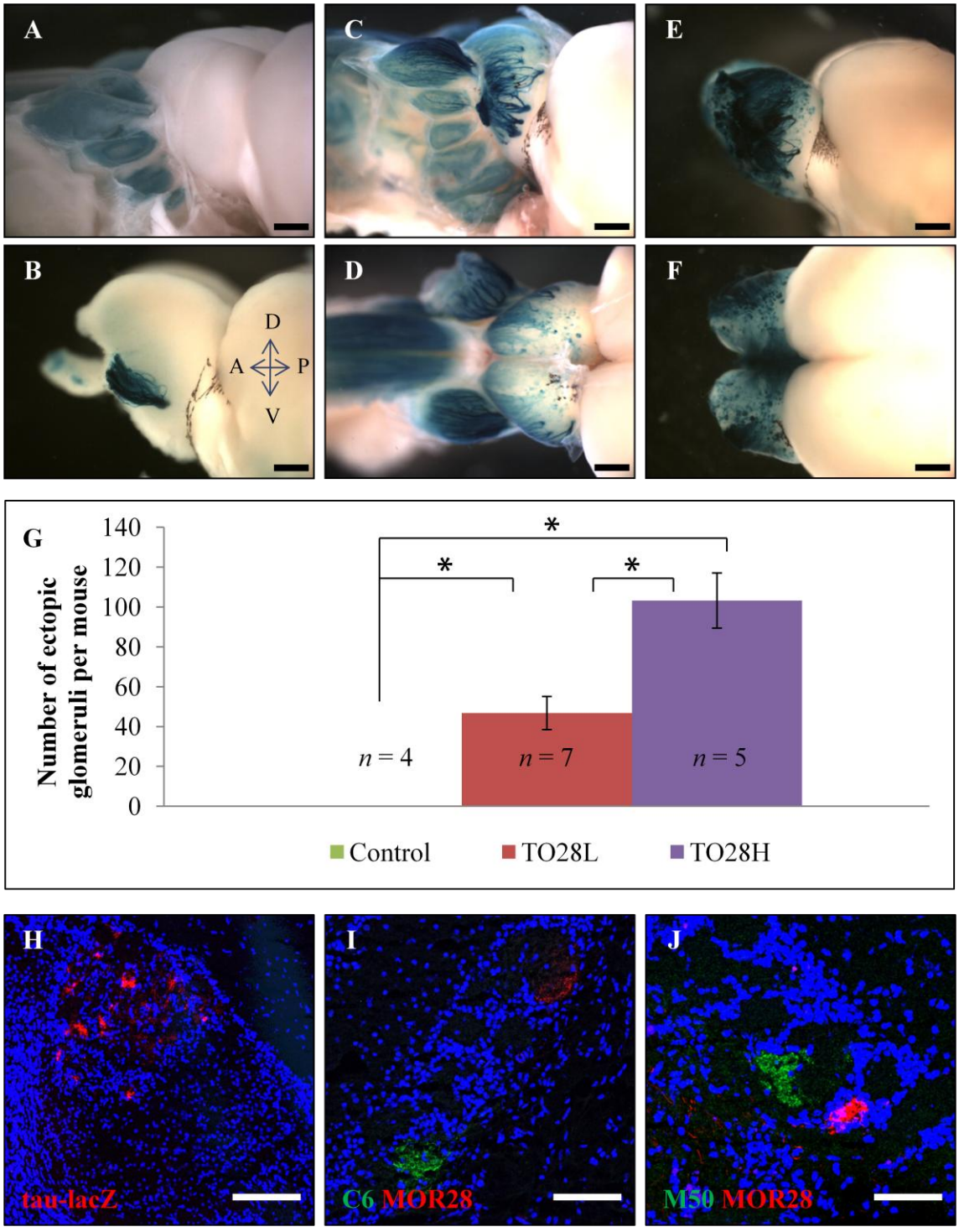

Figure 4. (legend continued on next page)

Figure 4. TO28 OSNs form ectopic glomeruli throughout the OB.

A-F) Whole mounts stained with X-gal to visualize TO28 OSNs. **A)** Sagittal view of a control expressing only MOR28-IRES-GFP. Diffuse background staining can be observed in the MOE. **B)** Sagittal view of a control expressing MOR28-IRES-tau-lacZ; X-gal staining indicates where the endogenous MOR28 OSNs normally form lateral glomeruli. A second glomerulus is located on the medial face of the OB (not shown). **C,D)** Sagittal and dorsal views of a mouse expressing TO28L. **E,F)** Sagittal and dorsal views of a mouse expressing TO28H. Ectopic glomeruli are distributed throughout the OB in a random manner that is not conserved even between the two OBs in a given mouse. **G)** Ectopic glomeruli are only found in mice expressing TO28 and there are significantly more in mice expressing TO28H versus TO28L. ($p < 0.050$. Error bars show standard error.) **H-I)** Coronal sections of the AOB and OB immunohistochemically stained for the proteins indicated. **H)** Ectopic glomeruli were observed throughout the AOB. **I,J)** Ectopic glomeruli were often observed in the vicinity of glomeruli targeted by endogenous C6 or M50 but TO28 axons did not co-innervate these glomeruli. Scale bars for A-F 1 mm. Scale bars for H-J 100 μm.

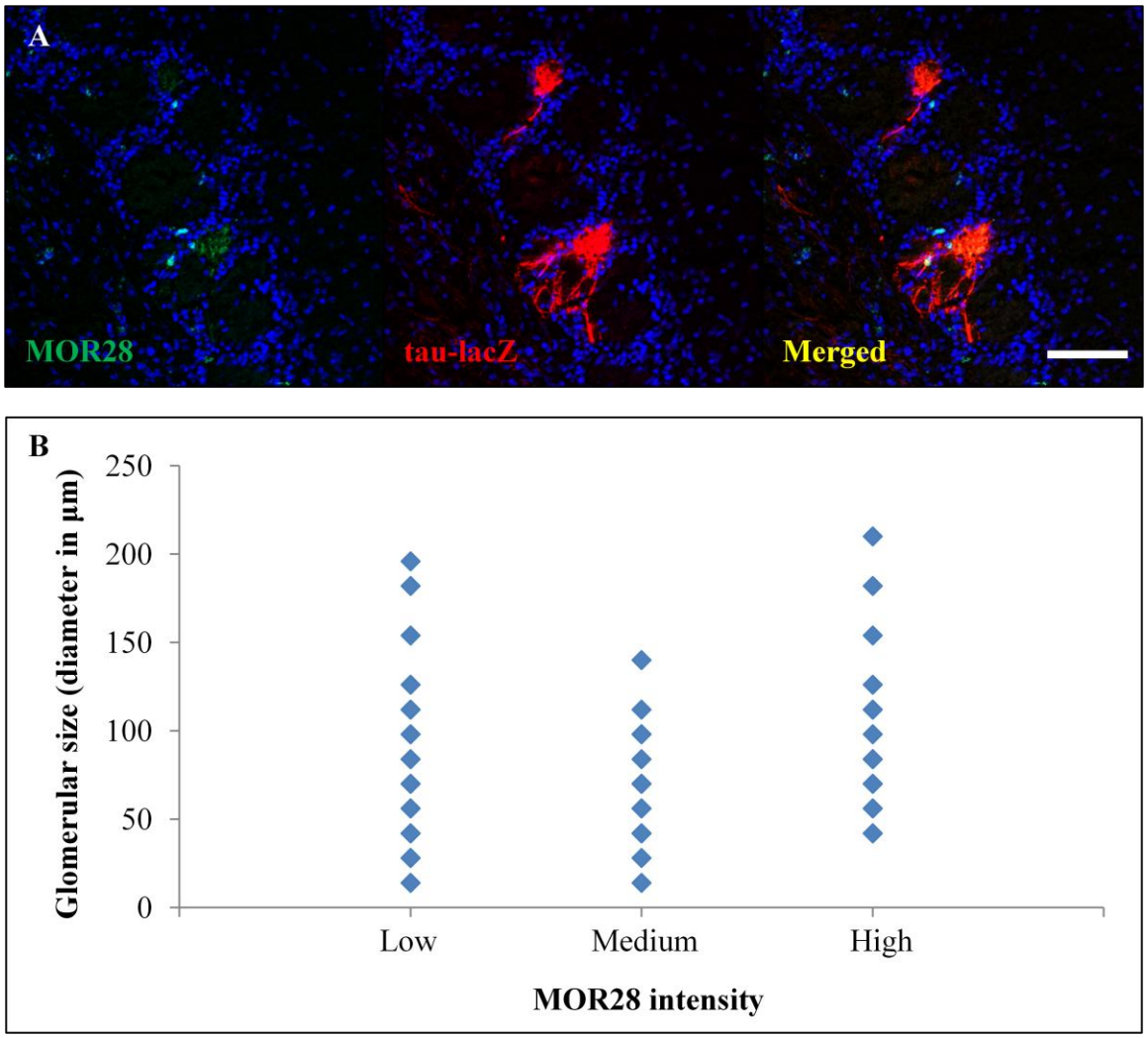

Figure 5. The size and MOR28 intensity vary independently in ectopic glomeruli.

A) Coronal section of the OB immunohistochemically stained for the proteins indicated. Representative ectopic glomeruli exhibiting different sizes and MOR28 intensity. **B)** Comparison of the size and MOR28 intensity of all ectopic glomeruli in a representative TO28L mouse. These two parameters varied independently of each other. Scale bars, 100 µm.

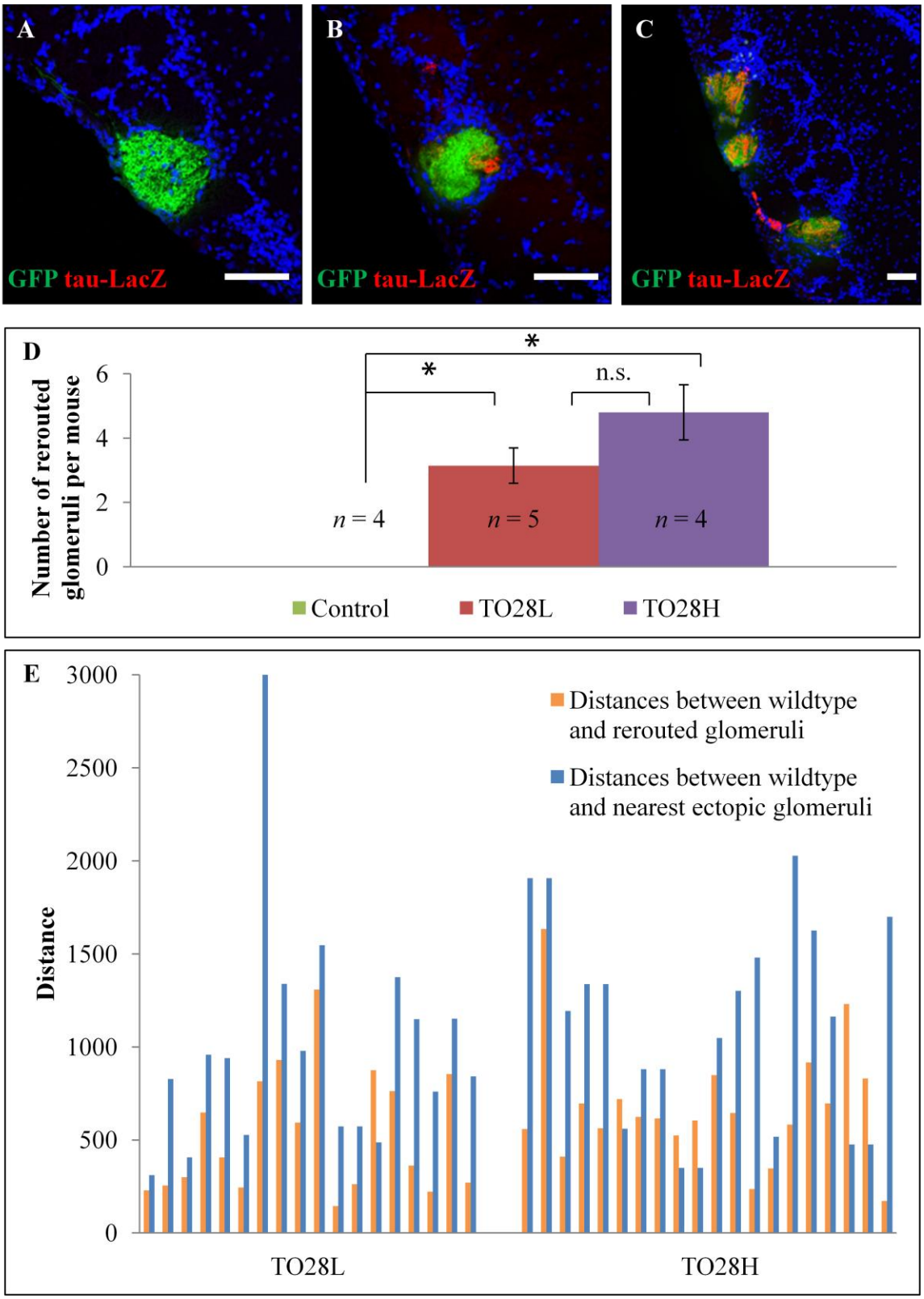

Figure 6. (legend continued on next page)

Figure 6. TO28 expression causes OSNs expressing endogenous MOR28 to form rerouted glomeruli.

A-C) Coronal sections of OB immunohistochemically stained for the indicated proteins. **A)** Control expressing only MOR28-IRES-GFP forms one lateral and one medial (not shown) glomerulus per OB. **B)** TO28L OSNs co-innervate the wildtype MOR28 glomerulus. **C)** In a mouse expressing TO28L, axons expressing only wildtype MOR28 form supernumerary glomeruli called rerouted glomeruli. **D)** Rerouted glomeruli are only found in mice expressing TO28 but there is no significant difference in the number formed by TO28H versus TO28L. ($p < 0.050$. Error bars show standard error.) **E)** Quantification of the distances between wildtype and rerouted or ectopic glomeruli. Each pair of bars represents the distance from a given wildtype MOR28 glomerulus to its rerouted or nearest ectopic glomeruli. Note only 6/33 rerouted glomeruli were farther than the nearest ectopic glomerulus. Scale bars, 100 μm.

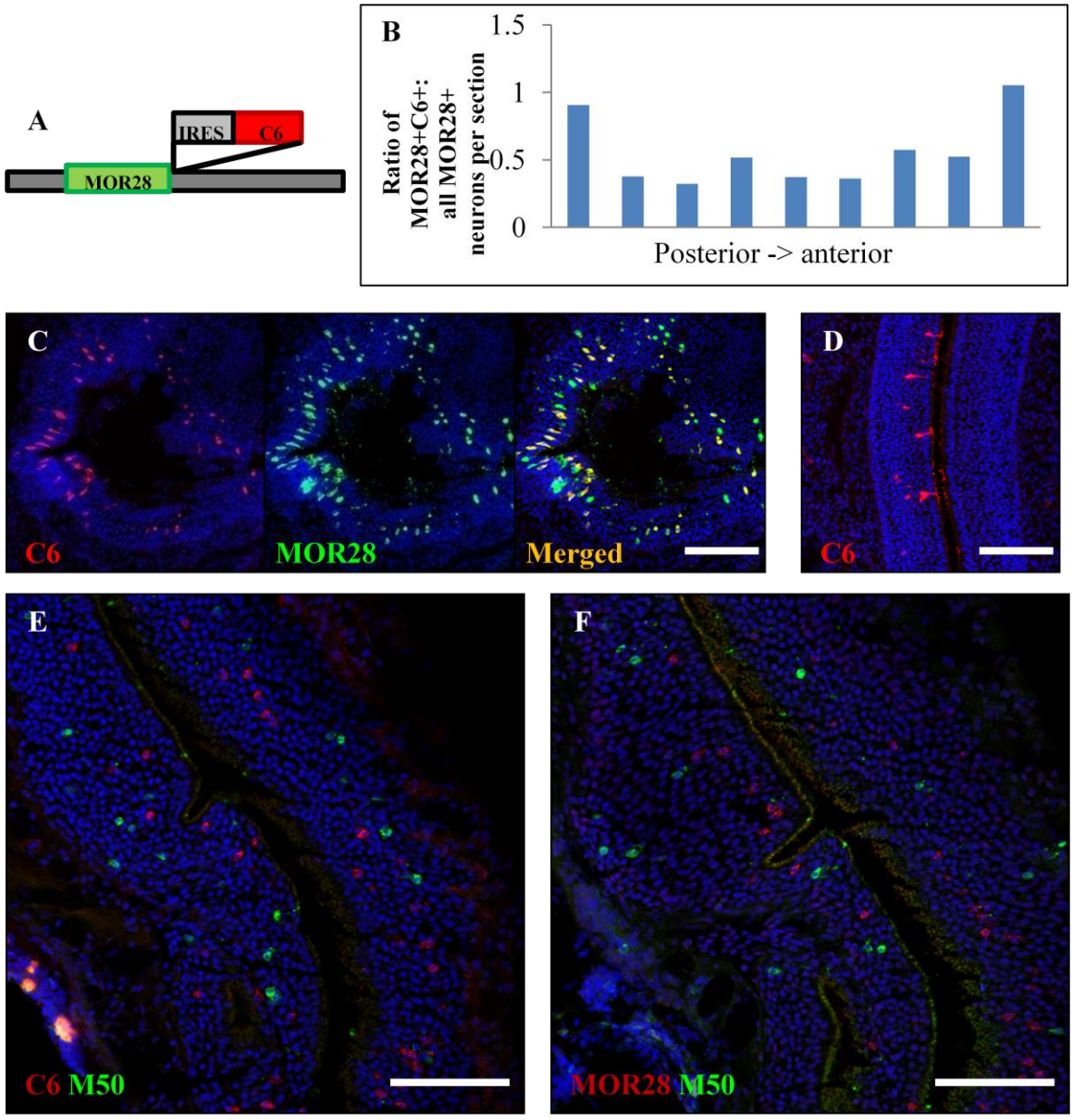

Figure 7. MOR28-IRES-C6 co-expresses MOR28 and C6.

A) MOR28-IRES-C6, drives C6 in OSNs expressing endogenous MOR28. **B)** Quantification of OSNs immunohistochemically stained for the proteins indicated. Each bar represents the ratio calculated from one section, starting from the posterior end of the MOE and progressing anteriorly. A MOR28-IRES-C6 heterozygote exhibits no bias in choosing to express the wildtype or modified allele. **C-F)** Coronal sections of MOE immunohistochemically stained for the proteins indicated. **C)** A MOR28-IRES-C6 heterozygote expresses C6 in half of the OSNs that express MOR28. **D)** The frequency and intensity of C6 staining is not affected in endogenous C6 OSNs when MOR28-IRES-C6 is expressed **E,F)** Co-expression of MOR28 and C6 does not cause OSNs to co-express MOR50. Scale bars, 100 μm.

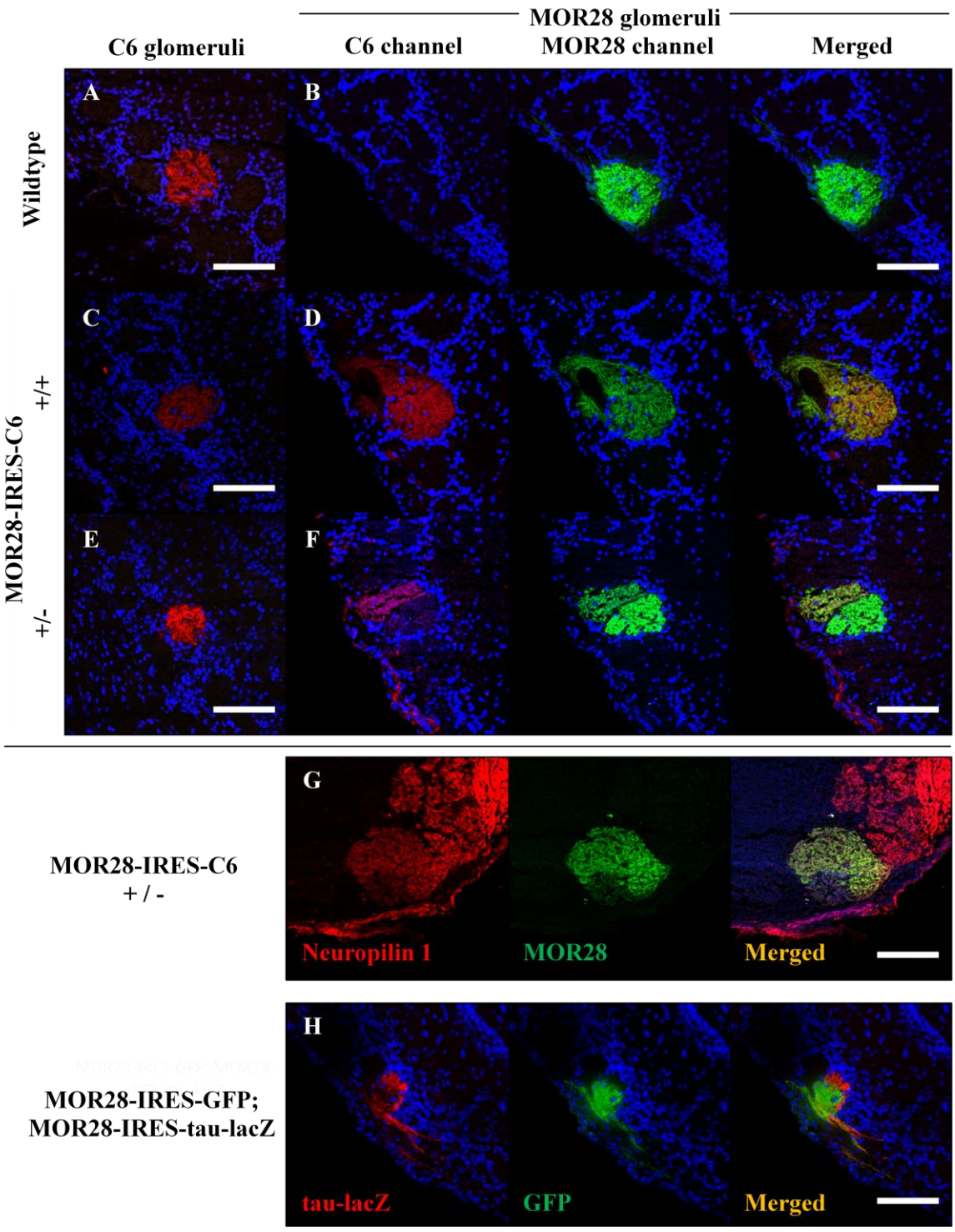

Figure 8. (legend continued on next page)

Figure 8. MOR28-IRES-C6 neurons express less MOR28 protein than wildtype MOR28 OSNs.

A-G) Coronal sections of OB immunohistochemically stained for the proteins indicated. **A,B)** Controls exhibit four C6 and four MOR28 glomeruli in different areas of the OB. **C,E)** The placement, number, and intensity of C6 glomeruli are not affected in mice expressing MOR28-IRES-C6. **D)** In a MOR28-IRES-C6 homozygote, the modified allele targets four glomeruli indistinguishable from the wildtype MOR28 glomeruli in terms of size and location. **F)** In a MOR28-IRES-C6 heterozygote, the axons expressing the modified allele co-innervate the wildtype MOR28 glomeruli. The concentration of MOR28 protein in MOR28-IRES-C6 axons is noticeably less than that seen in wildtype MOR28 axons. **G)** The expression of the canonical guidance protein Neuropilin 1 is decreased in the MOR28-IRES-C6 axons. **H)** In mice expressing both MOR28-IRES-GFP and MOR28-IRES-tau-lacZ, the two populations of MOR28 OSNs segregate within the glomerulus. Scale bars, 100 μm.

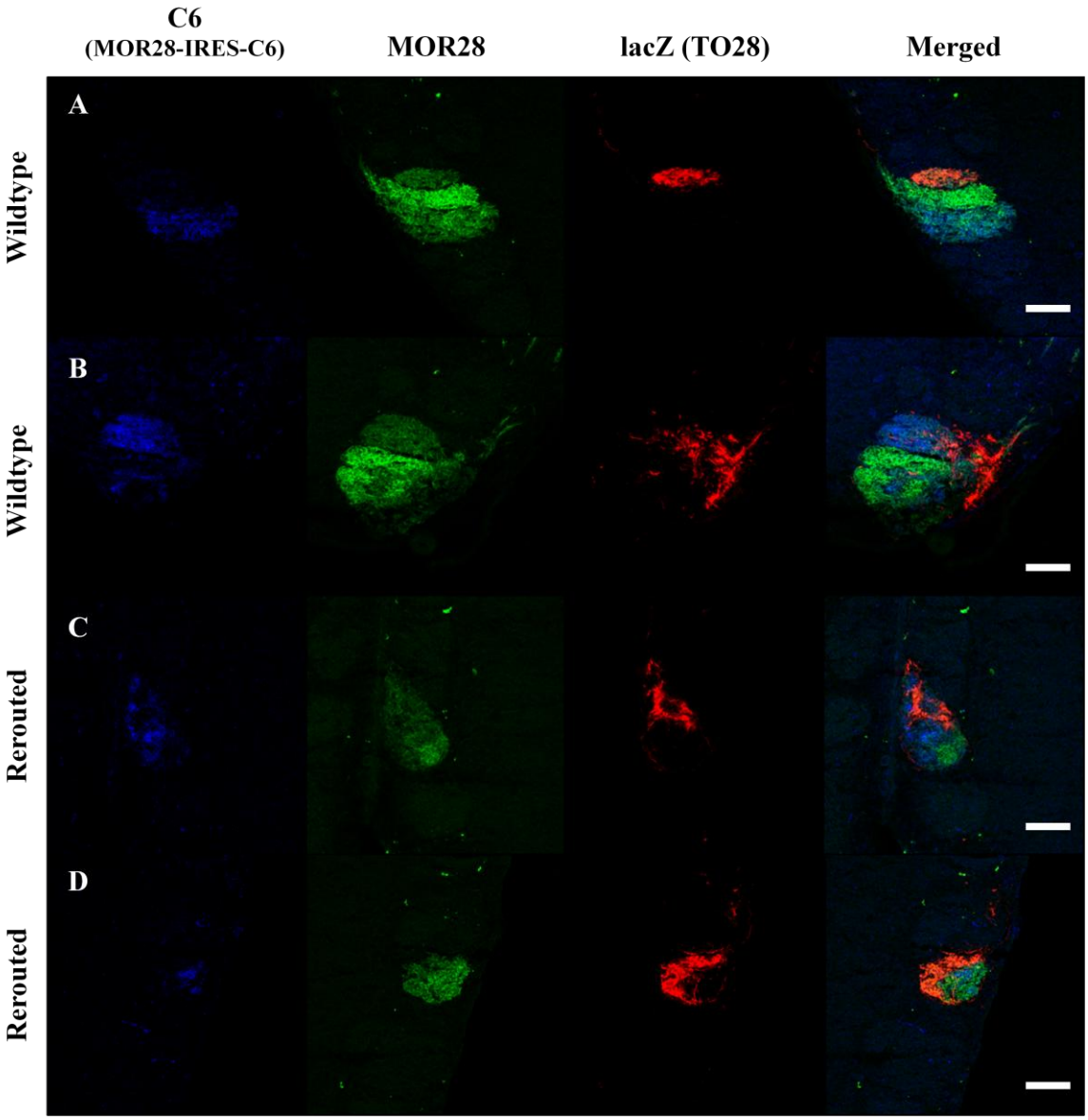

Figure 9. Wildtype and rerouted MOR28 glomeruli are equally innervated by MOR28-IRES-C6 and endogenous MOR28 axons.

A-D) Coronal sections of the OB from immunohistochemically stained for the proteins indicated. Mice express the alleles MOR28-IRES-C6, OMP-IRES-tTA, and TO28L. **A,B)** Representative wildtype MOR28 glomeruli and **C,D)** representative rerouted glomeruli. No difference was observed in the amount of innervation from MOR28-IRES-C6 or endogenous MOR28 axons. Scale bars, 100 μm.

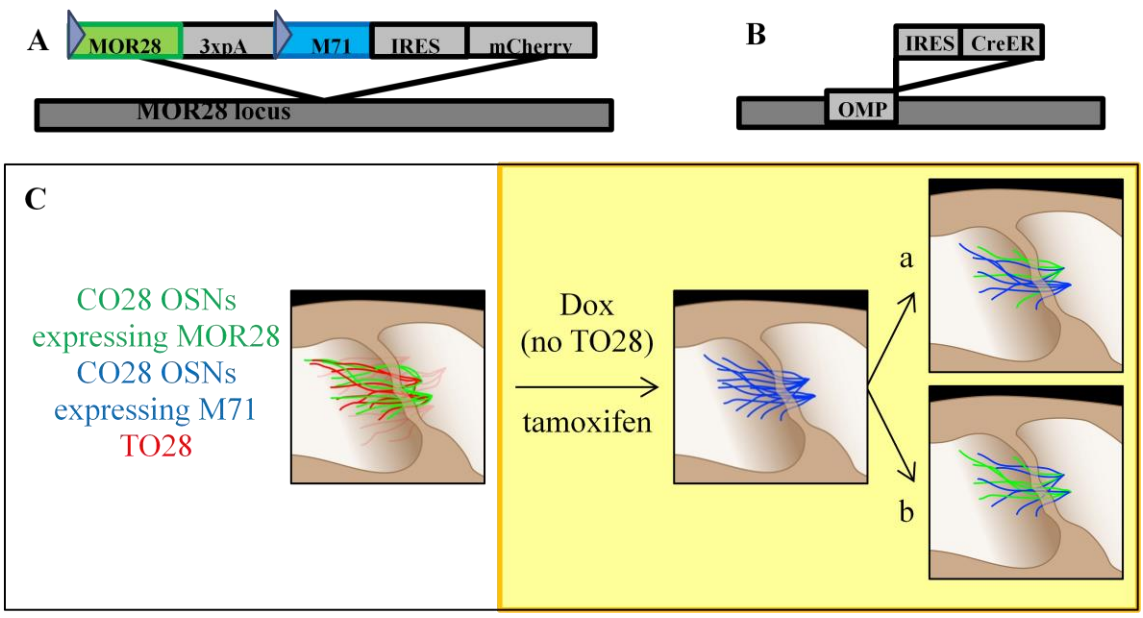

Figure 10. Distinguishing homotypic attraction from glomerular marking by glia and post-synaptic cells.

A) lox-MOR283xpA-lox-M71-IRES-mCherry (CO28), should not normally affect OSNs that normally express MOR28. After exposure to Cre recombinase, this allele will drive the expression of M71 instead of MOR28 as well as the reporter protein mCherry. **B)** OMP-IRES-CreER, drives tamoxifen-inducible Cre recombinase expression in all OSNs. **C)** Summary of experiment, depicted as schematics of sagittal views of the olfactory system. Mice will express TO28 and MOR28 from the CO28 allele until two months of age. They will be given a single dose of tamoxifen and placed on a dox regimen for two months. After this treatment, rerouted glomeruli will be only innervated by OSNs expressing M71. a) If later-born CO28 OSNs expressing MOR28 do not innervate rerouted glomeruli, this would suggest a lack of homotypic attraction to CO28 OSNs expressing M71. b) If later-born CO28 OSNs do co-innervate rerouted glomeruli with CO28 OSNs expressing M71, this would suggest that glia and post-synaptic cells marked the glomeruli for MOR28 OSNs.

Chapter 3

Glomerular identity is established within a critical period

ABSTRACT

Before the advent of modern mouse genetics, most of the studies regarding neuronal regeneration relied on non-specific physical or chemical ablation of neurons. These approaches often caused scarring and or other side effects in non-specific cell types that complicated the interpretation of the results. In the previous chapter we described a targeted genetic approach to assay the mechanisms of axonal guidance in adulthood. Not only do we avoid perturbing non-specific cell types, but we also alter solely the gene expression of olfactory sensory neurons. This subtle manipulation allows us to examine the axonal guidance mechanisms that are mediated specifically by the odorant receptors expressed by olfactory sensory neurons. Furthermore, the inducibility of our system allows us to distinguish the mechanisms that initially establish the glomerular map versus the mechanisms that maintain the map as olfactory sensory neurons regenerate later in life. In the previous chapter we determined that the expression of transgenic odorant receptor during early development causes the formation of rerouted glomeruli. In this chapter we provide evidence that rerouted glomeruli can *only* be formed during glomerular map establishment. The mechanisms that govern axonal guidance are different in the adult such that transgenic odorant receptors expressed after a critical period are no longer capable of causing rerouted glomeruli to form. Conversely, once the rerouted glomeruli have formed, their maintenance does not depend on the expression of transgenic odorant receptor. Even when the majority of olfactory sensory neurons are ablated, regenerating neurons will continue to innervate the rerouted glomeruli. Overall it appears that the mechanisms of axonal guidance later in life ensure that the adult glomerular map is maintained in the exact conformation that was

established early in life. This suggests that a critical characteristic of the adult glomerular map is that it is consistent with early circuitry.

INTRODUCTION

In this chapter I address the mechanisms of axonal guidance that guide OSNs during adulthood. In order to distinguish embryonic development from the processes that specifically maintain the pattern of axonal projections later in life, we needed a temporally controlled approach that perturbs the olfactory system at different stages of a mouse's life. Many of the techniques previously used in the field to affect OSNs, such as naris occlusion, axotomy, and bulbectomy, cause systemic injury and scarring. Not only do we want to avoid affecting non-OSN cells, but ideally we want to manipulate just the gene expression of OSNs without killing them at all.

Advances in the development of genetic tools have provided multiple strategies for manipulating gene expression. Endogenous alleles can be deleted, replaced with other genes, or modified to co-express other proteins. However, these three approaches alone cannot be used to study adult-specific axonal guidance because their effects last for the entire life of the animal. The technique that we described in the last chapter supplements a modified endogenous allele with an inducible transgene such that gene expression in OSNs can be temporally controlled. The same technique with a different transgene was used previously to modify the electrical activity of OSNs (Yu et al., 2004). Other labs even used the same technique to express transgenic ORs (Fleischmann et al., 2008; Nguyen et al., 2010; Nguyen et al., 2007; Takeuchi et al., 2010). However, the focus of these papers was not adult-specific axonal guidance and the experiments often did not take advantage of the temporal control provided by the inducible promoter.

In the previous chapter we characterized the effect that the TO28 transgene had on axonal guidance when it was expressed for the entire life of the animal. We established that TO28 axons form ectopic glomeruli throughout the OB. Furthermore, TO28 expression caused endogenous MOR28 axons to form rerouted glomeruli. This is presumably because ectopic glomeruli in the vicinity of the wildtype MOR28 glomeruli recruit endogenous MOR28 axons through mechanisms such as homotypic attraction.

In this chapter we begin by assaying whether TO28 can cause the formation of rerouted glomeruli regardless of when it begins to be expressed. Originally we hypothesized that this would be true, since OSNs are constantly being generated in the MOE and thus some aspects of axonal guidance must be operable in the adult olfactory system. Surprisingly, we found evidence that there is in fact a developmental time window, or critical period, during which the expression of TO28 can cause rerouted glomeruli to form. This suggests that there are distinct differences between the axonal guidance mechanisms controlling early-born versus later-born OSNs. Next we found that, once formed, rerouted glomeruli are stable and that they can persist despite major lesions. Overall our evidence suggested that even though the olfactory system constantly regenerates, it maintains whatever circuitry conformation is established during early development.

MATERIALS AND METHODS

*Animals***.** We used C57/Bl6 mice purchased from Jackson Labs as the wildtype strain for all of our experiments. The TO28 mice used in our experiments are on a mixed C57/BL6; 129 background. Mice were genotyped by PCR using primers that recognize TO28 (Int2 for: CTCTCCACAGGTGTCCACTCC and SP1 dA rev: AGATCTGTTGCCTCAGGG-CCACAAGG), tTA (tTA for: GCTTTGCTCGACGCCTTAGCCA and tTA rev: CCGT-AGGGGGCGGAGTCGTG), and GFP (GFP for: GACCCTGAAGTTCAGCTGC and GFP rev: TGTCGCCATGATATAGACG). EdU (Invitrogen, 3 mg/mL in PBS, final dosage 50 mg/kg body weight) was administered via a single intraperitoneal injection. Dox was administered via dox-supplemented chow (Bioserv, 200 mg/kg carrier chow) provided *ad libitum* and replaced once weekly. Methimazole (Sciencelab.com Inc., 10 mg/mL in PBS, final dosage 200 mg/kg body weight) was administered via intraperitoneal injections given once every 24 hours for 3 consecutive days. All animal procedures were in compliance with the guidelines of the institutional animal care and use committee (IACUC) of Brown University.

Immunohistochemistry. The mice were anesthetized via intraperitoneal injection of 2,2,2-tribromoethanol (1.2% in 2-methyl-2-butanol and water, final dosage 240 mg/kg body weight). Animals were transcardially perfused with 2% paraformaldehyde in PBS. The MOE and OBs were dissected separately and embedded in OCT (Sakura) or M1 (Shandon) in a dry ice/ethanol bath. 14 μm coronal sections were cut on a cryostat (Leica CM3050S) and collected on SuperFrost plus slides (Fisher). The sections were post-fixed with 1% paraformaldehyde in PBS for 10 minutes at room temperature, washed three times in PBS for 5 minutes, permeabilized in 0.1% Triton X-100 in PBS (PBS-T) for 30

minutes at room temperature, blocked in 5% heat in-activated donkey serum in PBS-T (P/T/S) for 30 minutes at room temperature, incubated with primary antibody in P/T/S under parafilm (Fisher) overnight in a humidified chamber at 4˚C, washed three times in PBS-T for 5 minutes, blocked with P/T/S for 30 minutes at room temperature, incubated with a fluorescent-conjugated secondary antibody in P/T/S with TOTO-3 (Invitrogen, 1:1000) for 2 hours at room temperature, washed three times in PBS-T for 5 minutes, and coverslipped with Prolong Gold (Invitrogen). Images were taken using a Zeiss LSM 510 DuoScan confocal microscope.

Primary antibodies included goat anti-β-galactosidase (Chemicon, 1:1000), rabbit anti-GFP (Invitrogen, 1:1000), goat anti-GFP (Rockland, 1:200), guinea pig anti-MOR28 (Barnea *et al.* 2004, 1:6000), guinea pig anti-VGLUT1 (Millipore, 1:1000), guinea pig anti-VGLUT2 (Synaptic Systems, 1:1000), rabbit anti-calbindin (Millipore, 1:1000), and rabbit anti-GAD65 (Millipore, 1:1000). Secondary antibodies used were donkey anti-goat Alexa Fluor® 488, donkey anti- guinea pig Alexa Fluor® 488, donkey anti-rabbit Alexa Fluor® 488, donkey anti-goat Alexa Fluor® 555, donkey anti-guinea pig Alexa Fluor® 549, and donkey anti-rabbit Alexa Fluor® 647 (Molecular Probes). EdU was visualized with the Click-iT® EdU kit (Invitrogen).

*Quantification of staining frequency***.** An Olympus BX41 fluorescent microscope was used to identify the number of OSNs per section that stained positive for EdU or the proteins indicated in the text. The six consecutive sections per mouse that exhibited peak expression were averaged to generate a single mean value per mouse.

RESULTS

The halflife of OSNs is 77 days

It is well established that OSNS are one of the few populations of neurons that normally regenerate throughout adulthood. However, the exact value of an OSN's halflife has been debated. Previous estimations ranged from 30-120 days (Astic and Saucier, 2001; Graziadei and Graziadei, 1979; Hinds et al., 1984; Mackay-Sim and Kittel, 1991) though even the authors of some of these sources point out that the values cited from these papers are sometimes merely the last time point taken and that the time course should be extended in order to calculate a true halflife (Mackay-Sim, 2003). In addition, these studies were not performed in the C57/BL6 strain that constitutes part of the genetic background for our mice. In order to interpret our results concerning the axonal guidance of regenerating OSNs, we first needed to determine an accurate halflife for the OSNs in our mice

We injected one age-matched cohort of wildtype mice with the thymidine analog EdU. These nucleosides are incorporated into proliferating cells and, since OSNs are post-mitotic, irreversibly mark all of the OSNs that are born shortly after EdU treatment. Every 15-30 days we assayed the number of these OSNs that remained in the MOE. These data were fit to an exponential decay to determine that the OSNs in our mice have a halflife of 77.0 days (Fig. 1). Not only does this value fall well within the 30-120 day range previously mentioned, but the time course extends well beyond 77 days, giving us confidence that the formula describes the data well.

Rerouted glomeruli can only form if the transgene is expressed during an early critical period

In the previous chapter we established that TO28 expression induces endogenous MOR28 axons to form rerouted glomeruli. Although we have not definitively identified the mechanisms that govern this process, we wanted to know whether in general these mechanisms still operated in the adult mouse. To do this, we took advantage of the inducibility of TO28 to begin transgene expression in an adult mouse only after it had already formed a mature glomerular map. Breeding pairs of mice were administered dox such that litters of pups capable of TO28 expression were kept phenotypically wildtype throughout gestation and until P0, P7, or P14. Dox was then removed for at least 8 months, or more than three times the half life of OSNs (Fig. 2Aa). At this point, new axons had replaced ~90% of the axons that were present within the average wildtype MOR28 glomeruli at 2 months of age. Some of the replacement neurons were endogenous MOR28 OSNs, others express TO28. TO28 axons also formed ectopic glomeruli nearby but endogenous MOR28 axons almost never formed rerouted glomeruli (Fig. 2B, C). In a few mice treated with dox until P0 or P7 (1/6 mice and 1/11 mice, respectively), endogenous MOR28 axons were observed in very small glomeruli. However, these structures co-stained for the same glomerular markers as the wildtype MOR28 glomeruli we have classified them as rerouted glomeruli (Fig. 3). Rerouted glomeruli of any kind was never observed when TO28 expression began after P14 (0/4 mice). We conclude that rerouted glomeruli can only be formed within an early developmental window, or critical period, that ends shortly after birth.

The percentage of OSNs that are actively outgrowing does not affect the critical period

Among the many differences between the developing and adult olfactory systems is the difference in the percentage of the total number of OSNs that are actively extending axons. In the embryonic olfactory system, most OSN axons synchronously target their glomeruli within a short period of time. However, in the adult olfactory system, only rare OSN axons are actively growing and most have synapsed within glomeruli. We wanted to test whether this difference in percentage explained the critical period for rerouted glomeruli formation.

To synchronize the growth of the majority of OSNs, we used the drug methimazole. It is thought to interact only with cells expressing specific variants of cytochrome P450, resulting in the apoptosis of only OSNs (Xie et al., 2011). Methimazole is better suited to our studies than other commonly used olfactory toxicants because it does not affect surrounding sustentacular cells like methyl bromide (Hurtt et al., 1988) and it does not cause permanent tissue damage like dichlobenil (Piras et al., 2003). In fact, a morphologically normal and functional MOE is restored within 2 months post-lesion (Suzukawa et al., 2011). We treated one age-matched cohort of MOR28-IRES-GFP mice and assayed the GFP expression in the OB and MOE at one day intervals after the last dose of methimazole. The number of endogenous MOR28 OSNs was drastically reduced, with the least expression observed 5 days after treatment (Fig. 4A). At this time point, only 0.2% of the normal number of MOR28 OSNs was left (Fig. 4B). Other chemoreceptors were even more drastically affected, with no C6, M71, TAAR4, or TAAR5 OSNs observed for the entire week post-methimazole. M50 expression was also completely abolished although the kinetics of its re-expression was

different. A few M50-expressing OSNs could be observed at 5 days post-methimazole (data not shown). A TO28L mouse given the same treatment also showed a severe decrease in TO28 expression, though trace amounts of MOR28 and lacZ protein were always observed in the MOR28 glomeruli (Fig. 4C).

Having identified a treatment that will synchronize the growth of 99.8% of the MOR28 OSNs, we assayed whether TO28 axons growing into a relatively sparsely-populated adult OB would be able to form new ectopic and rerouted glomeruli. Mice capable of TO28 expression were treated with dox beginning at conception so that no ectopic or rerouted glomeruli would form and possibly affect the glomerular map. At 2 months of age, after a mature glomerular map had formed, the mice were taken off dox and also treated with methimazole (Fig. 2Ab). TO28 was expressed and ectopic glomeruli were formed (data not shown) but we never observed rerouted glomeruli (Fig. 2D,E). These results indicate that the critical period is due to other characteristics that define the mature olfactory system, and not the difference in the proportion of outgrowing axons.

Rerouted glomeruli are maintained without continuous transgene expression

In the previous chapter, we observed that all rerouted glomeruli were co-innervated by both TO28 axons and endogenous MOR28 axons so we addressed whether TO28 expression was necessary to maintain the existence of rerouted glomeruli. We allowed mice to express TO28 until 2 months of age, at which point they had developed a mature glomerular map with both ectopic and rerouted glomeruli. Next we treated these mice with dox for at least 21 weeks, or roughly twice the half life of OSNs (Fig. 5Aa). These mice all expressed the same number of rerouted glomeruli as untreated TO28 mice,

even though at this point <30% of the axons present at 2 months of age were still present in the average rerouted glomerulus. Furthermore, none of the axons within the rerouted glomeruli expressed TO28 (Fig. 5B,C). These results indicate that, once formed, the maintenance of rerouted glomeruli does not depend on TO28 expression.

A small fraction of the MOR28 axon population may be sufficient to reconstitute rerouted glomeruli

The maintenance of the rerouted glomeruli is presumably due to the continued influence of homotypic attraction between the early-born endogenous MOR28 axons already in the glomeruli and the later-born endogenous MOR28 axons that were born after dox treatment. We wanted to test whether a small fraction of the early-born MOR28 axons is sufficient to maintain rerouted glomeruli. Since methimazole ablates 99.8% of the MOR28 OSNs, we examined whether the 0.2% remaining neurons were sufficient to recruit new MO28 axons. Mice expressing TO28L were allowed to form ectopic and rerouted glomeruli until 2 months of age. The mice were then treated with methimazole and placed on a dox regimen for an additional 2 months to allow the glomerular map to be restored without TO28 expression (Fig. 5Ab). All of the mice exhibited rerouted glomeruli (Fig. 5D,E). If recruitment is mediated by homotypic attraction, these results are consistent with the interpretation that 0.2% of the total population of MOR28-expressing axons is sufficient to guide new endogenous MOR28 axons to previously-formed rerouted glomeruli.

DISCUSSION

In this chapter we provide evidence that in order for the expression of TO28 to cause the formation of rerouted glomeruli, it must be expressed during a critical period that ends before P14. We use this term in the sense that a developmental process can only happen during a specific time window, not in the original sense used by Hubel and Wiesel to indicate a time during which experience-dependent neuronal activity affects neuronal circuitry. However, the existence of other types of supernumerary glomeruli is known to depend on odorant exposure. Extra M71 and M72 glomeruli are pruned by P60 unless the nose is blocked by naris occlusion (Zou et al., 2004). Perhaps the plasticity that allows this pruning is related to the plasticity that allows the formation of rerouted glomeruli so it would be interesting to see if the critical period for TO28 expression could be extended if mice were naris occluded at birth.

It is interesting to note that the mechanisms governing the formation of rerouted glomeruli had changed later in life even though the mechanisms that govern the formation of ectopic glomeruli had not changed. Some ectopic glomeruli were observed only one glomerulus away from wildtype MOR28 glomeruli and yet they did not recruit endogenous MOR28 axons. The differences may be due to subtle variation in the expression of transgenic versus endogenous MOR28. The MOR28 promoter is one of the strongest OR promoters (Young et al., 2003) and endogenous MOR28 axons clearly express more MOR28 protein than transgenic MOR28 axons (Chapter 2 Fig. 9). Perhaps these distinctions do not affect initial map formation but are a driving force behind maintaining the map. It would be interesting to repeat this experiment with mice expressing both MOR28-IRES-C6 and TO28. Since the levels of MOR28 in MOR28-

IRES-C6 axons were more closely matched to that in TO28 axons (Chapter 2 Fig. 9), MOR28-IRES-C6 axons may be more likely to reroute into ectopic glomeruli later in life. This result would be interesting because it would suggest that rather than axonal guidance mechanisms merely shutting off later in life, different mechanisms are actually activated and perhaps supplant earlier mechanisms.

We also found evidence that after rerouted glomeruli are formed, they do not depend on TO28 expression for maintenance and that they can even be reconstituted if more than 99.8% of OSNs are ablated. The latter experiment argues against one of the models proposed by Vassalli et al. for the rerouting of OSNs expressing endogenous ORs. In that paper, M71 or MOR23 expressed from a minigene also formed ectopic glomeruli that could recruit OSNs expressing endogenous M71 and MOR23 (Vassalli et al., 2002). The authors proposed that the recruited OSNs represent OSNs that are not normally observed because they are usually pruned during early development. If an OR is expressed in an abnormal zone, it would not be able to navigate to the glomeruli normally associated with that OR, causing it to die from lack of trophic support. When transgenes or minigenes increase the number of OSNs expressing the OR within these abnormal zones, the OSNs that would normally be pruned can now target ectopic glomeruli and be stably integrated into the circuit. However, the 0.2% of MOR28 axons left after methimazole ablation seems hardly sufficient for stabilizing any abnormally located endogenous MOR28 OSNs. Furthermore, we did not observe wildtype MOR28 OSNs in ectopic zones (Chapter 2 Fig. 1F). Instead of stabilized OSNs, the rerouted glomeruli appear to be ectopic glomeruli that have been modified with recruited endogenous MOR28 axons.

The results presented in this chapter all indicate that the olfactory system will maintain whatever glomerular map established during early development. This conservation of circuitry is a matter of course for neurons that are not replaced during adulthood, but perhaps surprising considering that OSNs do constantly regenerate. Perhaps maintaining the established map is necessary for an organism to perceive a given odorant in a consistent manner for the entirety of its lifetime. In this way, death and regeneration within the circuit will not impact cognitive processes such as learning conditioned responses to odorants. This phenomenon can also have clinical implications. Our results suggest that a subtle, transient change in gene expression during early development can permanently affect neuronal circuitry. Therefore it may be impossible to reverse certain neuronal birth defects caused by chemical imbalances during gestation. However, the observation that rerouted glomeruli are reconstituted after drastic chemical ablation can also provide hope for restoring smell to patients who have experienced extensive olfactory tissue damage. Concussive head trauma can shear OSN axons at the cribriform plate. As long as 0.2% of the OSNs are intact, perhaps the human glomerular map can also be repaired. Our work may delineate the extent to which medical interventions can impact neuronal circuitry later in life.

REFERENCES

Astic, L., and Saucier, D. (2001). Neuronal plasticity and regeneration in the olfactory system of mammals: morphological and functional recovery following olfactory bulb deafferentation. Cell Mol Life Sci *58*, 538-545.

Fleischmann, A., Shykind, B., Sosulski, D., Franks, K., Glinka, M., Mei, D., Sun, Y., Kirkland, J., Mendelsohn, M., Albers, M., *et al.* (2008). Mice with a "monoclonal nose:" perturbations in an olfactory map impair odor discrimination. Neuron *60*, 917-926.

Graziadei, P.P., and Graziadei, G.A. (1979). Neurogenesis and neuron regeneration in the olfactory system of mammals. I. Morphological aspects of differentiation and structural organization of the olfactory sensory neurons. J Neurocytol *8*, 1-18.

Hinds, J., Hinds, P., and McNelly, N. (1984). An autoradiographic study of the mouse olfactory epithelium: evidence for long-lived receptors. Anat Rec *210*, 375-383.

Hurtt, M.E., Thomas, D.A., Working, P.K., Monticello, T.M., and Morgan, K.T. (1988). Degeneration and regeneration of the olfactory epithelium following inhalation exposure to methyl bromide: pathology, cell kinetics, and olfactory function. Toxicol Appl Pharmacol *94*, 311-328.

Mackay-Sim, A. (2003). Handbook of Olfaction and Gustation, 2nd edn (New York, Dekker).

Mackay-Sim, A., and Kittel, P. (1991). On the Life Span of Olfactory Receptor Neurons. 3 *208-215*.

Nguyen, M., Marks, C., Belluscio, L., and Ryba, N. (2010). Early Expression of Odorant Receptors Distorts the Olfactory Circuitry. J Neuroscei *3*-, 9271-9279.

Nguyen, M., Zhou, Z., Marks, C., Ryba, N., and Belluscio, L. (2007). Prominent roles for odorant receptor coding sequences in allelic exclusion. Cell *131*, 1009-1017.

Piras, E., Franzen, A., Fernandez, E.L., Bergstrom, U., Raffalli-Mathieu, F., Lang, M., and Brittebo, E.B. (2003). Cell-specific expression of CYP2A5 in the mouse respiratory tract: effects of olfactory toxicants. J Histochem Cytochem *51*, 1545-1555.

Suzukawa, K., Kondo, K., Kanaya, K., Sakamoto, T., Watanabe, K., Ushio, M., Kaga, K., and Yamasoba, T. (2011). Age-related changes of the regeneration mode in the mouse peripheral olfactory system following olfactotoxic drug methimazole-induced damage. J Comp Neurol *519*, 2154-2174.

Takeuchi, H., Inokuchi, K., Aoki, M., Suto, F., Tsuboi, A., Matsuda, I., Suzuki, M., Aiba, A., Serizawa, S., Yoshihara, Y., *et al.* (2010). Sequential Arrival and Graded Secretion of Sema3F by Olfactory Neuron Axons Specify Map Topography at the Bulb. Cell *141*, 1056-1067.

Vassalli, A., Rothman, A., Feinstein, P., Zapotocky, M., and Mombaerts, P. (2002). Minigenes impart odorant receptor-specific axon guidance in the olfactory bulb. Neuron *35*, 681-696.

Xie, F., Zhou, X., Genter, M.B., Behr, M., Gu, J., and Ding, X. (2011). The tissue-specific toxicity of methimazole in the mouse olfactory mucosa is partly mediated through target-tissue metabolic activation by CYP2A5. Drug Metab Dispos *39*, 947-951.

Young, J., Shykind, B., Lane, R., Tonnes-Priddy, L., Ross, J., Walker, M., Williams, E., and Trask, B. (2003). Odorant receptor expressed sequence tags demonstrate olfactory expression of over 400 genes, extensive alternate splicing and unequal expression levels. Genome Biol *4*.

Yu, C., Power, J., Barnea, G., O'Donnell, S., Brown, H., Osborne, J., Axel, R., and Gogos, J. (2004). Spontaneous neural activity is required for the establishment and maintenance of the olfactory sensory map. Neuron *42*, 553-566.

Zou, D.J., Feinstein, P., Rivers, A.L., Mathews, G.A., Kim, A., Greer, C.A., Mombaerts, P., and Firestein, S. (2004). Postnatal refinement of peripheral olfactory projections. Science *304*, 1976-1979.

FIGURES

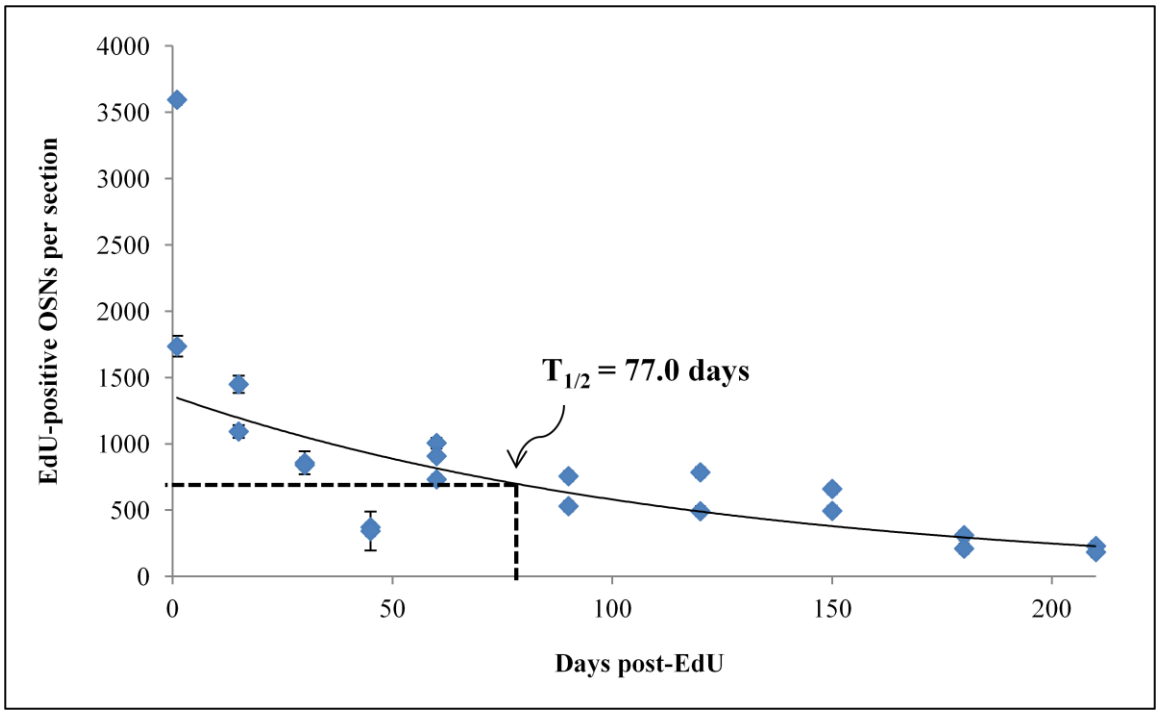

Figure 1. OSNs have a halflife of 77.0 days.

One cohort C57/BL6 mice was injected with EdU and two mice were assayed at the indicated times. The halflife of an OSN was calculated to be 77.0 days. The data were fit the formula $y = 1358.2e^{-0.009x}$ with an R^2 value of 0.6384; error bars shown are standard deviation.

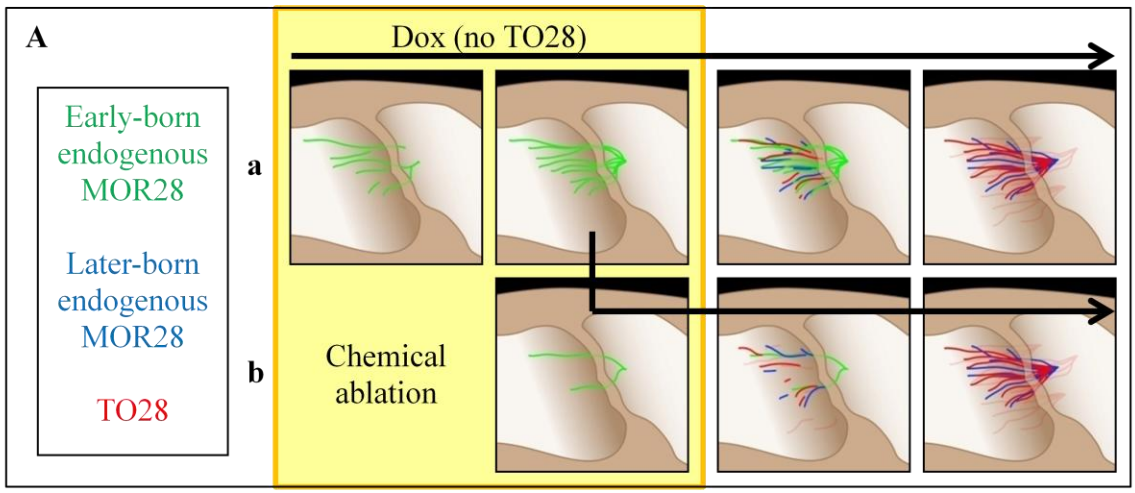

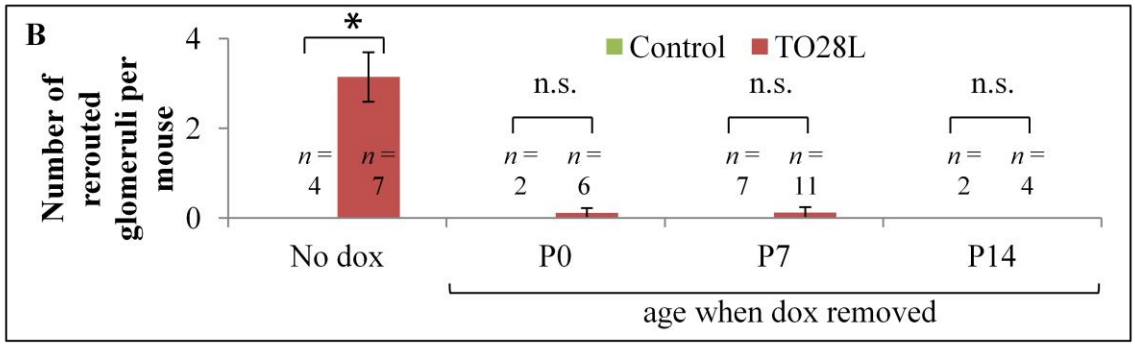

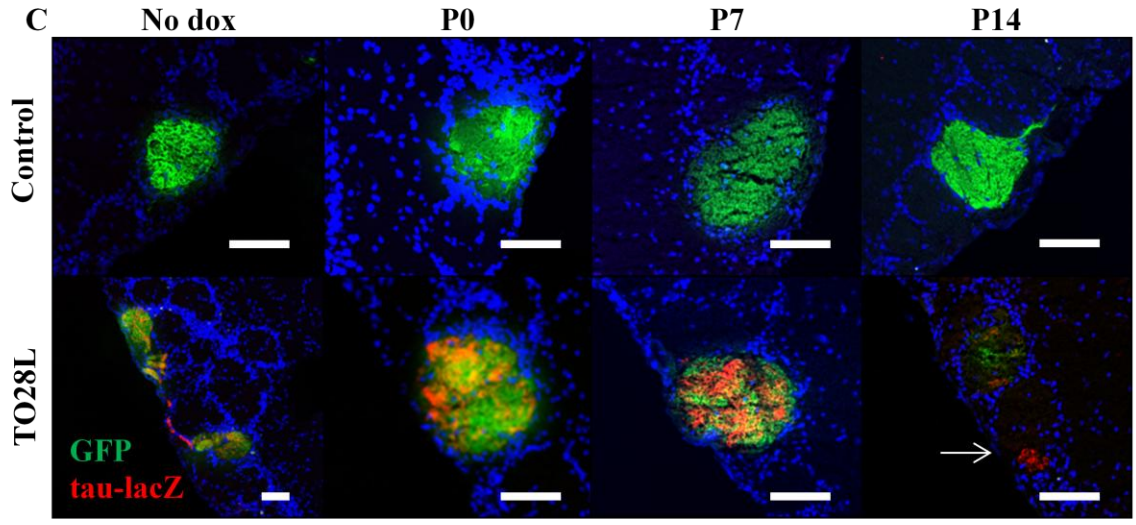

D	Pre-ablation	Post-ablation	Rerouted glomeruli
a	+ dox (no TO28)	+ dox (no TO28)	0 ± 0
b	+ dox (no TO28)	- dox (with TO28)	0 ± 0

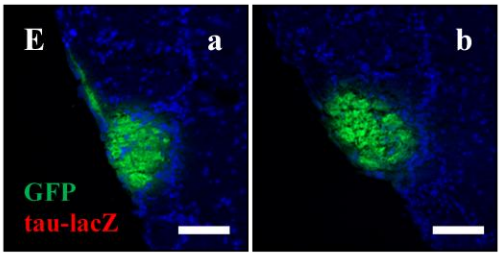

Figure 2. (legend continued on next page)

Figure. 2. Rerouted glomeruli can only be formed within a critical period.

A) Summary of experiments, depicted as schematics of sagittal views of the olfactory system. a) Mice capable of expressing TO28L were treated with dox from conception to P0, P7, or P14. The mice were assayed after 8+ months without dox. Ectopic glomeruli formed, but rerouting was rarely observed. b) Mice capable of expressing TO28L were treated with dox from conception until P60, injected with methimazole, and assayed after 2 additional months without dox. Again, ectopic glomeruli formed, but rerouting was never observed. **B)** The number of rerouted glomeruli observed when TO28L is only expressed post-natally is not significantly different from that seen in wildtype mice. ($p >$ 0.050, n.s. Error bars shown are standard error.) **C)** Representative images of the glomeruli quantified in B. Arrow, a nearby ectopic glomerulus that has not rerouted endogenous MOR28 axons. **D)** The number of rerouted glomeruli observed after 99.8% of MOR28 OSNs are ablated and TO28L is induced is not significantly different from that seen in phenotypically wildtype TO28L mice treated only with methimazole. (a, $n =$ 4; b, $n = 5$; $p > 0.050$, n.s. Errors shown are standard error.) **E)** Representative images of the glomeruli quantified in D. C,E show coronal sections of OB immunohistochemically stained for the proteins indicated. Scale bars 100 μm.

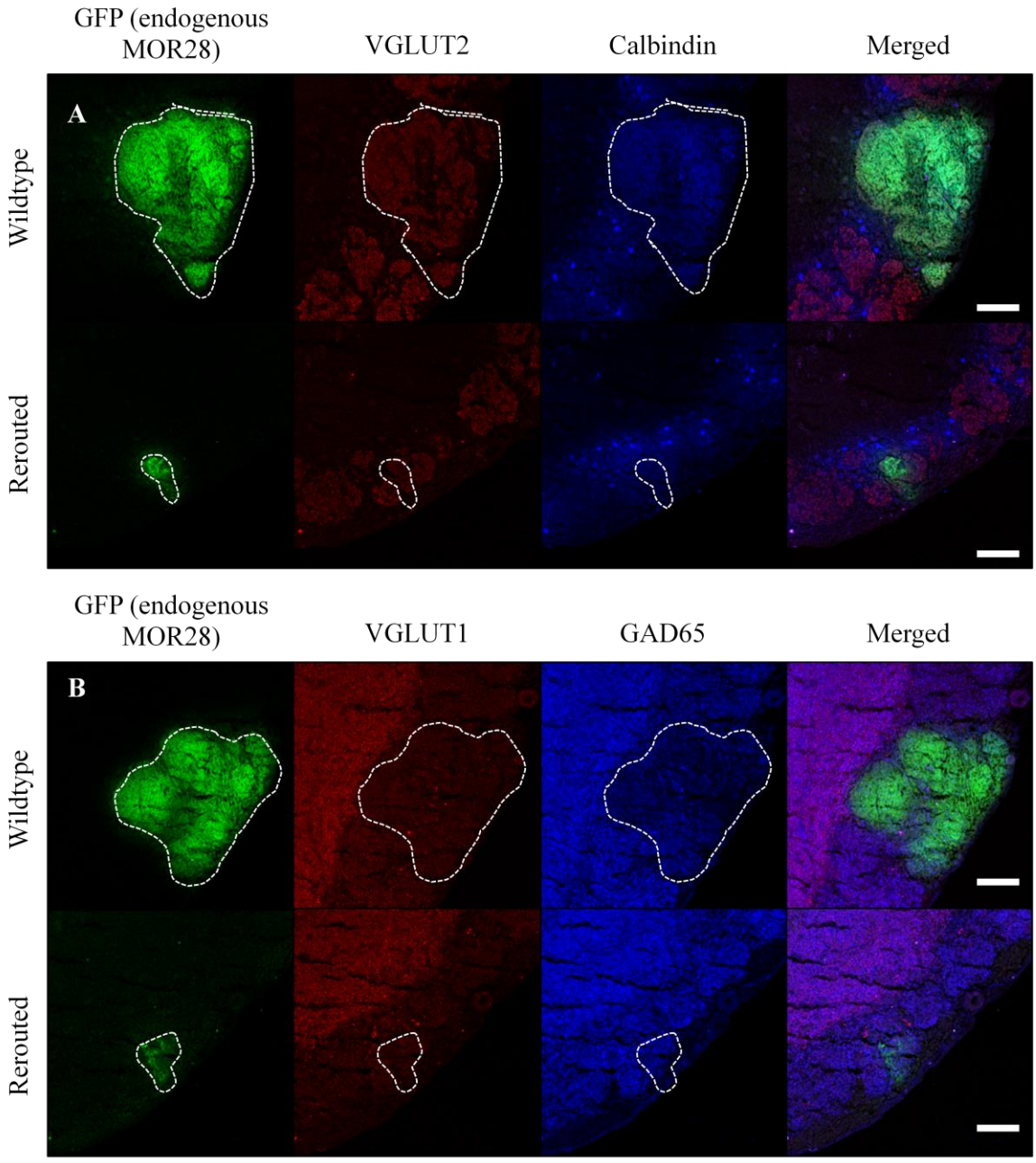

Figure 3. The small rerouted glomeruli observed after dox treatment co-stain for the same glomerular markers as wildtype MOR28 glomeruli.

TO28L mice were treated with dox until P7. 8 months later the OBs were coronally sectioned and immunohistochemically stained for the indicated proteins. **A)** Both wildtype and the small rerouted MOR28 glomeruli co-stain for VGLUT2 and Calbindin. **B)** Both wildtype and the small rerouted MOR28 glomeruli do not co-stain for VGLUT1 and partially co-stain for GAD65. Scale bars 100 μm.

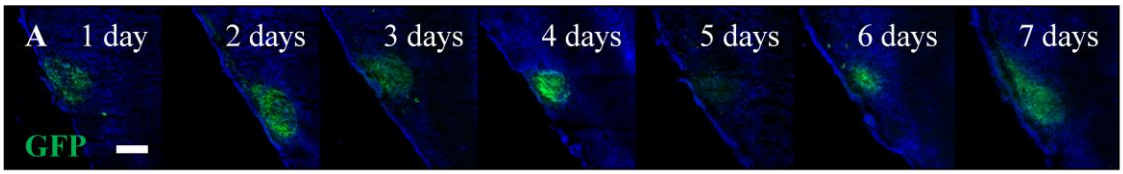

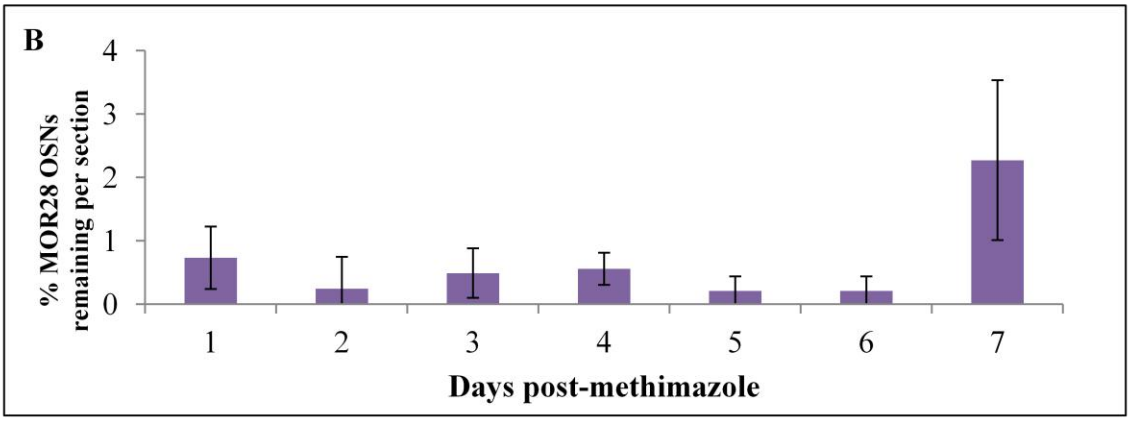

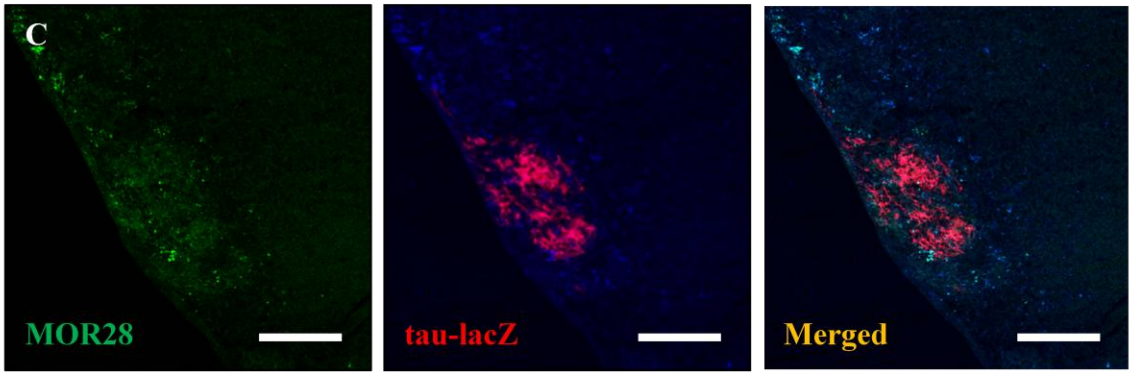

D	Pre-ablation	Post-ablation	Rerouted glomeruli	*n*
a	- dox	- dox	0 ± 0	1
b	- dox	+ dox	0 ± 0	3
c	+ dox	- dox	0 ± 0	2

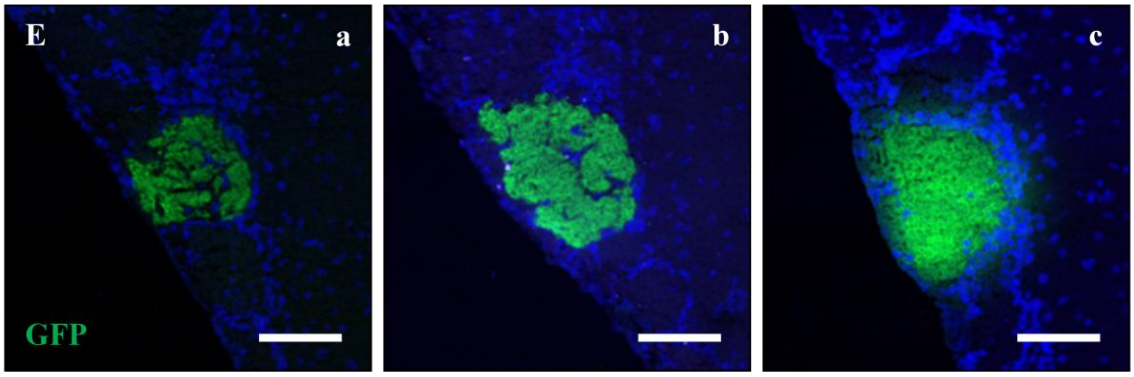

Figure 4. (legend continued on next page)

Figure. 4. Dox and the cell death caused by methimazole do not affect glomerular number.

A,B) Methimazole ablates 99.8% of MOR28 OSNs. Mice expressing MOR28-IRES-GFP were assayed at one day intervals post-methimazole. **A)** The fewest endogenous MOR28 axons were observed 5 days post-methimazole but the MOR28 glomeruli never completely disappear. **B)** Quantification of MOR28 OSNs per section in the MOE, expressed as the percentage of MOR28 OSNs per section in an untreated control. The lowest expression was observed 5 days post-methimazole (1 $\pm$ 1.095 OSNs out of 477 $\pm$ 48.9 in the control, or ~0.2%). Error bars shown are standard deviation. **C)** A mouse expressing TO28 assayed 5 days post-methimazole still expresses MOR28 and lacZ within the MOR28 glomeruli. **D)** Control mice given dox and methimazole do not form rerouted glomeruli. **E)** Representative images of the glomeruli quantified in C. A,C,E show coronal sections of OB immunohistochemically stained for the proteins indicated. Scale bars 100 μm.

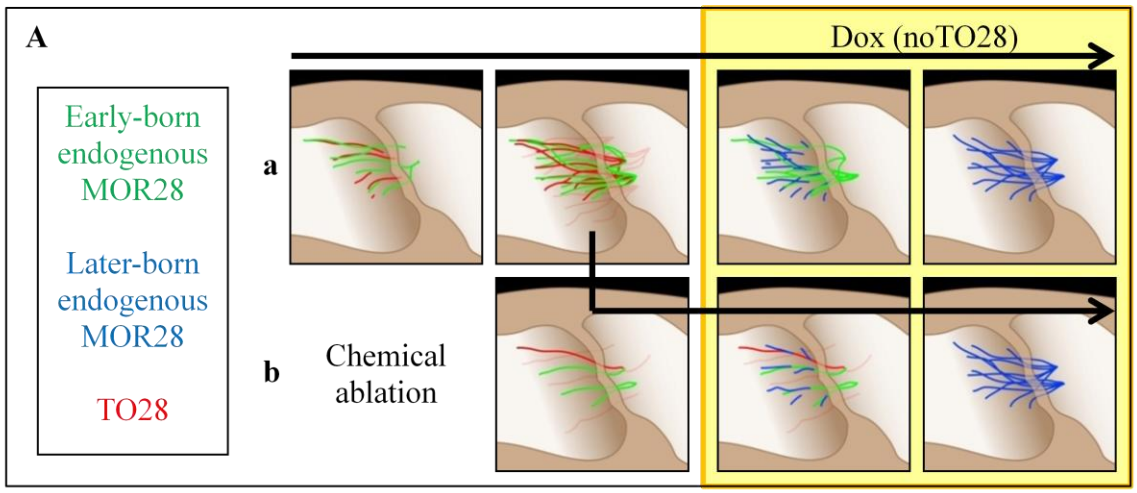

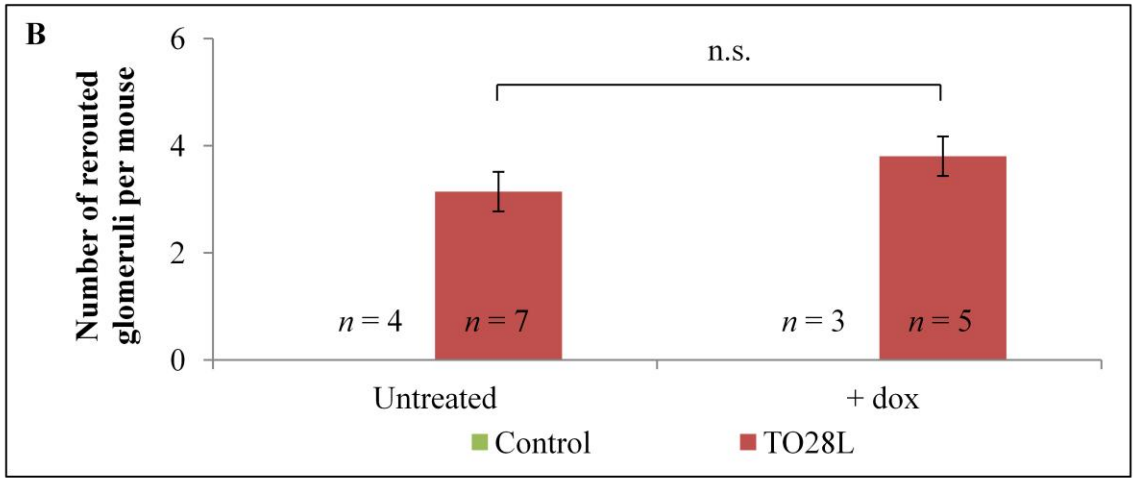

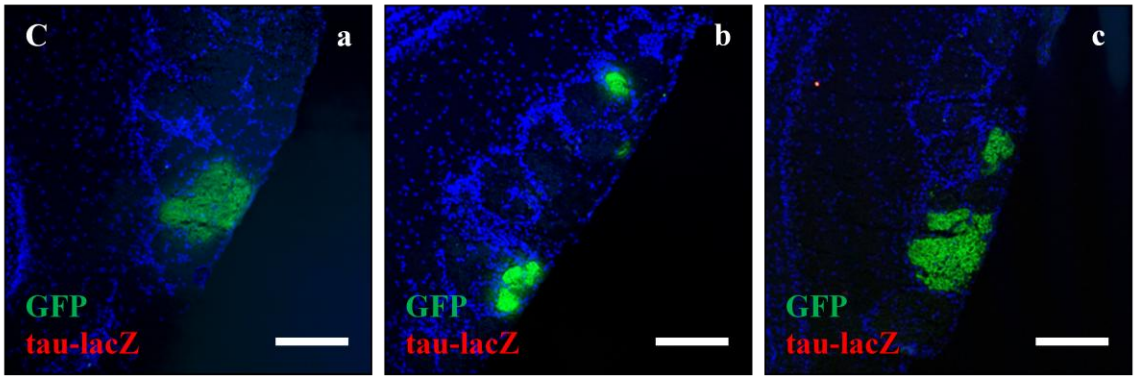

D	Pre-ablation	Post-ablation	Rerouted glomeruli
a	- dox (with TO28)	- dox (with TO28)	3.6 ± 0.98
b	- dox (with TO28)	+ dox (no TO28)	3 ± 1.15

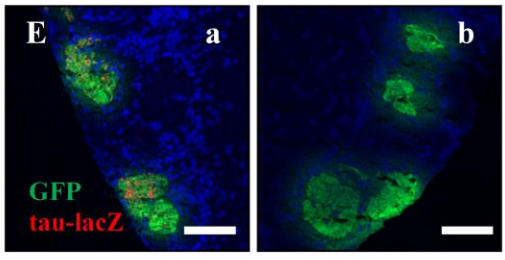

Figure 5. (legend continued on next page)

Figure 5. Rerouted glomeruli are maintained even without continuous transgene expression.

A) Summary of experiments, depicted as schematics of sagittal views of the olfactory system. a) Mice expressed TO28L until two months of age and were then treated with dox for ≥5 months. Later-born endogenous MOR28 axons continued to innervate rerouted glomeruli. b) Mice expressed TO28L until 2 months of age, were injected with methimazole, and then treated with dox for 2 months. Again, later-born endogenous MOR28 axons continued to innervate rerouted glomeruli. **B)** The number of rerouted glomeruli observed after TO28L has been silenced for more than 21 weeks is indistinguishable from that seen in untreated TO28L mice. ($p < 0.001$. Error bars shown are standard error.) **C)** Representative images of the glomeruli quantified in B. a) Control mouse treated with dox for 21 weeks. b) TO28L mouse treated with dox for 21 weeks. c) TO28L mouse treated with dox for 32 weeks. **D)** The number of rerouted glomeruli observed after 99.8% of MOR28 OSNs and TO28L expression are ablated is indistinguishable from that seen in TO28L mice treated only with methimazole. (a, $n = 5$; b, $n = 3$; $p > 0.050$, n.s. Errors shown are standard error.) **E)** Representative images of the glomeruli quantified in D. C,E show coronal sections of OB immunohistochemically stained for the proteins indicated. Scale bars 100 μm.

Chapter 4

Trace-amine associated receptor expressing neurons project to discrete glomeruli and constitute an olfactory subsystem

Acknowledgements and contributions

This work was supported by National Institute of Mental Health (NIMH) Grant 5R01MH086920 (to G.B.), by National Institute on Deafness and Other Communication Disorders (NIDCD) Grant RO3DC010273, a grant from the McKnight endowment fund for neuroscience (to S.L.), and by NIDCD Grant R01DC010155 (to S.D.L.). G.B. is a Pew Scholar.

L.Tsai performed the majority of the perfusions and dissections for all experiments. She conceived, collected data for, and worked with Andrew Loomis at Brown's Center for Computation and Visualization to generate the glomerular maps in figure 2. She wrote the methods and results sections for figure 2 and contributed to the review and revision of the drafts. She independently wrote the Appended Discussion with advice from G. Barnea.

*Johnson, M.A., *Tsai, L., Roy, D.S., Valenzuela, D.H., Mosley, C., Magklara, A., Lomvardas, S., Liberles, S.D., and Barnea, G. (2012). Neurons expressing trace amine-associated receptors project to discrete glomeruli and constitute an olfactory subsystem. Proc Natl Acad Sci U S A 109, 13410-13415.

*These authors contributed equally to this work

ABSTRACT

Some chemoreceptors of the TAAR family detect innately aversive odors and are proposed to activate hardwired olfactory circuits. However, the wiring of TAAR neurons, the regulatory mechanisms of *Taar* gene choice and the subcellular localization of TAAR proteins remain unknown. Here, we reveal similarities between TAAR and OR neurons, but also unexpected differences. Like ORs, TAARs appear to be monoallelically expressed and localized both in cilia, the site of odor detection, and in axons, where they may participate in guidance. TAAR neurons project to discrete glomeruli predominantly localized to a confined bulb region. *Taar* expression involves different regulatory logic than *OR* expression, as neurons choosing a *Taar5* knockout allele frequently express a second *Taar* without silencing the deleted allele. Moreover, the epigenetic signature of *OR* gene choice is absent from *Taar* genes. The unique molecular and anatomical features of the TAAR neurons suggest that they constitute a distinct olfactory subsystem.

INTRODUCTION

The rodent olfactory system is a powerful model for studying both learned and innate behaviors. Rodents detect a vast array of neutral odors that can be assigned behavioral relevance by learning, as well as pheromones and predator odors that stimulate instinctive responses. Thus, some olfactory circuits are highly plastic while others are hardwired (Dulac, 2000).

Odors are detected by several anatomically distinct areas in the nasal cavity that include the main olfactory epithelium (MOE), the vomeronasal organ (VNO) and the Grüneberg ganglion (Stowers and Logan). Neurons in each one of these sensory areas project to different regions of the main and accessory olfactory bulbs (Stowers and Logan, 2010), and the anatomical segregation between MOE and VNO persists in the projections to higher brain centers (Dulac and Torello, 2003). The sensory neurons in the olfactory system can be further classified based on the chemosensory receptors that they express. Sensory neurons in the MOE express odorant receptors (ORs) and trace amine-associated receptors (TAARs) (Buck and Axel, 1991; Liberles and Buck, 2006), and neurons in the VNO express three families of receptors (V1Rs, V2Rs and FPRs) (Liberles et al., 2009; Rivière et al., 2009; Stowers and Logan, 2010). Neurons that express V1Rs and V2Rs respond to different ligands, have different physical locations in the VNO, and project to different target regions of the accessory olfactory bulb (Dulac, 2000; Isogai et al., 2011). While TAAR and OR neurons are intermingled in the MOE, it is not known whether their axonal projections segregate to distinct anatomical regions of the olfactory bulb (OB).

Olfactory sensory neurons (OSNs) stochastically choose a single *OR* allele out of more than 2,000 possible alleles (Shykind, 2005). We have recently shown that certain chromatin modifications are involved in *OR* silencing and that silencing occurs prior to *OR* expression and thus forms the foundation for *OR* choice (Magklara et al., 2011). About 25% of mouse *OR* genes are pseudogenes (Young and Trask, 2002; Zhang and Firestein, 2002). When a pseudogene is selected for expression, it is turned off and the neuron switches to express another receptor gene (Lewcock and Reed, 2004; Serizawa et al., 2003; Shykind et al., 2004). A mechanism by which the functional OR generates a feedback signal to stop switching has been proposed to control this process (Shykind, 2005). Once expressed, ORs are found in cilia, where they detect odors, as well as in axons, where they instruct axon guidance (Barnea et al., 2004). OSNs expressing the same OR, while randomly dispersed within a broad zone of the epithelium, project axons to two spatially invariant glomeruli in each OB (Mori and Sakano, 2011). Second order projection neurons called mitral cells then transmit olfactory information to several cortical and limbic areas (Sosulski et al., 2011). Several lines of evidence indicate that some MOE receptors mediate innate, odor-driven responses to potential mates, intruders, offspring, and predators (Kobayakawa et al., 2007; Mandiyan et al., 2005) and must therefore couple to hardwired neural circuits. Consistent with this notion, the projections from specific glomeruli to the cortical amygdala are more spatially concentrated and stereotyped than those to the piriform cortex (Sosulski et al., 2011).

TAARs belong to a distinct and evolutionarily conserved family of G protein-coupled receptors that are distantly related to biogenic amine receptors and not related to ORs. There are 15 intact *Taar* genes in the mouse, 14 of which are expressed in a

dispersed pattern of OSNs similar to *OR* genes. TAAR OSNs do not co-express other TAARs or any of the ORs examined (Liberles and Buck, 2006). All olfactory TAARs, with the exception of TAAR6 and at least one member of the TAAR7 subfamily, are expressed in the dorsal MOE (Ferrero et al., 2011). Known ligands for olfactory TAARs include volatile and highly aversive amines, such as 2-phenylethylamine, a carnivore odor that repels rodents, and isoamylamine, a leucine metabolite that is avoided by mice (Ferrero et al., 2011; Ferrero et al., 2012; Kobayakawa et al., 2007; Liberles and Buck, 2006). TAARs that detect aversive odors have been proposed to activate stereotyped neural circuits. However, the projection patterns of TAAR OSNs to the OB, the subcellular localization of TAARs, and the gene choice mechanisms controlling *Taar* expression have not yet been characterized.

Here, we show that TAAR OSNs are similar to OR OSNs in some regards, but also have some unexpected and unique features. Like ORs, TAARs are localized to cilia, where they can detect odors, and also to axons. TAAR OSNs project to discrete glomeruli, but the OSNs expressing each TAAR form 4-6 glomeruli per bulb while OR OSNs converge on only 2 glomeruli per bulb. Most of the TAAR glomeruli are confined to a specific region in the dorsal OB. Surprisingly, TAAR OSNs express the cell adhesion molecule OCAM, which is predominantly expressed in OSNs that project to the ventrolateral OB (Yoshihara et al., 1997). Examination of knockout mice in which the coding sequence of *Taar5* is replaced by *LacZ* suggests that TAARs are expressed monoallelically, and that neurons choosing the deleted allele reselect another *Taar* with ~50% frequency. Remarkably, unlike switching from expression of an OR pseudogene, the reselection of another *Taar* does not involve shutting off the original pseudogene,

indicating that the mechanisms of switching and perhaps of receptor choice are distinct in TAAR OSNs. Consistent with this notion, we found that the epigenetic hallmarks of *OR* gene choice are not found on *Taar*s. Taken together, our observations suggest that the TAAR OSNs constitute a distinct olfactory subsystem.

MATERIALS AND METHODS

Animals. C57/Bl6 mice were purchased from Jackson Labs, and Taar5 knockout mice were purchased live from the Knockout Mouse Project Repository. All animal procedures were in compliance with guidelines of the institutional animal care and use committees of Brown, Harvard, and University of California, San Francisco. Genotyping information is provided in SI Materials and Methods.

Antibody Generation. Antibodies were generated as previously described (Barnea et al., 2004). Immunogen information is provided in SI Materials and Methods

Immunohistochemistry. All of the images shown are from tissue from adult mice. Protocol details are provided in SI Materials and Methods.

Two-Color RNA FISH. Two-color RNA FISH experiments were performed as described previously (Liberles et al., 2009), except that hybridizations were done at 58 °C. Probe information is provided in SI Materials and Methods.

Glomerular Distribution Maps. Flattened 2D plots of the dorsal OB were reconstructed from coronal sections stained with antibodies against each receptor. In each plot, the top is the anterior part of the bulb, and the bottom is the posterior part. The position of the center of each glomerulus was defined as the distance from the anterior tip of the OB (y axis) and the distance from the midline (x axis). Additional details are provided in SI Materials and Methods. Whole-Mount X-Gal Staining. Whole-mount preparations were dissected and stained with X-gal. Images were taken using a Nikon SMZ1500 stereomicroscope. Additional details are provided in SI Materials and Methods.

Epigenetic Analysis. Native chromatin preparations were performed as previously described (Magklara et al., 2011). Details are provided in SI Materials and Methods.

SUPPORTING MATERIALS AND METHODS

Fluorescence in situ *hybridization with immunohistochemistry*

Fluorescence RNA *in situ* hybridization combined with immunohistochemistry experiments were performed as described (Liberles et al., 2009). We used sense and antisense RNA probes specific for *Taar4, Taar5* and *Taar6* transcripts that were labeled with digoxigenin. The sequences of these probes correspond to nucleotides 1–226 of *Taar4* (accession number NM_001008499), nucleotides 816–1014 of *Taar5* (accession number NM_001009574), and nucleotides 739–988 of *Taar6* (accession number NM_001010828). The probes were detected with sheep anti-digoxigenin-POD (Roche Applied Science) followed by Cy3 tyramide (PerkinElmer).

Generation of degenerate OR probe for in situ hybridization

Degenerate primers were used to amplify OR sequence segments from TM3-TM6 as described (Liberles and Buck, 2006). The sequence of the degenerate primers were as follows except that a 25 bp T7 promoter sequence was added to the P27 primer:

P26: GCITA(C/T)GA(C/T)CGITA(C/T)GTIGCIATITG

P27_T7: AATTGTAATACGACTCACTATAGGG

ACIACIGAIAG(G/A)TGIGAI(G/C)C(G/A)CAIGT

Degeneracy of the probe template was validated by restriction digest with HinfI as described (Liberles and Buck, 2006).

Reverse transcription PCR

RNA was isolated from main olfactory epithelia using the PureLink Micro-to-Midi Total RNA Purification System (Invitrogen). cDNA was reverse transcribed using the Superscript III First-Strand Synthesis System (Invitrogen). cDNAs prepared from the various mouse strains were used as PCR templates with Phusion polymerase (Finnzymes) and specific primers pairs designed to amplify < 1 kb fragments of M71, MOR28, Taar5, LacZ or Cre.

RESULTS

TAARs are expressed on the dendrites of OSNs

To reveal the subcellular localization of TAARs within OSNs, we generated antibodies against three members of the murine family (TAAR4, TAAR5 and TAAR6). Antibody specificity was validated by staining HEK293 cells transfected with expression vectors bearing *Taar4*, *Taar5* or *Taar6* (Fig. S1A) and by staining histological sections from the MOE in conjunction with fluorescence *in situ* hybridization (FISH) using specific cRNA riboprobes (Fig. S1B–D). Each antibody labeled only HEK293 cells transfected with the appropriate plasmid and OSNs marked by the appropriate cRNA riboprobe.

Histological staining experiments with the three antibodies revealed non-overlapping populations of OSNs in broad zones in the MOE (Fig. 1). As revealed by previous RNA FISH experiments (Ferrero et al., 2011; Liberles et al., 2009), TAAR4 and TAAR5 neurons are found in the dorsal area of the MOE while TAAR6 neurons are located more ventrally (Fig S2). Furthermore, subcellular analysis indicated that like ORs (Barnea et al., 2004), these three TAARs are highly expressed on the dendrites of OSNs and in perinuclear compartments likely corresponding to the endoplasmic reticulum and Golgi apparatus (Fig. 1). The high levels of dendritic expression strongly support the proposed role for TAARs as *bona fide* receptors for volatile amines in the environment.

The axons of TAAR neurons converge on distinct glomeruli

To test whether OSNs expressing a given TAAR converge on particular glomeruli, we performed antibody staining of OB histological sections. Each TAAR

antibody stained 4 to 6 glomeruli within the dorsal part of each bulb (Fig. 2A–C), with some glomeruli occupying a medial position while others are slightly more lateral. Co-staining experiments with antibodies against TAAR4 and TAAR5 revealed some adjacent but distinct glomeruli (Fig. 2*D–F*). These results indicate that neurons expressing TAARs converge on distinct glomeruli like those expressing ORs. However, we observe more variability in the exact positions and numbers of the TAAR glomeruli than is the case with OR glomeruli (Fig. 2*G–K* and Fig. S3). We have not detected consistent differences in the positions or numbers of glomeruli between males and females (Fig. S3).

Neurons choosing a Taar5-deletion allele reselect other Taars

We next analyzed MOE from mice carrying a modified allele (*Taar5*^{LacZ}*)* in which the coding sequence of *Taar5* is deleted and replaced by *LacZ*, which encodes the enzyme β-galactosidase (β-gal). In these mice, neurons that select the modified allele (*Taar5*^{LacZ}) express β-gal instead of TAAR5. Histological MOE sections from *Taar5*$^{LacZ/+}$ animals were analyzed (Fig. 3A and B) by two-color FISH using a probe for *LacZ* (red), which identifies the modified allele, and probes for various *Taars* and *ORs* (green). As a control, two *LacZ* probes (green and red) labeled identical OSNs (Fig. 3A). We found populations of *LacZ*+ OSNs that were co-labeled by each of 8 different *Taar* probes (Fig. 3B), with frequencies that ranged from 2.5% (*Taar3*) to 10% (*Taar9*). Probes for *Taar7a* and *Taar8a* recognize multiple members of the same subfamily. Combining the frequencies of reselection of all *Taars* indicates that ~50% of the OSNs that initially chose the *Taar5*^{LacZ} allele reselected another *Taar*. For comparison, intact *Taar* genes are not co-expressed in the same neurons in wild-type (WT) animals (Liberles and Buck, 2006). Interestingly, we obtained evidence that *LacZ*+ neurons can reselect *Taar5*. Most

LacZ+ neurons (220/228) were negative for *Taar5*, consistent with the notion that like *ORs*, *Taar5* is expressed monoallelically in these neurons. The intensity of signal with *Taar5* was equivalent to that of other probes. Other *LacZ*+ neurons (8/228) were co-labeled with *Taar5*, revealing that *Taar* reselection can occur in trans, like *OR* switching (13), and that there is no preferential reselection of *Taar5* among *Taar* genes. In an attempt to account for the remaining 50% of *LacZ*+ neurons, we probed for 5 different *ORs* that are expressed in the *Taar5* zone of the MOE and with a degenerate probe that recognizes multiple *ORs* (Fig. S4). We observed 0% overlapped cells (0/503) for four *OR* probes, ~1% overlapped cells (2/194) for the fifth, and ~1% overlapped cells (2/187) for the degenerate *OR* probe. Thus, neurons expressing the $Taar5^{LacZ}$ allele exhibit a strong bias to reselect a second *Taar*.

As expected, when we stained MOE from $Taar5^{LacZ/LacZ}$ mice with antibodies against β-gal and TAAR5, we observed β-gal+ but not TAAR5+ neurons (Fig. 3C). Some LacZ+ neurons were also labeled by antibodies to TAAR4 and TAAR6, indicating that reselection of a new *Taar* allele results in stable protein expression (Fig. 3D–F).

Expression of the Taar5-deletion allele persists after reselecting other Taars

To examine whether the $Taar5^{LacZ}$ allele is turned off in neurons that reselect other *Taars*, we stained wholemount preparations of OBs from 7-month-old $Taar5^{LacZ/LacZ}$ mice with X-gal. Surprisingly, expression of the deleted allele persists and neurons that express it innervate many glomeruli in a dorsal band in the OB (Fig. 4*A*). This is in stark contrast to what is observed in mice bearing an equivalent allele of an OR gene. In mice bearing the $P2^{LacZ}$ allele, the number of *LacZ*+ OSNs significantly

diminishes with time, and the β-gal+ fibers do not converge on the P2 glomerulus (Wang et al., 1998). The decrease in β-gal+ fibers is due to shut off of the deleted P2 allele (Shykind et al., 2004). We further confirmed the persistence of expression from the *Taar5*^{LacZ} allele by RT-PCR experiments that revealed that while the message of a deleted *OR* allele shut off, the deleted *Taar* allele continued to be expressed in the MOE of adult mice (Fig. S5).

We then co-stained histological sections from the OBs of *Taar5*$^{LacZ/+}$ mice with antibodies against β-gal and TAAR4 (Fig. 4*B*), TAAR5 (Fig. 4*C*) or TAAR6 (Fig. 4*D*). Consistent with the wholemount staining results, we observed multiple β-gal+ glomeruli spread over a dorsal band in the OB. For each one of the three receptors examined, we observed glomeruli that receive β-gal+ fibers. Thus, expression of *Taar* alleles persists even in the absence of a full-length TAAR, unlike *OR*s, where the production of full-length protein is necessary for maintaining the transcriptional stability of a chosen allele (Zhang and Firestein, 2002). OSNs that initially choose the *Taar5*^{LacZ} allele reselect another receptor with a strong bias towards other *Taars* and continue to express the original allele. Furthermore, OSNs that switch to a new *Taar* incorporate into the neural circuit of the new receptor.

Unlike the dorsal OR glomeruli, the TAAR glomeruli express OCAM

The cell adhesion molecule OCAM labels the axons of OR OSNs that converge on glomeruli in the ventrolateral OB (Yoshihara et al., 1997). OCAM is believed to participate in the initial sorting of the axons destined to these glomeruli from the axons heading to the dorsomedial portion of the OB (Chehrehasa et al., 2005). To molecularly

define the portion of the OB where the TAAR glomeruli are located, we stained bulbs from adult wild-type mice with antibodies against OCAM together with the antibodies against TAAR4, TAAR5 or TAAR6. To reveal all of the glomeruli, we also stained with antibodies against the vesicular glutamate transporter VGLUT2. As expected, most OCAM+ glomeruli are located in the ventrolateral portion of the OB. However, a small population of dorsomedial glomeruli and the axonal bundles that innervate them are also OCAM+. To our surprise, the TAAR4, TAAR5 and TAAR6 glomeruli were all among the OCAM+ ones (Fig. 5*A*–*C*). Staining of OBs from *Taar5*$^{LacZ/+}$ mice with antibodies against OCAM and β-gal revealed that the β-gal+ fibers innervated only OCAM+ glomeruli, suggesting that expression of OCAM is a general feature of TAAR OSNs (Fig. 5*D*).

Unlike the OR gene clusters, the Taar cluster is not covered by repressive heterochromatic marks

The observation that deletion of the coding sequence of *Taar5* does not affect the transcriptional stability of the mutant allele raises important questions regarding the molecular differences between the regulation of expression of *OR*s and *Taar*s. We have recently shown that *OR*s undergo an unusual heterochromatic silencing prior to *OR* activation and that the chosen *OR* allele is free from the trimethyl marks found on lysine 9 of histone H3 and lysine 20 of histone H4 (H3K9me3 and H4K20me3, respectively) (Magklara et al., 2011). Since our genetic data suggest a different regulatory logic behind *OR* and *Taar* choice, we examined whether this could be a reflection of the epigenetic state of *Taars* in the MOE. Analysis of the data collected in our previously described whole genome ChIP-on-chip experiments (Magklara et al., 2011) with a focus on

chromosome 10, the chromosome where the *Taar* genes are clustered, shows that *Taars* are indeed devoid of both H3K9me3 and H4K20me3 in chromatin preparations from the MOE, whereas *OR* genes located on chromosome 10 have high levels of both modifications (Fig. 6*A* and *B*). To verify the whole genome analysis, we performed ChIP-qPCR analysis using chromatin prepared from the MOE and measured the enrichment of H3K9me3 and H4K20me3 on *Taar1*, *Taar3* and *Taar5* in this tissue. In agreement with our ChIP-on-chip data, the three *Taar* genes are devoid of these modifications (Fig. 6*C* and *D*).

To further assess whether epigenetic silencing is involved in the transcriptional repression of *Taars,* we tested whether two other heterochromatin marks, dimethyl on lysine 9 of histone H3 (H3K9me2) and trimethyl on lysine 27 of histone H3 (H3K27me3) are enriched on these genes. H3K9me2 is found on *OR* genes in the stem cells of the MOE (HBCs) but is converted to H3K9me3 in the cells that commit to the neuronal lineage of this tissue. The levels of H3K9me2 on *Taars* are very low compared to our positive control (*Wnt2*), suggesting that this modification is also absent on these genes in the MOE (Fig. 6*E*). Finally, we examined whether *Taars* are subject to a Polycomb mediated repression like other clustered and developmentally regulated genes (i.e. *Hox* genes). H3K27me3 is considered an accurate epigenetic imprint for Polycomb repression, but this mark is also absent from the *Taars* tested (Fig. 6*F*). In conclusion, our ChIP-on-chip and Chip-qPCR analyses for all of the known repressive epigenetic marks have not revealed any evidence for an epigenetic silencing of *Taar* genes in the MOE. These observations strongly suggest that different mechanisms control *OR* and *Taar* gene choice.

DISCUSSION

Most of the odors that rodents detect acquire valence through experience that involves learning and association. Some odors, however, elicit innate and stereotyped behavioral responses towards members of the same species (pheromones) or other species (kairomones and allomones). Several lines of evidence suggest that some pheromones and kairomones are detected by OSNs in the MOE and not only by neurons in the VNO (Ferrero et al., 2011; Kobayakawa et al., 2007; Mandiyan et al., 2005). The activation of some neurons in a broad dorsal area of the MOE is implicated in innate odor avoidance responses (Kobayakawa et al., 2007). The ligands for olfactory TAARs include volatile and highly aversive amines (Ferrero et al., 2011; Kobayakawa et al., 2007; Liberles and Buck, 2006). TAARs have therefore been proposed to perform specialized functions by binding specific odors that activate hardwired neural circuits and ultimately elicit stereotyped, innate behaviors. A better understanding of the specialized roles of TAARs in mediating innate behaviors requires characterization of the projections of TAAR OSNs to the OB and of the mechanisms controlling *Taar* expression.

Our results reveal that TAAR OSNs converge on distinct sets of 4 to 6 glomeruli in the dorsal portion of the OB. It is noteworthy that most OR OSNs converge on only 2 glomeruli in each bulb. Thus, the convergence on multiple glomeruli could be a unique feature of TAAR OSNs. Interestingly, the locations of the TAAR glomeruli are less stereotyped than the positions of OR glomeruli. The TAAR glomeruli are located in a discrete dorsal region of the OB. Remarkably, OSNs expressing TAAR6, which are mostly located in a ventral zone of the MOE, also project dorsally in the OB. This is in contrast to OR OSNs that maintain a general organization where OSNs located ventrally

in the MOE tend to project to ventral glomeruli, and OSNs located in the dorsal zone of the MOE project dorsally in the OB (Miyamichi et al., 2005). This observation may reflect unique properties of the "TAAR region" of the OB, such as the projections from these glomeruli further into the brain.

The projection of the ventral TAAR6-expressing OSNs to dorsal glomeruli may also indicate that the axon guidance mechanisms involved in wiring the TAAR OSNs are different than those controlling the projection of OR neurons. Consistent with this notion, the axons of TAAR OSNs express the cell adhesion molecule OCAM that is predominantly associated with OR OSNs that project to the ventrolateral part of the bulb (Yoshihara et al., 1997). Indeed, one of the TAAR6 glomeruli is at the very dorsal end of the OCAM region of the lateral bulb (Fig. 5*C*).

Our experiments reveal that TAARs are highly expressed on dendrites, consistent with binding environmental ligands. Like ORs, TAARs are also expressed on axons suggesting that they may participate in axon guidance in a similar manner to the mechanism proposed for ORs (Barnea et al., 2004; Yoshihara et al., 1997). This mechanism whereby a receptor that functions primarily on the dendrite is also expressed at low levels on the axon and participates in guidance may be unique to the olfactory system. Such a dual function of receptors encoded by the non-related gene families of *ORs* and *Taars* could thus be an example of convergent evolution. Alternatively, this solution for the problem of axon guidance could be used in other neural circuits, and the massive convergence of axons on a glomerulus enables us to detect it.

Our results suggest that like *OR*s, *Taars* are expressed monoallelically. Furthermore, like OR OSNs, when TAAR OSNs choose an allele that does not encode a functional receptor, they allow the expression of another receptor allele. The high frequency of reselection of other *Taars* may indicate that these OSNs are dedicated to expressing *Taar*s. However, we cannot rule out that TAAR OSNs could also express certain *OR*s or perhaps other receptors. Reselection is not restricted to the adjacent genes in the cluster although there may be a bias for genes that are downstream of *Taar5*. The high frequency of reselection of *Taar6,* which is normally expressed more ventrally than *Taar5*, indicates that the zonal restriction of *Taar* expression operates only in earlier developmental stages of the OSN. Finally, the observation that heterozygous mice turn on the other *Taar5* allele indicates that the reselection can occur in trans.

Each TAAR OSN expresses only one functional *Taar* (Liberles and Buck, 2006). We observe that neurons expressing a *Taar*-deletion allele express a second *Taar*, consistent with a role for the *Taar* coding sequence in preventing expression of a second receptor. Surprisingly, the expression of the *Taar*-deletion allele persists even after another gene is chosen. By contrast, OR OSNs only allow transcription of a single *OR* allele at a time, so for a new functional allele to be activated the initially chosen pseudogene must be turned off (Lewcock and Reed, 2004; Serizawa et al., 2003; Shykind et al., 2004). What we observe with *Taar*s is therefore not gene switching, but rather reselection of another *Taar* allele and permission for concomitant expression. Whereas in OR OSNs the coding sequence of the expressed *OR* is necessary both to inhibit switching to another *OR* and to stabilize receptor choice, in TAAR OSNs, the coding sequence of

the expressed *Taar* inhibits the selection of another *Taar* but does not affect the stability of receptor choice.

In view of our observation that deleting the coding sequence of *Taar5* does not affect the transcriptional stability of the mutant allele, we analyzed the molecular differences between the regulation of expression of *ORs* and *Taar*s. We previously showed that *ORs* undergo an unusual heterochromatic silencing by the addition of H3K9me3 and H4K20me3 marks before *OR* activation and that the chosen allele is free from these marks (Magklara et al., 2011). Examination of the *Taar* genes revealed that *Taars* are devoid of these marks whereas *ORs* located on the same chromosome are highly enriched for them. Furthermore, our analyses for all of the known repressive epigenetic marks have not revealed any evidence for epigenetic silencing of *Taar*s in the MOE. These observations strongly suggest that different mechanisms control *OR* and *Taar* gene choice. Most *ORs* are organized in clusters on almost all of the chromosomes. By contrast, the *Taar* family is a single cluster on chromosome 10. Our data suggest that TAAR OSNs are mostly limited to choosing *Taars*. Thus, the challenge of choosing a single allele is reduced in these OSNs, and may allow for a different mechanism of choice. In mice, 25% of *OR*s are pseudogenes (Young and Trask, 2002; Zhang and Firestein, 2002), but only *Taar7c* is a pseudogene. Thus, the burden of pseudogene selection is significantly lower in TAAR OSNs. Furthermore, if TAARs detect mostly aversive odors, there may have been less selective pressure for a mechanism to assure singular *Taar* expression. Our data regarding *Taar* reselection are reminiscent of the *Drosophila* opsins that generate a feedback signal, the absence of which allows

photoreceptor neurons to express an additional opsin gene without terminating transcription of the originally selected allele (Vasiliauskas et al., 2011).

Our data suggest that TAAR OSNs constitute a distinct olfactory subsystem since they differ from OR OSNs in their mechanisms of gene choice, some aspects of axon guidance, and in their projection patterns in the OB. The similarities between *Taar*s and *ORs* also raise interesting evolutionary questions. It seems that these two distinct families of chemoreceptors evolved to be expressed monoallelically in the MOE, but the mechanisms controlling singular expression appear to be different. The receptors from both families evolved to be expressed both on the dendrites of OSNs, where they function as chemoreceptors, and on their axons, where they may participate in guidance. TAAR OSNs are posed to extract specific environmental cues and participate in circuits that evoke uniform and innate responses. Our analysis of the projection patterns of TAAR OSNs in the OB may facilitate dissection of the next level of these circuits to determine whether they are indeed hardwired.

APPENDED DISCUSSION

Chapters 2 and 3 of this thesis focused on the axonal guidance of OR-expressing OSNs. These neurons have been associated with circuits that mediate learned behaviors in response to chemical cues. Classically, the various olfactory subsystems were thought to be divided by the class of behaviors they mediated, with the entire MOE associated with learned behaviors and the VNO associated with pheromonal behaviors. However, it has become increasingly clear that this view is an oversimplification of the system. The VNO does not mediate all pheromonal behavior since TrpC2 (a transient receptor potential channel) knockout mice lacking functional vomeronasal sensory neurons still exhibit some pheromone-mediated behaviors such as mating (Kimchi et al., 2007). Furthermore, there are other innate, experience-independent behaviors that are not pheromonal. Besides responding to other members of their own species, mice also show stereotyped avoidance behavior in response to predators and spoiled food. Strong evidence that these other types of innate behaviors are mediated by the MOE comes from Kobayakawa et al. when they found that mice lacking only subsets of OSNs in the MOE lost their innate aversion to molecules produced by spoiled food and predators. However, these mice were still capable of detecting these odors and could be learn to associate them with a fear response (Kobayakawa et al., 2007). This strongly suggests that parallel but independent processing streams mediate innate and learned behaviors.

If OR-expressing OSNs mediate learned responses to odorants, what other neurons in the MOE could be mediating these innate aversive behaviors? A relatively new class of OSNs, discovered in 2006 by Liberles and Buck, expresses not ORs but TAARs (Liberles and Buck, 2006). In more recent studies the Liberles lab has verified *in*

vitro that murine TAARs are indeed activated by compounds found specifically in the urine of carnivores (Ferrero et al., 2011; Li et al., 2013). Pacifico et al. also verified *in vivo* that glomeruli innervated by TAAR-expressing OSNs are the glomeruli most sensitive to amines, molecules that are produced in decomposing tissue (Pacifico et al., 2012; Silla Santos, 1996). These lines of evidence strongly implicate TAAR-expressing OSNs in mediating innate behavior. To gain insight into TAAR-specific chemosensory processing, we compared and contrasted the axonal guidance of OR- and TAAR-expressing OSNs.

In this chapter we mapped the axonal projections of OSNs expressing TAAR4, TAAR5, and TAAR6. We did find some similarities between these OSNs and OR-expressing OSNs. For example, each neuron expressed only one allele of one TAAR and the TAAR proteins were also found at the axon tips of OSNs. If this localization occurs during axonal outgrowth, TAARs may also be involved in axonal guidance. In further support of this possibility, the population of OSNs expressing a given TAAR converged on a small number of homogeneous glomeruli. Similar results were concomitantly reported by another lab (Pacifico et al., 2012).

There were also striking differences in the axonal guidance of TAAR-expressing OSNs. Where one population of OR-expressing OSNs almost invariably project to two glomeruli per OB (Mombaerts et al., 1996; Potter et al., 2001; Ressler et al., 1994; Strotmann et al., 2000; Vassar et al., 1994), we found that each population of OSNs expressing TAAR4, TAAR5, or TAAR6 project to 4-6 glomeruli per OB. Not only were there more glomeruli than for OR-expressing OSNs, but the number of glomeruli was much less stereotyped, being different even between the two OBs in a given mouse.

Pacifico et al. also saw variability in the number of glomeruli targeted by a given TAAR though they reported only 2.5 $\pm$ 0.5 glomeruli per OB for TAAR4 (Pacifico et al., 2012). The difference in number between our results may be due to the difference in the way glomerular number was assayed. Pacifico et al. imaged only the dorsal surface of whole-mounts and used autofluorescence from TAAR-IRES-YFP or TAAR4-IRES-RFP mouse lines to identify glomeruli. Since their labeling technique visualizes the entirety of all labeled axons, and glomeruli are located in a layer beneath the axon tracts, their method may have obscured any glomeruli covered by TAAR-expressing axons. In contrast, we reconstructed glomeruli from coronal sections where only the axon tips are labeled so our method likely had higher spatial resolution and was able to identify all glomeruli.

One of the most striking observations about the axonal guidance of TAAR-expressing OSNs was that they did not strictly adhere to the mechanisms that cause OR-expressing OSNs in the dorsomedial MOE to project to the dorsal OB and the ventrolateral OSNs to project to the ventral OB. Specifically, TAAR6 was observed in the ventrolateral MOE and yet projected only to dorsal glomeruli. Similarly, expression of OCAM was previously only reported in ventrolateral OR-expressing OSNs (Yoshihara et al., 1997) and yet the dorsomedial TAAR-expressing OSNs that we mapped all expressed OCAM.

Pacifico et al. also quantified some additional differences between the TAAR- and OR-expressing OSNs. For example, they found that the TAAR glomeruli are more tightly clustered, with an average distance of 491 μm instead of the usual 700-1000 μm seen for ORs. Additionally, TAARs guide axons to glomeruli in a new zone they called the DIII zone. The TAAR glomeruli here are spatially segregated from the glomeruli targeted by

the class II OR-expressing OSNs in the DII zone and, while overlapping with part of the DI zone, are not co-innervated by the OSNs expressing class I ORs. Finally, they observed that some TAAR glomeruli are "fused" in that they are innervated by both medial and lateral axons (Pacifico et al., 2012). In contrast, the medial and lateral dorsal glomeruli formed by ORs such as M71 are cleanly segregated (Feinstein and Mombaerts, 2004). Perhaps the fusion of the two populations in TAAR glomeruli indicates that TAARs participate in a single processing stream dedicated to innate behavior and so the distinction between medial and lateral was not selectively preserved.

The most interesting questions concerning neuronal wiring in innate versus learned olfactory learning will likely lie beyond the glomeruli in how the OR and TAAR glomeruli signal into the olfactory cortex. The mapping of the TAAR glomeruli described here will facilitate these studies by identifying the relevant starting points for these future experiments. It will also be interesting to map the tufted cells that receive input from TAAR glomeruli. Will their axonal collaterals link the glomeruli expressing the same TAAR similar to that seen with glomeruli expressing the same ORs? Or is this sort of linkage only required to synchronize the mirrored glomeruli that otherwise signal independently?

Several of the above observations provide intriguing evidence that the TAAR-expressing OSNs comprise a new OSN subtype that is molecularly distinct from OR-expressing OSNs beyond just the expression of the chemoreceptor. Accordingly, when OSNs expressed a TAAR allele lacking a coding region, they predominantly switched to express a second TAAR rather than a new OR. Pacifico et al. reached a similar conclusion when they provided evidence that these OSNs are predisposed toward TAARs

as a first choice, before ever choosing a modified deletion allele. They also mention preliminary evidence that when TAAR subtype OSNs are forced to express a class I OR instead, they still project to the DIII zone along with unmodified TAAR-expressing OSNs (Pacifico et al., 2012). It would be interesting to force OSNs to co-express TAARs and ORs to see the relative contributions of these chemoreceptors to axonal guidance.

The work described in this chapter has also paved the way for studying other aspects of TAAR-expressing OSNs beyond their axonal guidance. For example, we are currently undertaking experiments addressing the behaviors mediated by TAAR-expressing OSNs and how input from TAAR-expressing OSNs is mapped onto the olfactory cortex. In conclusion, we have identified interesting similarities and differences in the axonal guidance of OR- and TAAR-expressing OSNs while also paving the way for future experiments to elucidate the function of these fascinating TAARs.

REFERENCES

Barnea, G., O'Donnell, S., Mancia, F., Sun, X., Nemes, A., Mendelsohn, M., and Axel, R. (2004). Odorant receptors on axon termini in the brain. Science *304*, 1468.

Buck, L., and Axel, R. (1991). A novel multigene family may encode odorant receptors: a molecular basis for odor recognition. Cell *65*, 175-187.

Chehrehasa, F., St John, J., and Key, B. (2005). The sorting behaviour of olfactory and vomeronasal axons during regeneration. J Mol Histol *36*, 427-436.

Dulac, C. (2000). Sensory coding of pheromone signals in mammals. Curr Opin Neurobiol *10*, 511-518.

Dulac, C., and Torello, A.T. (2003). Molecular detection of pheromone signals in mammals: from genes to behaviour. Nat Rev Neurosci *4*, 551-562.

Feinstein, P., and Mombaerts, P. (2004). A contextual model for axonal sorting into glomeruli in the mouse olfactory system. Cell *117*, 817-831.

Ferrero, D., Lemon, J., Fluegge, D., Pashkovski, S., Korzan, W., Datta, S., Spehr, M., Fendt, M., and Liberles, S. (2011). Detection and avoidance of a carnivore odor by prey. Proc Natl Acad Sci *108*, 11235-11240.

Ferrero, D.M., Wacker, D., Roque, M.A., Baldwin, M.W., Stevens, R.C., and Liberles, S.D. (2012). Agonists for 13 trace amine-associated receptors provide insight into the molecular basis of odor selectivity. ACS Chem Biol *7*, 1184-1189.

Isogai, Y., Si, S., Pont-Lezica, L., Tan, T., Kapoor, V., Murthy, V., and Dulac, C. (2011). Molecular organization of vomeronasal chemoreception. Nature *478*, 241-245.

Kimchi, T., Xu, J., and Dulac, C. (2007). A functional circuit underlying male sexual behaviour in the female mouse brain. Nature *448*, 1009-1014.

Kobayakawa, K., Kobayakawa, R., Matsumoto, H., Oka, Y., Imai, T., Ikawa, M., Okabe, M., Ikeda, T., Itohara, S., Kikusui, T., *et al.* (2007). Innate versus learned odour processing in the mouse olfactory bulb. Nature *450*, 503-508.

Lewcock, J., and Reed, R. (2004). A feedback mechanism regulates monoallelic odorant receptor expression. PNAS *101*, 1069-1074.

Li, Q., Korzan, W.J., Ferrero, D.M., Chang, R.B., Roy, D.S., Buchi, M., Lemon, J.K., Kaur, A.W., Stowers, L., Fendt, M., *et al.* (2013). Synchronous evolution of an odor biosynthesis pathway and behavioral response. Curr Biol *23*, 11-20.

Liberles, S., and Buck, L. (2006). A second class of chemosensory receptors in the olfactory epithelium. Nature *442*, 645-650.

Liberles, S., Horowitz, L., Kuang, D., Contos, J., Wilson, K., Siltberg-Liberles, J., Liberles, D., and Buck, L. (2009). Formyl peptide receptors are candidate chemosensory receptors in the vomeronasal organ. Proc Natl Acad Sci *106*, 9842-9847.

Magklara, A., Yen, A., Colquitt, B., Clowney, E., Allen, W., Markenscoff-Papadimitriou, E., Evans, Z., Kheradpour, P., Mountoufaris, G., Carey, C., *et al.* (2011). An epigenetic signature for monoallelic olfactory receptor expression. Cell *145*, 555-570.

Mandiyan, V.S., Coats, J.K., and Shah, N.M. (2005). Deficits in sexual and aggressive behaviors in Cnga2 mutant mice. Nat Neurosci *8*, 1660-1662.

Miyamichi, K., Serizawa, S., Kimura, H., and Sakano, H. (2005). Continuous and overlapping expression domains of odorant receptor genes in the olfactory epithelium determine the dorsal/ventral positioning of glomeruli in the olfactory bulb. J Neurosci *25*, 3586-3592.

Mombaerts, P., Wang, F., Dulac, C., Chao, S., Nemes, A., Mendelsohn, M., Edmonson, J., and Axel, R. (1996). Visualizing an olfactory sensory map. Cell *87*, 675-686.

Mori, K., and Sakano, H. (2011). How is the olfactory map formed and interpreted in the mammalian brain? Annu Rev Neurosci *34*, 467-499.

Pacifico, R., Dewan, A., Cawley, D., Guo, C., and Bozza, T. (2012). An olfactory subsystem that mediates high-sensitivity detection of volatile amines. Cell Rep *2*, 76-88.

Potter, S., Zheng, C., Koos, D., Feinstein, P., Fraser, S., and Mombaerts, P. (2001). Structure and emergence of specific olfactory glomeruli in the mouse. J Neurosci *21*, 9713-9723.

Ressler, K., Sullivan, S., and Buck, L. (1994). Information coding in the olfactory system: evidence for a stereotyped and highly organized epitope map in the olfactory bulb. Cell *79*, 1245-1255.

Rivière, S., Challet, L., Fluegge, D., Spehr, M., and Rodriguez, I. (2009). Formyl peptide receptor-like proteins are a novel family of vomeronasal chemosensors. Nature *459*, 574-577.

Serizawa, S., Miyamichi, K., Nakatani, H., Suzuki, M., Saito, M., Yoshihara, Y., and H, S. (2003). Negative feedback regulation ensures the one receptor-one olfactory neuron rule in mouse. Science *302*, 2088-2094.

Shykind, B., Rohani, S., O'Donnell, S., Nemes, A., Mendelsohn, M., Sun, Y., Axel, R., and Barnea, G. (2004). Gene switching and the stability of odorant receptor gene choice. Cell *117*, 801-815.

Shykind, B.M. (2005). Regulation of odorant receptors: one allele at a time. Hum Mol Genet *14 Spec No 1*, R33-39.

Silla Santos, M.H. (1996). Biogenic amines: their importance in foods. Int J Food Microbiol *29*, 213-231.

Sosulski, D., Bloom, M., Cutforth, T., Axel, R., and Datta, S. (2011). Distinct representations of olfactory information in different cortical centres. Nature *472*, 213-216.

Stowers, L., and Logan, D.W. (2010). Olfactory mechanisms of stereotyped behavior: on the scent of specialized circuits. Curr Opin Neurobiol *20*, 274-280.

Strotmann, J., Conzelmann, S., Beck, A., Feinstein, P., Breer, H., and Mombaerts, P. (2000). Local permutations in the glomerular array of the mouse olfactory bulb. J Neurosci *20*, 6927-6938.

Vasiliauskas, D., Mazzoni, E.O., Sprecher, S.G., Brodetskiy, K., Johnston, R.J., Jr., Lidder, P., Vogt, N., Celik, A., and Desplan, C. (2011). Feedback from rhodopsin controls rhodopsin exclusion in Drosophila photoreceptors. Nature *479*, 108-112.

Vassar, R., Chao, S., Sitcheran, R., Nuñez, J., Vosshall, L., and Axel, R. (1994). Topographic organization of sensory projections to the olfactory bulb. Cell *79*, 981-991.

Wang, F., Nemes, A., Mendelsohn, M., and Axel, R. (1998). Odorant receptors govern the formation of a precise topographic map. Cell *93*, 47-60.

Yoshihara, Y., Kawasaki, M., Tamada, A., Fujita, H., Hayashi, H., Kagamiyama, H., and Mori, K. (1997). OCAM: A new member of the neural cell adhesion molecule family related to zone-to-zone projection of olfactory and vomeronasal axons. J Neurosci *17*, 5830-5842.

Young, J.M., and Trask, B.J. (2002). The sense of smell: genomics of vertebrate odorant receptors. Hum Mol Genet *11*, 1153-1160.

Zhang, X., and Firestein, S. (2002). The olfactory receptor gene superfamily of the mouse. Nat Neurosci *5*, 124-133.

FIGURES

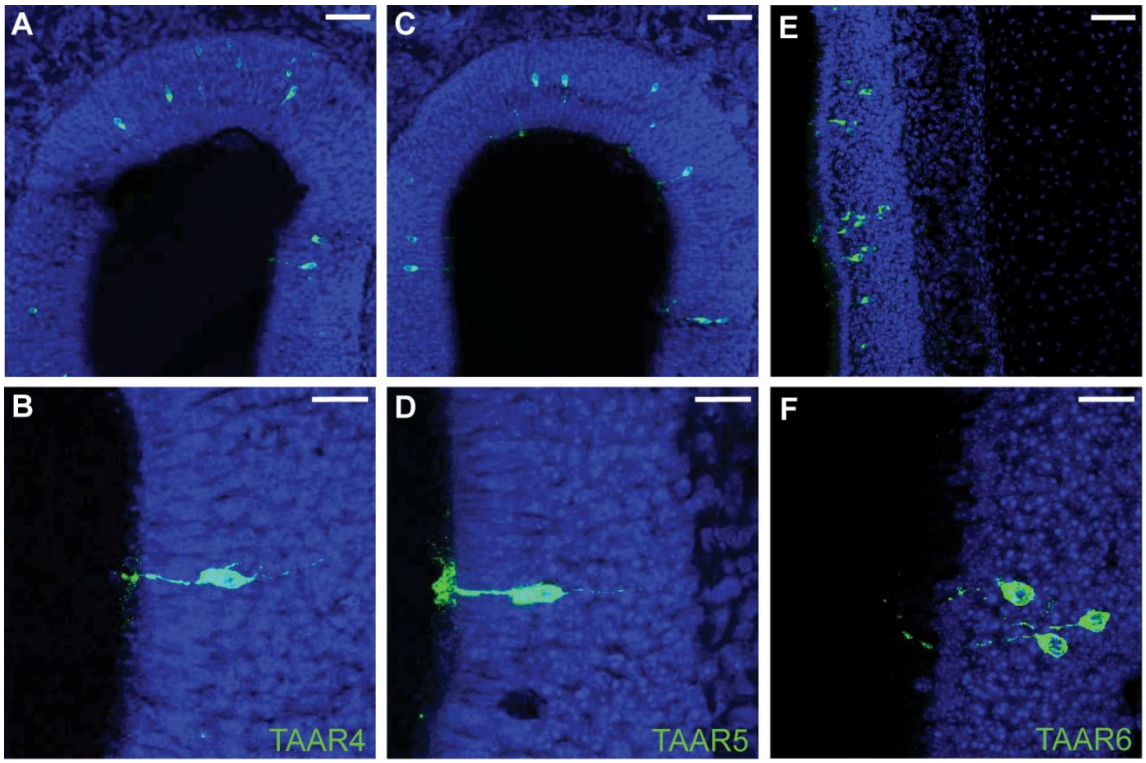

Figure 1. TAARs are highly expressed on dendrites.

Sections of MOE were stained with antibodies against TAAR4 (*A–C*), TAAR5 (*D–F*) or TAAR6 (*G–I*). Antibodies against TAAR4 and TAAR5 recognized distinct OSN populations in the dorsal MOE (*A* and *D*). TAAR6+ OSNs are more ventral in the MOE (*G*). High levels of staining are observed on dendrites and in perinuclear structures. Scale bars: 300 µm *A*, *D* and *G*; 50 µm *B*, *E* and *H*; 20 µm *C*, *F* and *I*.

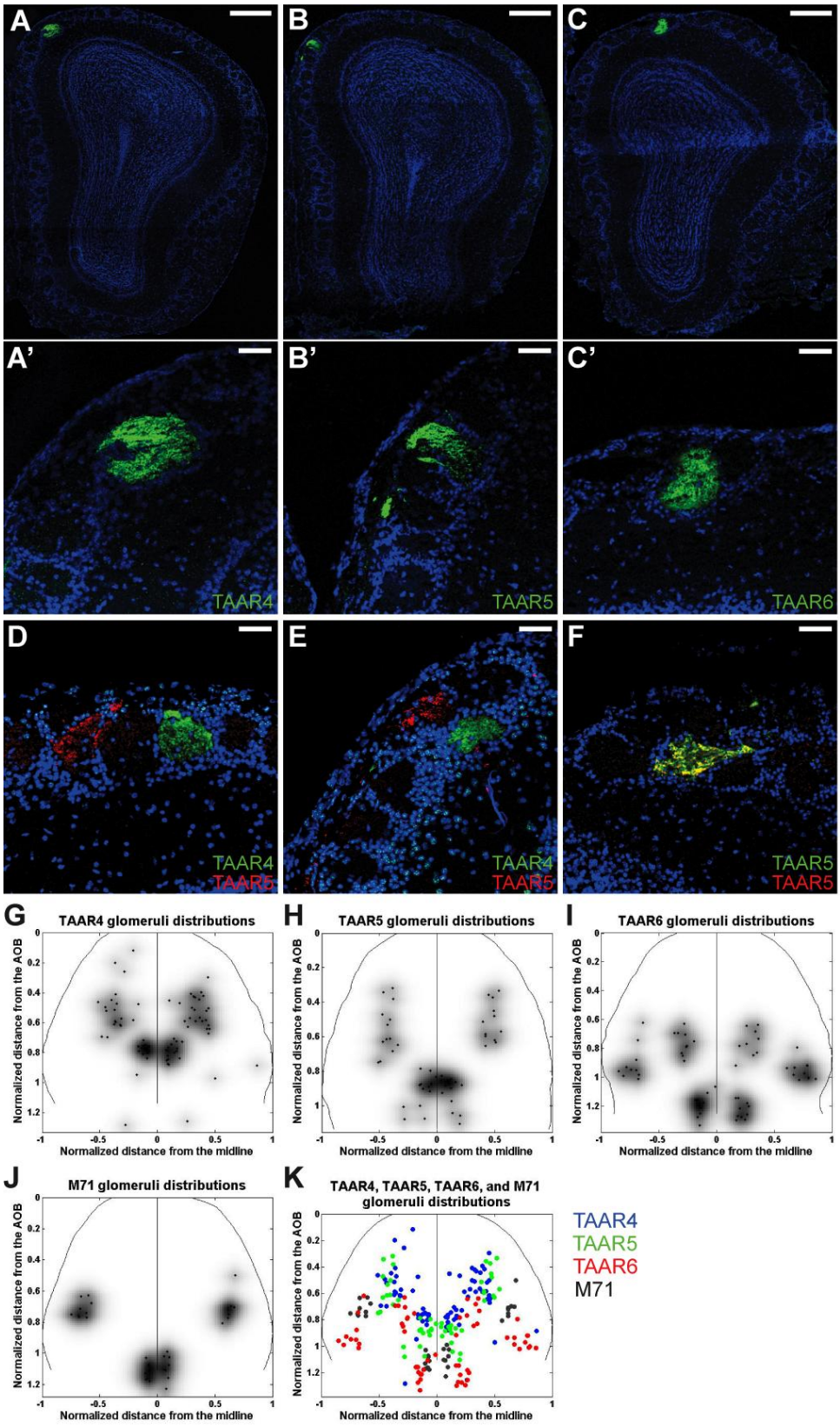

Figure 2. (legend continued on next page)

Figure 2. TAAR neurons project to distinct glomeruli.

Sections of OB were stained with antibodies against TAAR4 (*A* and *A'*), TAAR5 (*B* and *B'*) or TAAR6 (*C* and *C'*). Each antibody recognized a distinct group of glomeruli. We show representative glomeruli for each TAAR. Scale bars: 300 µm *A–C*; 50 µm *A'–C'*. (*D* and *E*) Co-staining with rabbit antisera against TAAR5 (red) and guinea pig antisera against TAAR4 (green) demonstrates that OSNs expressing different TAARs project to adjacent, but non-overlapping glomeruli. (*F*) Rabbit (red) and guinea pig (green) antisera against TAAR5 label the same glomerulus. Scale bars: 50 µm. (*G–K*) Smoothed density plots for the glomeruli of TAAR4 (*G*), TAAR5 (*H*), TAAR6 (*I*), and M71 (*J*). The normalized distance from the AOB is presented on the Y-axis (1 is the anterior tip of the AOB). The normalized distance from the midline is presented on the X-axis (0 is the boundary between the two bulbs). (*K*) Composite distribution of all TAAR4, TAAR5, TAAR6, and M71 glomeruli. Blue: TAAR4, green: TAAR5, red: TAAR6, black: M71.

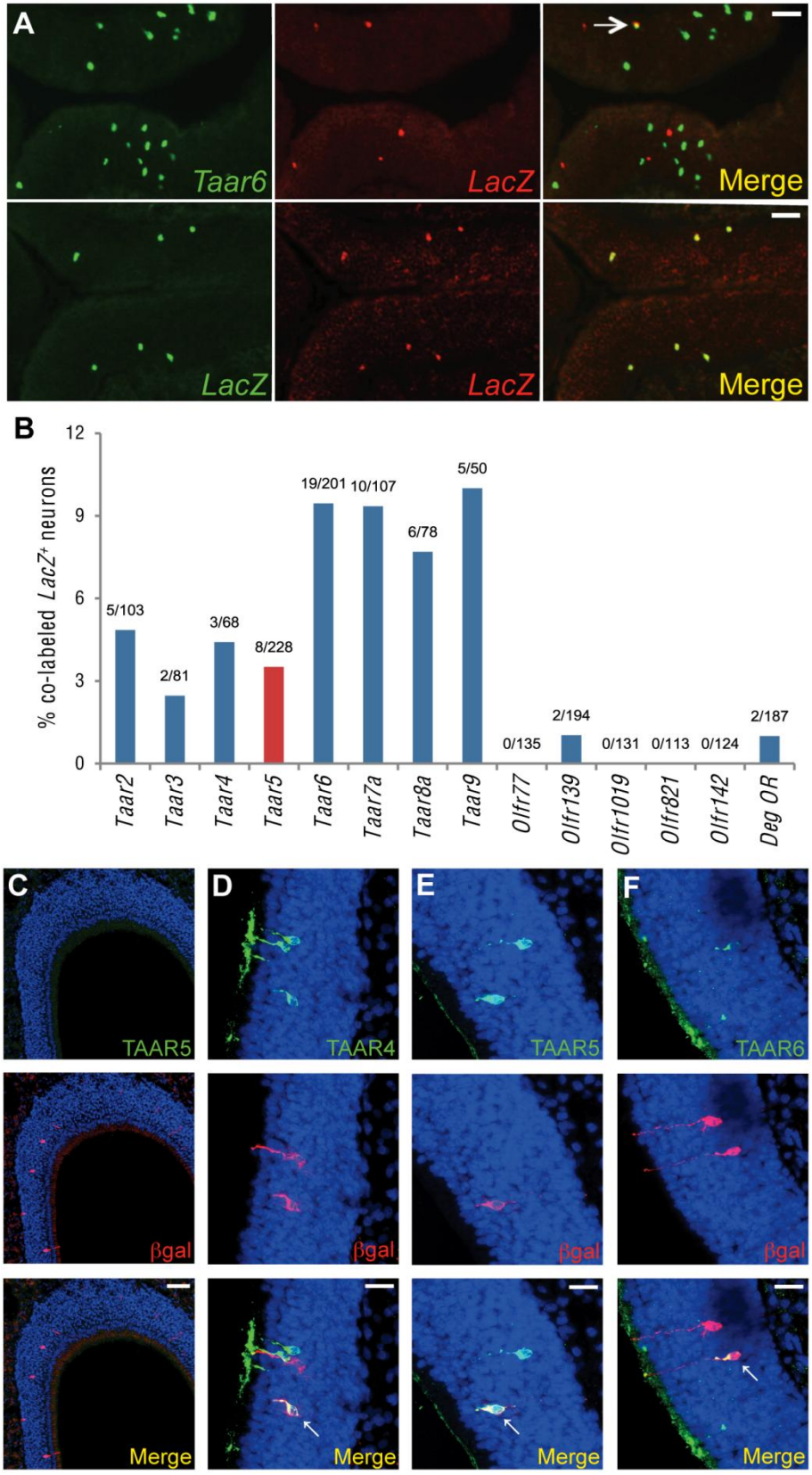

Figure 3. (legend continued on next page)

Figure 3. OSNs that choose a deleted Taar5 allele predominantly reselect other Taars.

MOE sections from mice that have the *Taar5* coding sequence replaced by *LacZ* (*Taar5*^{LacZ}) were analyzed by two-color FISH and by immunostaining. Except where indicated, *Taar5*$^{LacZ/+}$ animals were analyzed in all experiments. (*A*) A representative two-color FISH experiment with probes for *Taar6* (green) and *LacZ* (red) reveals distinct but overlapping populations of OSNs. The arrow marks a cell labeled by both probes. In a control experiment, two probes for *LacZ* (green and red) label the same OSNs. (*B*) Compilation and quantification of two-color FISH experiments with probes for *LacZ* and for the various *Taars* or *ORs* (including a degenerate probe that detects multiple *ORs*), as indicated. The bars represent the percent of *LacZ*+ neurons that were also labeled by the probe for each receptor, with specific cell counts indicated above. The red bar indicates neurons that are positive for *Taar5* and for *LacZ* (indicating switching to the WT allele of *Taar5*). Note that the probes for *Taar7a* and *Taar8a* recognize the entire respective *Taar* subfamily. Scale bars: 100 μm. (*C*) MOE of *Taar5*$^{LacZ/LacZ}$ stained with antibodies against TAAR5 (green) and β-gal (red). As expected, no signal is observed with the antibody against TAAR5. Scale bars: 100 μm. (*D*–*F*) MOE sections of *Taar5*$^{LacZ/+}$ were co-stained with antibodies against β-gal (red in all three panels) and TAAR4 (green in *D*), TAAR5 (green in *E*) or TAAR6 (green in *F*). Arrows in the Merge panels mark OSNs co-expressing β-gal and the corresponding receptors, indicating OSNs that switched from the deleted *Taar5* allele to express a new TAAR. Scale bars: 50 μm.

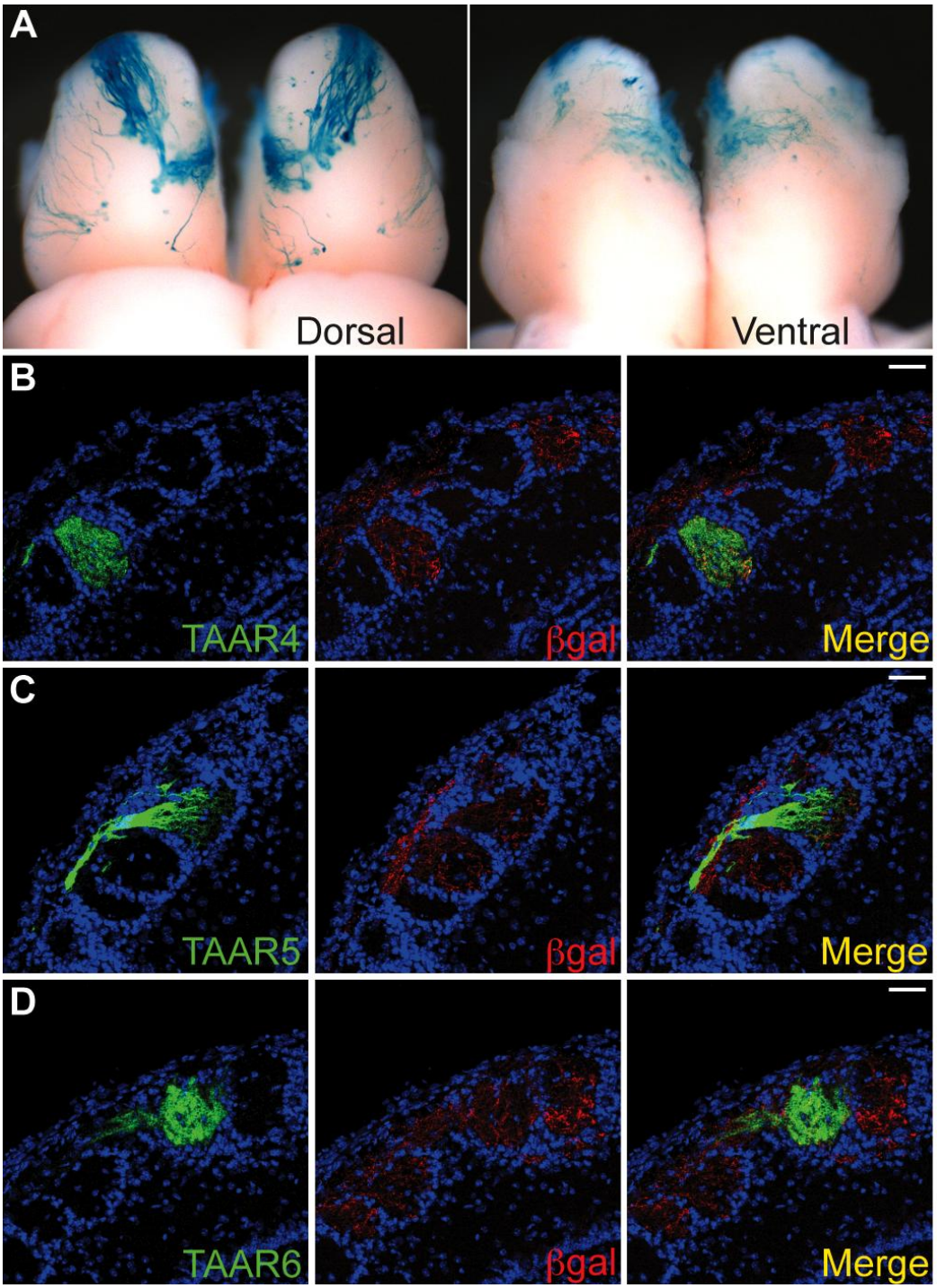

Figure 4. Expression of the Taar5-deletion allele persists after selecting another Taar.

(*A*) X-gal staining of wholemount preparations of OB from 7-month-old *Taar5*$^{LacZ/+}$ mice. Both dorsal and ventral views are presented. (*B–D*) Co-staining of OB sections from *Taar5*$^{LacZ/+}$ mice with antibodies against β-gal (red in all panels) and TAAR4 (green in *B*), TAAR5 (green in *C*), and TAAR6 (green in *D*). β-gal+ axons are observed in glomeruli for each TAAR. Scale bars: 50 μm.

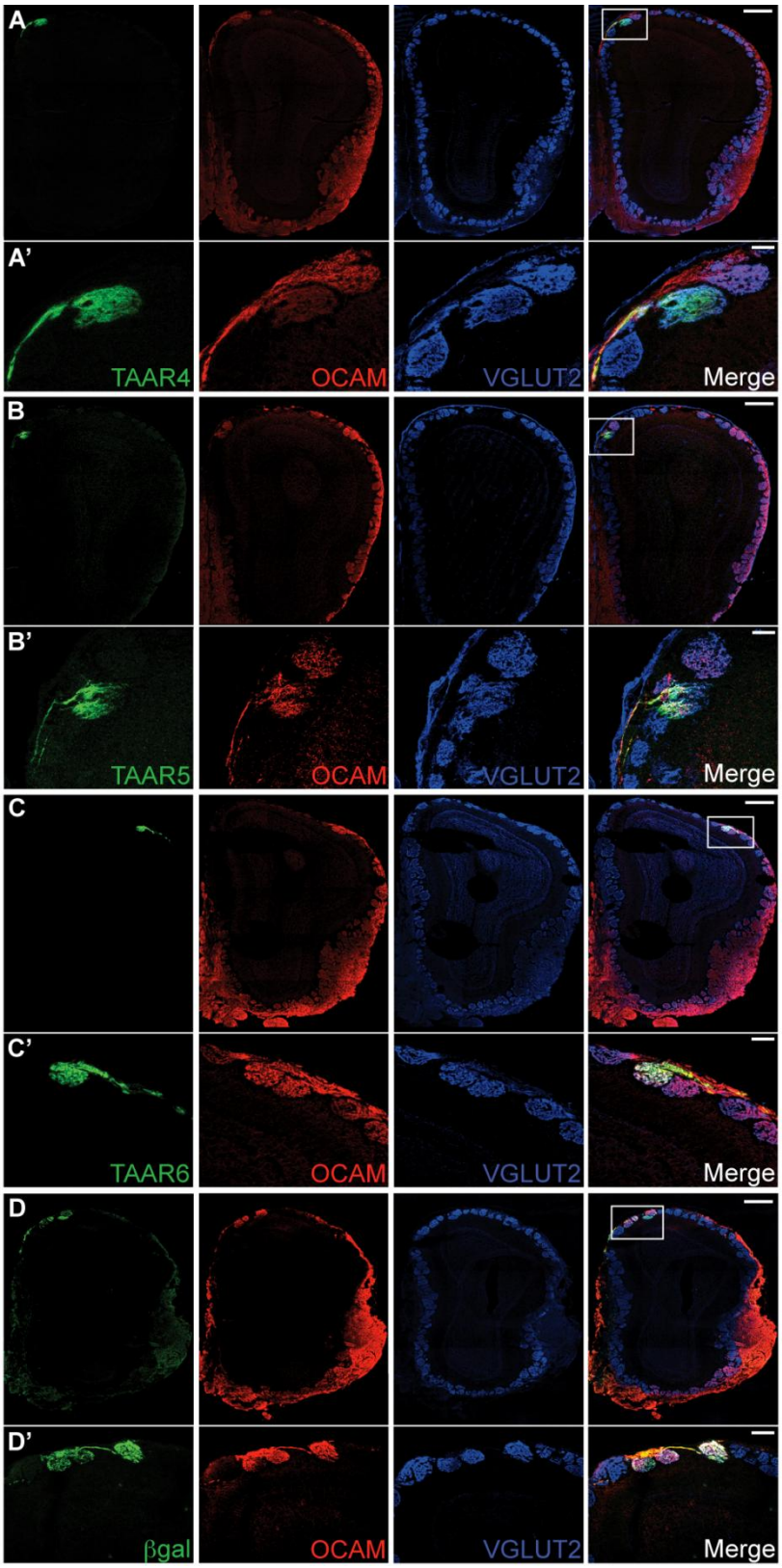

Figure 5. (legend continued on next page)

Figure 5. The TAAR glomeruli express the cell adhesion molecule OCAM.

OB sections from WT (*A–C*) or *Taar5*$^{LacZ/+}$ mice (*D*) were stained with antibodies against OCAM (red), the presynaptic marker vesicular glutamate transporter VGLUT2 (blue), and TAAR4 (green in *A* and *A'*), TAAR5 (green in *B* and *B'*), TAAR6 (green in *C* and *C'*) or β-gal (green in *D* and *D'*). Panels *A'–D'* represent high magnification images of the regions contained in the white boxes in the corresponding low magnification panels *A–D*. In all cases co-staining of OCAM and the various TAARs or β-gal is observed. Note that OCAM+ fibers innervate a cluster of dorsal glomeruli that include the TAAR glomeruli. Scale bars: 300 μm *A–D*; 50 μm *A'–D'*.

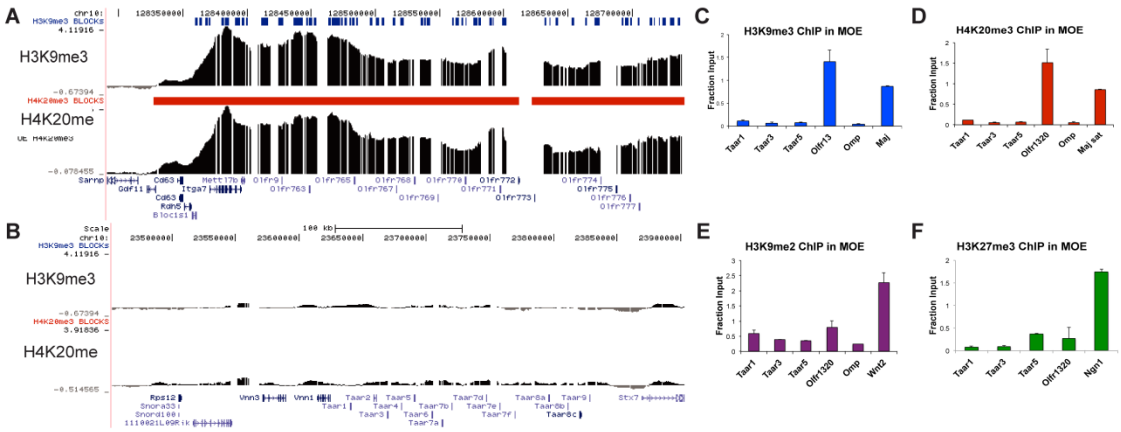

Figure 6. The Taar cluster is not covered by repressive heterochromatic marks.

(*A* and *B*) ChIP-on-chip experiments for H3K9me3 and H4K20me3 in the MOE as described (Magklara et al., 2011). (*A*) Part of an *OR* cluster on chromosome 10. The blue (H3K9me3) or red (H4K20me3) bars represent significant peaks (FDR ≤ 5%) identified by MA2C using parameters: window=10 kb, min number of probes=20 and max gap=1 kb. The black bars represent the enrichment of signal hybridization intensity over input DNA. (*B*) The *Taar* cluster, also on chromosome 10, is devoid of H3K9me3 or H4K20me3. (*C–F*) ChIP-qPCR analysis using native chromatin preparations from the MOE with various antibodies for repressive chromatin marks. In each case different genes serve as positive controls and *Omp* is used as a negative control as indicated. The gene *Olfr1320* is shown here as a representative *OR*. Values are the mean of duplicated qPCR. Error bars indicate SEM. (*C*) H3K9me3 ChIP-qPCR and (*D*) H4K20me3 ChIP-qPCR. Both *Olfr1320* and major satellite repeats (maj sat) serve as positive controls (Magklara et al., 2011). (*E*) H3K9me2 ChIP-qPCR. *Wnt2*, which is not particularly enriched on *OR*s from a whole MOE preparation (10), serves as a positive control. (*F*) H3K27me3 ChIP-qPCR. *Neurogenin1*, a developmentally regulated gene in the MOE, serves as a positive control. The *OR* clusters do not exhibit Polycomb mediated repression (Magklara et al., 2011).

SUPPORTING FIGURES

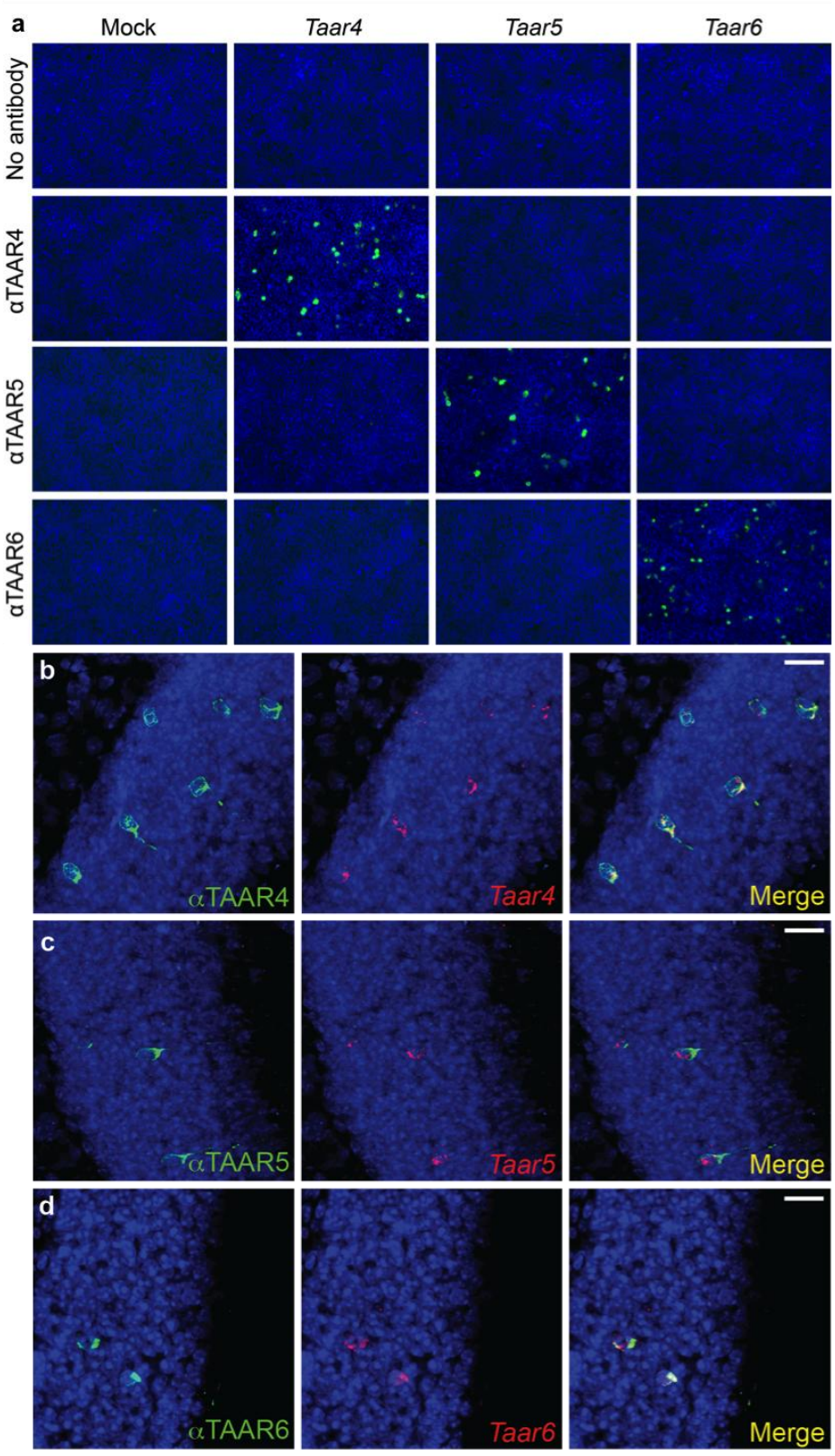

Figure S1. (legend continued on next page)

Figure S1. Validation of the specificity of the antibodies against TAAR4, TAAR5 and TAAR6.

(*A*) HEK293 cells were transfected with expression vectors encoding TAAR4, TAAR5 or TAAR6 and stained with the three antibodies. Vertical columns represent HEK293T cells that were transfected either with empty expression vector (*Mock*) or with an expression vector encoding TAAR4, TAAR5 or TAAR6. Horizontal rows were stained either with no primary antibody or with antibodies specific for TAAR4, TAAR5 or TAAR6. TAAR proteins are stained in green; nuclei are counterstained in blue. (*B–D*) Histological sections through the main olfactory epithelium were analyzed by immunostaining with the antibodies against TAAR4, TAAR5 or TAAR6 (green) and by RNA *in situ* hybridization with the specific probes for the corresponding receptors (red). Merged images indicate that in all cases identical neurons are detected by both methods. (*B*) TAAR4; (*C*) TAAR5; (*D*) TAAR6. Scale bars in *B–D*: 20 µm.

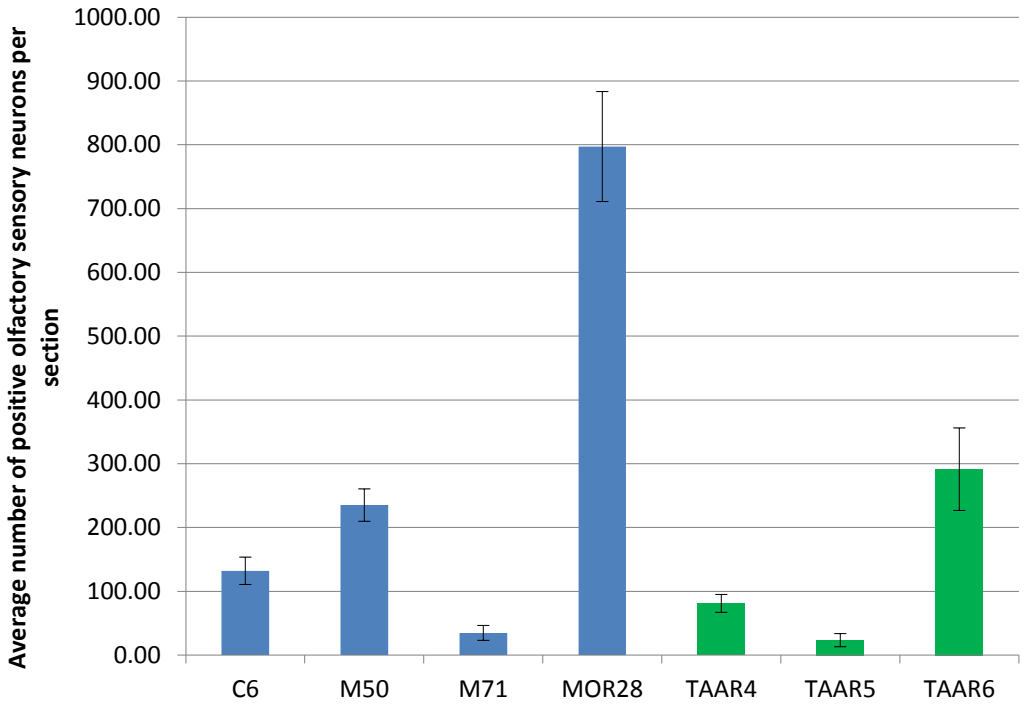

Figure S2. Expression frequencies of various TAARs and ORs in the main olfactory epithelium.

The main olfactory epithelia from three adult C57/Bl6 mice were cryosectioned into 14 µm sections and stained with antibodies against the ORs C6, M50, M71, MOR28 and the TAARs: TAAR4, TAAR5 or TAAR6. The olfactory sensory neurons expressing each of these chemoreceptors were counted in the 6 consecutive sections with peak expression. The mean and standard deviation of the numbers of positive neurons were calculated from those 6 sections.

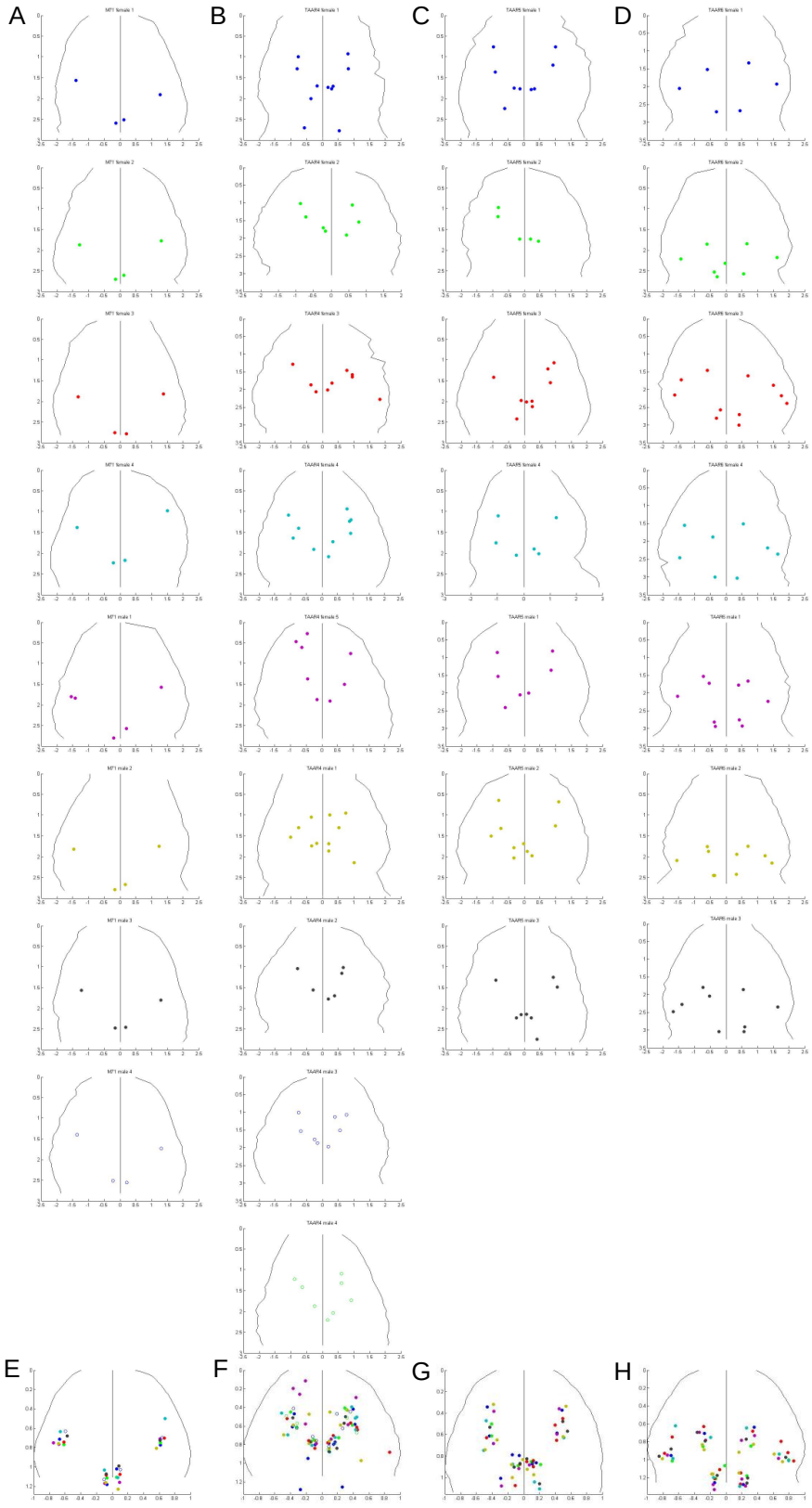

Figure S3. (legend continued on next page)

Figure S3. Distribution of TAAR glomeruli in individual C57/Bl6 mice.

(*A* and *E*) M71, (*B* and *F*) TAAR4, (*C* and *G*) TAAR5, (*D* and *H*) TAAR6. Flattened two-dimensional reconstruction of the dorsal aspect of the OB. *Top*, anterior; *bottom*, posterior. The distance in mm from the anterior tip of the OB is indicated on Y-axis. The distance in mm from the midline is indicated on the X-axis. Maps in *A*–*D* represent individual animals and maps in *E*–*H* are overlays of glomeruli from all of the individuals plotted for a given TAAR. Mice were 4-6 weeks old.

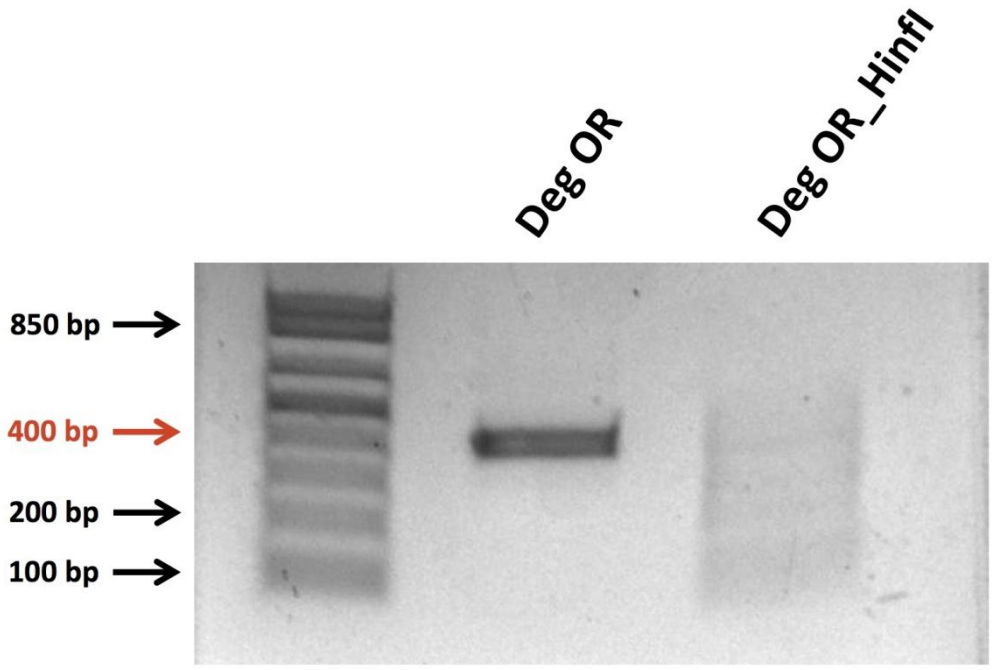

Figure S4. Validation of the complexity of the degenerate OR probe for *in situ* hybridization.

Degenerate primers were used to amplify OR sequence segments from TM3-TM6 as described[47]. To validate the complexity of the probe, a sample of it was digested with the enzyme HinfI. From left to right: (*Lane 1*) 1 kb+ DNA ladder; (*Lane 2*) undigested template for the degenerate OR probe; (*Lane 3*) template for the degenerate OR probe digested with HinfI.

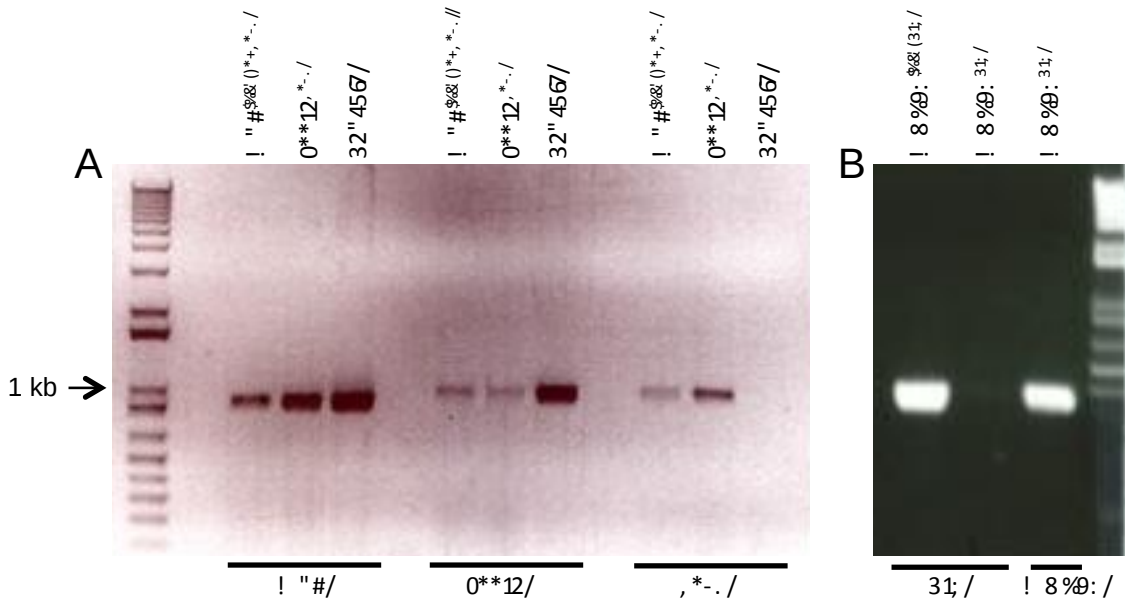

Figure S5. RT-PCR validation of persistent expression of the *Taar5*^{LacZ} allele.

(*A*) PCR amplification of fragments of M71, TAAR5 or LacZ using cDNA prepared from main olfactory epithelia from adult M71$^{IRES\text{-}tauLacZ}$, in which β-galactosidase is expressed from the genomic locus of the OR M71 together with the receptor[49]; Taar5^{LacZ}, in which β-galactosidase is expressed from the genomic locus of TAAR5 and replaces the coding sequence of the receptor, or C57/Bl6 mice. (*B*) PCR amplification of fragments of CRE or MOR28 using cDNA prepared from main olfactory epithelia of adult MOR28$^{IRES\text{-}CRE}$ or MOR28^{CRE} mice in which CRE is expressed from the MOR28 locus either together with the receptor or instead of it, respectively (Barnea et al., 2004). 1 kb+ DNA ladder was used.

Chapter 5

Discussion

Nothing in biology makes sense except in the light of evolution.

– Theodosius Dobzhansky

The theory of evolution was originally proposed to explain the diversity and distribution of living organisms. Today, the principles of evolution are used to explain numerous phenomena observed in various fields such as cancer biology, antibiotic resistance, and even machine learning. One of the basic tenets of evolution can be paraphrased as "whatever works, works." This can shed light on how certain living systems are so efficient. They had to be efficient, or perish. It can also explain how other living systems are seemingly inefficient. If something suffices, it will be sustained and passed on. Since the evolutionary history of a system can inform our understanding of the system's function, I will be framing my discussion of the axonal guidance of OSNs in the light of evolution and its functional consequences.

Multiple aspects of the axonal guidance in the olfactory system have drawn much attention and subsequent research. Some of these include the "one receptor per neuron" rule, the "one receptor per glomerulus" rule, the stereotyped distribution of glomeruli within the glomerular map, the distinction between the circuits mediating learned versus innate olfactory behavior, and the maintenance of the glomerular map despite regeneration. In this discussion I will separately address each of these aspects as well as how they interact with one another.

Monoallelic expression – the "one receptor per neuron" rule

The sequences of ORs contain indications of their evolutionary past. The class I ORs are most similar to those found in fish and may originally have been specialized for detecting water-soluble odorants. Class II ORs are more common in mammals and appear to be responsible for detecting volatile odors (Freitag et al., 1995). However, this distinction is merely a consequence of the evolutionary lineage of the genes and not an evolutionary constraint. ORs classified as class I receptors may have diverged to bind volatile odorants and conversely some class II ORs may bind water-soluble odorants. No law dictates that any receptor must bind ligands with specific chemical properties. Likewise, no law dictates that a receptor must belong to a specific gene family and indeed, several types of GPCRs do serve as olfactory chemoreceptors (Fleischer et al., 2009). The organization of the genes suggests that these receptors evolved by duplication. The OR, V1R, V2R, TAAR, and FPR genes are predominantly arranged in clusters within the genome, with highly-similar genes often closely apposed. Gene duplication causes redundancy, which allows one copy of the receptor to evolve without compromising the function of the original receptor. However, in order for the nervous system to capitalize on this receptor diversity, it must be able to distinguish the activation of one receptor from the activation of another. OSNs seem to have achieved this by ensuring monoallelic receptor expression. In this way, each receptor variant activates separate populations of neurons which can integrate into separate neuronal circuits to mediate separate responses. Monoallelic expression can also generate olfactory discrimination from the two alleles of a given gene if multiple allele variants are present within the species.

The mechanisms of monoallelic expression seem to be mediated by negative feedback from functional receptor proteins (Serizawa et al., 2003; Shykind et al., 2004; Shykind, 2005). Using the receptor protein itself as the salient signal for monoallelic expression minimizes evolutionary constraints. In this way, promoter and regulatory elements can evolve independently of the receptor coding sequence while preserving the "one receptor per neuron" rule. Indeed, our transgenic ORs can be viewed as novel OR genes with evolutionarily divergent promoters. Since the presence of the OR protein alone is sufficient to mediate negative feedback, the fact that it is encoded by a transgene does not affect monoallelic expression and thus we and others rarely observe co-expression of transgenic and endogenous ORs within a single OSN (Fleischmann et al., 2008; Nguyen et al., 2007).

Convergence – the "one receptor per glomerulus" rule

The convergence of the OSNs expressing the same OR also seems to be mediated by the receptor protein. The transgenic origin of TO28 did not prevent TO28 axons from converging into MOR28 glomeruli. Indeed, the recruitment of endogenous MOR28 axons into rerouted glomeruli can be viewed as an extension of the mechanisms that cause MOR28 axons to converge on the same glomeruli. Convergence may have evolved as a consequence of the evolutionary history of olfactory chemoreceptors. Monoallelic expression allows newly evolved receptors to be expressed in a dedicated population of OSNs. However, these OSNs must integrate into neuronal circuitry in order to allow the organism to perceive the ligands bound by this receptor. All the sensory neurons identified in the olfactory system converge in glomeruli before synapsing on mitral and tufted cells (Fleischer et al., 2009; Johnson et al., 2012; Pacifico et al., 2012). This

organizational strategy serves to minimize evolutionary constraints. When OSNs begin expressing a newly-evolved receptor, the organism is not required to concurrently evolve unique second order neurons to synapse with each of these OSNs. Instead, these OSNs are only required to aggregate in one location, which allows them all to synapse together with a small number of pre-existing second order neurons.

Convergence into glomeruli may also facilitate olfactory processing by enabling coincidence detection, which increases the signal-to-noise ratio within the system. To illustrate this point, I will use the activation of the M71 glomerulus. Since ORs bind many ligands, exposure to any odorant likely results in a small degree of non-specific M71 activation. Each M71 axon would have a small probability of firing. However, since the M71 glomerulus consists of many M71 axons, the overall activity within the glomerulus is low and there is little noise. Conversely, when the mouse is exposed to the M71-specific ligand acetophenone, the axons expressing M71 will fire in unison, amplifying the signal. The second order neurons in the glomerulus are most likely activated only when a threshold number of M71 OSNs fire, and consequently the M71 glomerulus is only activated when an M71-specific ligand is present. Thus aggregation of M71 axons simultaneously decreases noise while increasing the strength of the signal.

Additionally, convergence of the OSNs expressing the same OR may be used to aggregate the axonal guidance cues that affect each OSN. In this way, multiple weak cues could sum into a stronger cue. This would serve to provide a level of redundancy within axonal guidance that may make the process more efficient and less prone to targeting errors.

Convergence may be mediated by homotypic attraction between OSNs expressing the same OR. Possible mechanisms include direct interaction between the OR proteins, interaction via adapter proteins, or indirect interaction where the activity of ORs results in the differential expression of other guidance cues. Homotypic attraction most likely does not occur through direct interaction. If OR proteins interacted across membranes, they must do so via their extracellular domains. However, the residues that vary the most between ORs are located predominantly in the transmembrane helices (Fleischer et al., 2009). Indeed, the extracellular residues are not sufficient for determining axonal guidance. Mutating a single amino acid within the cytoplasmic end of the fifth transmembrane helix of M71 was sufficient to cause formation of a new glomerulus (Feinstein and Mombaerts, 2004). Moreover, the structurally unrelated β-adrenergic receptor can mediate the convergence of OSNs (Feinstein et al., 2004). The β-adrenergic receptor is not a chemosensor and it is highly unlikely that the evolutionary selection that would be necessary to allow the protein to bind another β-adrenergic receptor on another axon would also affect this gene.

The same reasoning suggests that homotypic attraction is not mediated by direct interaction via adapter molecules. The selective pressure to maintain the ability to bind guidance-specific adapter molecules is unlikely to affect the β-adrenergic receptor. It is possible that the adapter molecules bind to ORs and the β-adrenergic receptor via highly conserved residues that are found in all GPCRs. However, sequence conservation usually occurs when the sequence is responsible for a critical function that undergoes positive selection. Moreover, the binding site for the adapter molecule would be predicted to change from one OR to another if it was required to mediate homotypic attraction only

between axons expressing the same OR. It seems unlikely that a sequence could serve a critical function in both ORs and the β-adrenergic receptor while being allowed to vary from one OR to another.

Multiple lines of reasoning suggest that convergence mediated by homotypic attraction could occur through an indirect interaction mediated by OR activity. Since convergence occurs prenatally before exposure to exogenous ligands, this activity must be intrinsic and ligand-independent. The intrinsic activity of ORs is thought to couple with the $G\alpha_s$ protein, which modulates the levels of cAMP and results in changes in the expression of type I guidance molecules such as Robo2, Slit1, Sema3F, and Nrp2 (Mori and Sakano, 2011). The β-adrenergic receptor also couples to $G\alpha_s$, which is consistent with the observation that this receptor causes convergence. The vomeronasal receptor V1rb2 does not couple to $G\alpha_s$, consistent with the observation that this receptor does not cause OSNs to converge into glomeruli (Feinstein and Mombaerts, 2004). Moreover, the OR proteins on the growth cone have been shown to mediate local cAMP levels (Maritan et al., 2009). This observation suggests that homotypic attraction determines local events in axonal guidance such as convergence rather than global events such as mapping the dorsomedial-ventrolateral axis of the MOE onto the dorsoventral axis of the OB. Finally, homotypic attraction through indirect interactions is consistent with the phenotype of cAMP mutants. P2 expressing OSNs that also expressed mutant effectors in the cAMP pathway formed P2 glomeruli in ectopic locations. Importantly, the endogenous P2 OSNs were not rerouted to these glomeruli (Imai et al., 2006). If homotypic attraction were mediated by direct interaction or via adapter proteins, the two populations of P2 OSNs would have interacted and induced rerouting. Since altering only the downstream cAMP

pathway was sufficient to prevent homotypic attraction, it is most likely the effector pathway for this mechanism.

Convergence mediated by cAMP-dependent homotypic attraction is also the most parsimonious with functional and evolutionary considerations. Since mice predominantly navigate via chemosensory cues, natural selection would favor those mice with the most olfactory discrimination. In order to achieve the highest degree of olfactory discrimination, the glomeruli in an animal must distinguish as many different odorants as possible. This would require each OR with a unique ligand specificity to mediate the formation of unique and separate glomeruli. An efficient way to ensure this dictates that homotypic attraction is mediated by the residues of the OR that also mediate ligand specificity. This specificity is most likely mediated by the transmembrane domains, since the residues here are most variable between ORs (Fleischer et al., 2009). If homotypic attraction occurred through the direct interaction of OR proteins, it would incur a tremendous evolutionary constraint. Changes deep in the receptor protein would be required to also affect the extracellular domain in such way that the OR could still bind its cognate on a different axon while distinguishing it from other very similar ORs. However, homotypic attraction through intrinsic ligand-independent activity would introduce no additional evolutionary constraints. Since intrinsic activity would likely involve the same residues that mediate ligand-dependent activity, mutations that affect ligand specificity would be likely to change activity-dependent homotypic attraction as well.

The convergence of OSNs expressing the same OR onto one location can be viewed as a variation of chemoaffinity. As mentioned previously, convergence into

glomeruli abrogates the requirement for a specific population of second order neurons to evolve concurrently with the generation of new ORs. This suggests that the OSNs expressing a given OR do not synapse on specific, predetermined mitral cells. Instead, the critical requirement for olfactory function is that these OSNs all converge together on one set of mitral cells. In this case, chemoaffinity is not employed to match pre- and post-synaptic cells, but rather to match the OSN axons expressing the same OR. Instead of occurring at synaptogenesis, chemoaffinity would operate during axon-axon sorting within the fascicles streaming toward the OB. After convergence and synaptogenesis, the identity of the second order neurons would be defined by the activity patterns of their OSN afferents. As long as these second order neurons are consistently activated upon exposure to specific odorants, then a defined perception would be associated with those odorants. It is possible that the entire olfactory percept is procedurally generated in this way. An analogy could be made to the human visual system. There is no universal perception of the color green. However, the perception of "green" wavelengths of light is internally consistent because it is functionally defined as the color that lies between yellow and blue on the spectrum. This internal consistency is sufficient for most functions, as illustrated by the anecdotal evidence that colorblindness may not be diagnosed until late in life. Identifying a similar "smellblindness," or individual difference in the perception of smells, may be impossible, given that ligands cannot be organized on a spectrum. If olfaction is functionally determined in this way, consistency in the neuronal circuitry over the lifetime of a given individual is critical for generating the perception of smell.

Stereotypy of the glomerular map

The glomeruli dedicated to specific ORs are normally observed in stereotyped locations in the glomerular map. One mechanism that could explain this stereotypy is that glomeruli are genetically pre-determined targets. However, convergence and glomerular order on anteroposterior axis was maintained even when the OB tissue was genetically or physically ablated (St John et al., 2003). Furthermore, axons do not innervate pre-existing structures in the glomerular layer (Bailey et al., 1999; LaMantia and Purves, 1989; Treloar et al., 1999). Instead, it seems that axon-axon interactions are sufficient to generate the glomerular map (Feinstein and Mombaerts, 2004; Imai and Sakano, 2011). This process may be error prone, but mistakes in axonal targeting would be solved by pruning and elimination during development. Indeed, ectopic glomeruli are known to be eliminated during the first few weeks after birth while protoglomeruli are being refined into the discrete glomeruli observed in adults (Conzelmann et al., 2002; Potter et al., 2001; Zou et al., 2004). Moreover, the glomerular map can only be assayed once in any given animal. Studies that only examine axonal guidance in adulthood would miss any axons that had already been pruned. Reminiscent of the evolution of life, the individuals present at a given time are merely the individuals that have survived and do not necessarily represent all the individuals that were eliminated throughout history.

Anatomical and technical constraints currently prevent researchers from following the axonal guidance of OSNs through time. We cannot count all of the OSNs that failed to integrate into neuronal circuits for one organism. However, we can approximate total neuronal death by counting the number of apoptotic OSNs at a given time point. In Chapter 2, the expression of TO28 was observed to cause an increase in apoptosis

throughout the MOE. The OMP driver could be causing TO28 expression in OSNs that were already expressing endogenous ORs. This would break the "one receptor per neuron" rule. In addition, TO28 could be expressed in OSNs that had already innervated a glomerulus dedicated to another OR. This would break the "one receptor per glomerulus" rule. Both of these situations would likely impact the activity-dependent competition of these axons and they would be eliminated. Thus the axon-axon interactions that generate the glomerular map impart robustness to the system that maintains glomerular convergence even when ORs are regulated by novel promoters. Axon-axon interactions also impart flexibility to allow the formation of ectopic glomeruli without violating the "one receptor per glomerulus" rule. Our transgenic promoter is artificially introduced, but robustness and flexibility would also allow the integration of ORs in cases where a promoter had changed over the course of natural evolution.

The ability to induce the formation of stable ectopic glomeruli suggests that natural selection does not necessarily favor stereotypy *per se*. Indeed, olfactory function was largely unaffected in mice where stereotypy was abolished by the expression of M71 in most glomeruli (Fleischmann et al., 2008). Since natural selection only operates on functional outcomes, these mice would not have had decreased chances of survival despite their abnormal glomerular maps. Stereotypy may arise merely as a consequence of the mechanisms that govern axonal guidance. Furthermore, the degree of stereotypy that has been reported may be an artefact. The studies that first examined the organization of the glomerular map were performed in mouse strains that were inbred for many generations (Potter et al., 2001; Ressler et al., 1994; Vassar et al., 1994). Truly wild mice are likely much more heterogeneous and it remains to be seen if their glomerular maps

are similarly stereotyped (Mombaerts, 2006). Regardless of the true extent of stereotypy, it seems to arise independently of glomerular convergence. Mice that were mutants for specific type I guidance molecules lost the rough topographical mapping of the dorsomedial-ventrolateral axis of the MOE onto the dorsolateral axis of the OB. However, the axons expressing the same ORs still converged into dedicated glomeruli (Imai et al., 2009; Schwarting et al., 2004; Takeuchi et al., 2010).

If stereotypy is not critical, what explains the loosely topographical mapping of the dorsomedial-ventrolateral axis of the MOE onto the dorsolateral axis of the OB? The glomerular map may result from the need to spatially segregate individual glomeruli. In the same way that tiling between the dendrites of one neuron class allows the neurons to maximize the number of afferents they receive (Hattori et al., 2008), glomeruli may tile across the surface of the OB to maximize the distinction of one glomerulus from another. Spatial segregation would prevent the activation of one glomerulus from cross-activating the second order neurons synapsing within the neighboring glomerulus. In this way, convergence would be the critical characteristic of the glomerular map and glomerular tiling would be a modification that facilitates the read-out of the map. Tiling also allows glomeruli to occupy a defined layer of the OB which may aid connections with second order neurons. Indeed, mitral cells seem to be genetically programmed to extend dendrites into the glomerular layer since they will do so even when the glomeruli within the layer have been ablated (Kobayakawa et al., 2007). This is reminiscent of the lock and key versus the induced fit models of ligand binding. In the same way that receptor proteins are not pre-shaped to perfectly fit a ligand, mitral cells are not pre-determined to innervate a specific glomerulus. Instead, ligands influence the shape of the receptor as

they dock, the same way that the OR expressed by OSNs could specify the identity of the mitral cell after synaptogenesis.

The mechanisms that tile glomeruli in space could also explain the patches of chemotopy within the glomerular map, or the observation that adjoining glomeruli sometimes share ligand binding properties (Johnson and Leon, 2007; Johnson et al., 2009; Mori et al., 2006; Soucy et al., 2009). As a duplicated pair of ORs evolves and diverges, the changes in the amino acid sequence result in changes in the activation of the cAMP pathway. These differences cause the original and diverged ORs to converge on different glomeruli. However, duplication likely results in many similarities between the two promoters regulating these two ORs. The diverged OR is likely to be expressed in the same zone of the MOE and co-expressed with the same repertoire of type I molecules such that the new glomerulus is near the glomerulus dedicated to the original OR. The shared evolutionary history between these two ORs also likely results in many similarities in their ligand binding properties. Thus nearby glomeruli tend to be activated by ligands that are chemically and structurally similar. However, a given OR has a low likelihood of duplication, so clusters of related glomeruli are small and infrequent. Therefore chemotopy is not widely observed in the OB.

The observation that ectopic glomeruli formed by TO28 are not eliminated suggests that not all changes to the glomerular map necessitates pruning. Indeed, the ectopic glomeruli could be viewed as a level of functional redundancy, which could serve as a substrate for generating diversity. It is possible that the redundancy in having a medial and lateral glomerulus for each OR allowed the development of different processing streams. These would be analogous to the “what” and “where” streams in the

visual system. It would be interesting to examine whether the ectopic glomeruli formed by TO28 were linked by tufted cells in the way that the medial and lateral glomeruli for a given OR are linked (Belluscio et al., 2002). We could also address the separate streams using optogenetics. We could condition mice to respond to light-induced activation of only one subset of ectopic glomeruli. Then we would light-induce another subset of ectopic glomeruli and look for the conditioned behavior. Presence of the conditioned behavior would suggest that the glomeruli are functionally linked. Absence of the conditioned behavior would suggest that the glomeruli participate in independent processing streams that could later evolve separate functions.

Learned versus innate olfactory behaviors

Innate behaviors most likely did not evolve as a matter of course after the segregation of processing streams. Innate behaviors are behaviors that are so critical to the reproductive success of an individual that it has undergone positive selection. Mice that did not exhibit these behaviors would not exist today and thus all conspecifics must exhibit these behaviors. The ability for all conspecifics to respond in the same manner to a given stimulus likely involves hardwired circuits. Since positive selection would only operate on the functions that affect reproductive fitness, unrelated functions mediated by these hardwired circuits may be allowed to drift, perhaps leaving a dedicated set of neurons that mediate only the innate behavior. Indeed, the projection patterns of some mitral cells into the olfactory cortex suggest that some circuits are organized in a manner similar to labeled lines. Some mitral innervate a broad range of targets in the piriform cortex such that a given third order neuron receives input from many mitral cells representing many different glomeruli. This could be the neural substrate for Hebbian

plasticity, allowing “fire together wire together” mechanisms to associate global patterns of glomerular activation. Conversely, other mitral cells innervate a smaller number of third order neurons in the amygdala. This appears to generate less crosstalk from the activation of different glomeruli (Sosulski et al., 2011). The authors speculate that the former circuits mediate learned behavior while the latter, more streamlined, circuits mediate innate behaviors.

The circuitry mediating innate behaviors also seems much less adaptable that mediating learned behaviors. When transgenic M71 was expressed in >95% of OSNs, the mice were capable of discriminating similar mixtures of odorants but their innate behaviors were impaired (Fleischmann et al., 2008). If the ligands that evoke innate behaviors must be processed through specific circuits, the axons expressing M71 may dilute the sensitivity of those circuits by increasing noise from unrelated ligands. Conversely, the circuits mediating learned behavior may merely be required to associate a firing pattern with specific stimuli. Furthermore, olfaction may be relative. Recall the analogy that “green” is defined as the color between yellow and blue. Even if the entire spectrum were overlaid with a color filter, the relationship between yellow, green, and blue remains the same so “green” can still be discriminated from closely related colors. Since transgenic M71 affected all glomeruli equally, the relative differences between the similar mixtures still had the same salience and thus could still be distinguished.

In Chapter 4 we observed that the number of glomeruli dedicated to a given TAAR was more variable than the number of glomeruli normally dedicated to an OR. It is possible that this difference reflects a divergence in the way learned versus innate behavior is processed. The function of TAARs may require merely the activation of a

specific hardwired circuit. In this case, increasing the number of glomeruli may increase the likelihood that exposure to a TAAR ligand will result in circuit activation. This strategy could introduce a level of functional redundancy since all glomeruli would be equally capable of mediating the innate behavior. Conversely, the discrimination of OR ligands is facilitated by precision in the circuitry since precision minimizes the noise within the system. This would explain the selective pressures that ensure two glomeruli dedicated to each OR. It would be interesting to test this hypothesis by generating a mouse where an OR was co-expressed by a TAAR-expressing OSN. We could test whether the odorant that activated the OR would evoke an innate reaction. If so, this would suggest that any activation of the hardwired circuit is sufficient to trigger a preprogrammed behavior.

Maintenance of the glomerular map

The studies described in Chapter 3 provide the first evidence for any type of critical period in the olfactory system. Previously, no observations had been reported that perturbations in gene expression had different results on the glomerular map depending on when they were applied. Similarly, no publications previously reported that changes in the map will be maintained after the original perturbation is removed. Overall, the olfactory system appears to maintain the glomerular map that is established during development. This may be requisite if the perception of an odor arises from the association of glomerular activity patterns and specific populations of second and third order neurons. It would be interesting to use a similar experimental set up to compare and contrast the maintenance of the glomeruli dedicated to learned versus innate behaviors. If the function of TAARs merely requires the activation of a specific hardwired circuit,

there may be no selective pressure to maintain the specific map that was established during development. As long as TAAR ligands continue to activate the labeled line, glomeruli could be added or removed later in life with no effect on innate behavior.

Maintenance of the glomerular map may depend on a mechanism similar to guidance via pioneer neurons. In this case, pioneers would not be defined as a transient, morphologically distinct population of neurons that appear early in development. Since regeneration occurs throughout adulthood, this sort of pioneer neuron would not be present during the maintenance of the map. Instead, pioneers could be defined as any existing OSNs that express the same OR as the regenerating OSN. These early-born OSNs already extend along the entire future path of the later-born OSN, allowing them to serve as scaffolds for axonal growth. Homotypic attraction would enable followers to distinguish between multiple possible pioneers, allowing them to identify only the ones that express the same OR. This mechanism was first proposed by Gogos et al. when they reported that the olfactory map was restored after the majority of the P2 OSNs were genetically ablated (Gogos et al., 2000). However, their mice had exhibited stereotyped glomerular maps before ablation and the wildtype maps were simply reconstituted after ablation so the results could also be explained if all of the axonal guidance mechanisms that operate during early development were still operating in adulthood. Since the glomerular map is variable and does not appear to be genetically pre-determined, the use of pioneer neurons would also be a simple mechanism that ensures consistency between early and late development regardless of any variations. Furthermore, the effect of early TO28 expression on the glomerular map is similar to an effect that has been described as a hallmark of pioneer neurons (Chao et al., 2009). Since followers make few axonal

guidance decisions on their own, manipulating the axonal trajectory of the pioneer neurons is sufficient to change the axonal trajectory of followers, regardless of their genotype.

Implications and future directions

One of our major conclusions was that early neuronal circuitry can dictate the conformation of later circuitry. Perhaps this can serve to delineate the limitations and possibilities for clinical interventions. Once a neuronal circuit has been established in an abnormal conformation, there may be little hope of amending the circuit later in life. Thus it is critical to safeguard fetuses and young children against any chemicals or perturbations that could alter axonal guidance. However, the maintenance of the glomerular map could also suggest an immense potential in restoring a neuronal circuit after neurodegeneration or injury. Current trials investigating the therapeutic potential of neural stem cells have resulted in some successes but also highlighted obstacles such as therapeutically relevant levels of integration into host tissue (Dutta et al., 2013; Simara et al., 2013). The work described in Chapter 3 could be used as a justification for continuing to search for ways to overcome these obstacles.

The mechanisms that govern the axonal guidance of ONSs in adulthood could also be developed into therapeutic strategies for controlling the axonal guidance of neural stem cells. Currently, it is known that some canonical guidance molecules such as semaphorins, netrins, slits, and ephrins are expressed in vertebrate adults (Koeberle and Bähr, 2004). However, their function in mediating adult axonal guidance is often limited. Perhaps one day a variant of homotypic attraction could be used to bring pre- and post-

synaptic cells into proximity. This possibility would be especially feasible if homotypic attraction is mediated by cAMP. Most cells already express components of the cAMP pathway and it is known to modulate the expression of semaphorins as well as semaphorin receptors (Imai and Sakano, 2008). ORs could be virally introduced into the pre- and post-synaptic cells of interest or functionally replaced by other molecules that could activate the cAMP pathway to a similar degree.

Elucidating the molecular details of homotypic attraction could also impact other fields of study beyond axonal guidance. Several labs have suggested that ORs function in other tissues. MOR23 is expressed in muscle and in mouse sperm, and the odorant bourgenal can affect the chemotaxis of human sperm (Griffin et al., 2009; Spehr et al., 2003). If these ORs truly have a function *in vivo* and the mechanisms of OR-dependent axonal guidance are fully elucidated, some day we may be able to use ORs to induce chemotaxis of non-neuronal cell types. This could impact the development of fertility treatments and strategies for muscle repair. ORs have even been implicated in preventing the advancement of prostate cancer (Neuhaus et al., 2009). Gaining a full understanding of OR function would inform studies on this putative role.

Loss of olfaction often precedes the onset of the movement or cognitive symptoms of Alzheimer's disease and Parkinson's disease (Rahayel et al., 2012; Wong et al., 2010). While restoring the sense of smell would not restore many of the functions lost from neurodegeneration, therapies that repaired the olfactory system would improve the quality of life of these patients. Moreover, elucidating the mechanisms underlying the development of the olfactory system may inform the understanding of these cases where olfaction is lost. Since olfaction in humans is idiosyncratic and perhaps functionally

defined in a relative manner, it can be difficult to diagnose subtle changes in olfactory perception. Studying olfactory system development could possibly identify new biomarkers for objectively detecting disease-associated perturbations in olfaction at a point when clinical intervention could prevent disease progression.

Intriguingly, the steroid hormones androstenone and androstadienone have been identified as OR ligands (Keller et al., 2007). There may be as-yet unknown roles for ORs in pheromone detection in humans or hormonal modulation of smell. Studies today, such as the ones described in this thesis, that contribute to our full understanding of the olfactory system may impact future studies in new fields that have yet to be identified.

In conclusion, the research presented in this thesis offers new insights into the development and maintenance of the glomerular map. This work can also impact studies regarding other aspects of the olfactory system, such as gene regulation, the distinction between learned versus innate behavior, and the structural basis of olfactory perception. Contributing to our knowledge of the olfactory system may someday even impact research on disease, therapies, and the possibility of novel functions. Since the sense of smell is subjective and difficult to quantify, it has traditionally been less researched than the visual or somatosensory systems. However, it has become increasingly clear that understanding the biology of olfaction can produce very objective, tangible benefits to mankind.

REFERENCES

Bailey, M.S., Puche, A.C., and Shipley, M.T. (1999). Development of the olfactory bulb: evidence for glia-neuron interactions in glomerular formation. J Comp Neurol *415*, 423-448.

Belluscio, L., Lodovichi, C., Feinstein, P., Mombaerts, P., and Katz, L. (2002). Odorant receptors instruct functional circuitry in the mouse olfactory bulb. Nature *419*, 296-300.

Chao, D., Ma, L., and Shen, K. (2009). Transient cell-cell interactions in neural circuit formation. Nat Rev Neurosci *10*, 262-271.

Conzelmann, S., Levai, O., Breer, H., and Strotmann, J. (2002). Extraepithelial cells expressing distinct olfactory receptors are associated with axons of sensory cells with the same receptor type. Cell Tissue Res *307*, 293-301.

Dutta, S., Singh, G., Sreejith, S., Mamidi, M.K., Husin, J.M., Datta, I., Pal, R., and Das, A.K. (2013). Cell therapy: the final frontier for treatment of neurological diseases. CNS Neurosci Ther *19*, 5-11.

Feinstein, P., Bozza, T., Rodriguez, I., Vassalli, A., and Mombaerts, P. (2004). Axon guidance of mouse olfactory sensory neurons by odorant receptors and the beta2 adrenergic receptor. Cell *117*, 833-846.

Feinstein, P., and Mombaerts, P. (2004). A contextual model for axonal sorting into glomeruli in the mouse olfactory system. Cell *117*, 817-831.

Fleischer, J., Breer, H., and Strotmann, J. (2009). Mammalian olfactory receptors. Front Cell Neurosci *3*, 9.

Fleischmann, A., Shykind, B., Sosulski, D., Franks, K., Glinka, M., Mei, D., Sun, Y., Kirkland, J., Mendelsohn, M., Albers, M., *et al.* (2008). Mice with a "monoclonal nose:" perturbations in an olfactory map impair odor discrimination. Neuron *60*, 917-926.

Freitag, J., Krieger, J., Strotmann, J., and Breer, H. (1995). Two classes of olfactory receptors in Xenopus laevis. Neuron *15*, 1383-1392.

Gogos, J., Osborne, J., Nemes, A., Mendelsohn, M., and Axel, R. (2000). Genetic ablation and restoration of the olfactory topographic map. Cell *103*, 609-620.

Griffin, C., Kafadar, K., and Pavlath, G. (2009). MOR23 promotes muscle regeneration and regulates cell adhesion and migration. Dev Cell *17*, 649-661.

Hattori, D., Millard, S., Wojtowicz, W., and Zipursky, S. (2008). Dscam-mediated cell recognition regulates neural circuit formation. Annu Rev Cell Dev Biol *24*, 597-620.

Imai, T., and Sakano, H. (2008). Odorant receptor-mediated signaling in the mouse. Curr Opin Neurobiol *18*, 251-260.

Imai, T., and Sakano, H. (2011). Axon-axon interactions in neuronal circuit assembly: lessons from olfactory map formation. Eur J Neurosci *34*, 1647-1654.

Imai , T., Suzuki, M., and Sakano, H. (2006). Odorant receptor-derived cAMP signals direct axonal targeting. Science *314*, 657-661.

Imai, T., Yamakazi, T., Kobayakawa, R., Kobayakawa, K., Abe, T., Suzuki, M., and Sakano, H. (2009). Pre-target axon sorting establishes the neural map topography. Science.

Johnson, B.A., and Leon, M. (2007). Chemotopic odorant coding in a mammalian olfactory system. J Comp Neurol *503*, 1-34.

Johnson, B.A., Xu, Z., Ali, S.S., and Leon, M. (2009). Spatial representations of odorants in olfactory bulbs of rats and mice: similarities and differences in chemotopic organization. J Comp Neurol *514*, 658-673.

Johnson, M.A., Tsai, L., Roy, D.S., Valenzuela, D.H., Mosley, C., Magklara, A., Lomvardas, S., Liberles, S.D., and Barnea, G. (2012). Neurons expressing trace amine-associated receptors project to discrete glomeruli and constitute an olfactory subsystem. Proc Natl Acad Sci U S A *109*, 13410-13415.

Keller, A., Zhuang, H., Chi, Q., Vosshall, L., and Matsunami, H. (2007). Genetic variation in a human odorant receptor alters odour perception. Nature *449*, 468-472.

Kobayakawa, K., Kobayakawa, R., Matsumoto, H., Oka, Y., Imai, T., Ikawa, M., Okabe, M., Ikeda, T., Itohara, S., Kikusui, T., *et al.* (2007). Innate versus learned odour processing in the mouse olfactory bulb. Nature *450*, 503-508.

Koeberle, P., and Bähr, M. (2004). Growth and Guidance Cues for Regenerating Axons: Where Have They Gone? J Neurobiol *59*, 162-180.

LaMantia, A.S., and Purves, D. (1989). Development of glomerular pattern visualized in the olfactory bulbs of living mice. Nature *341*, 646-649.

Maritan, M., Monaco, G., Zamparo, I., Zaccolo, M., Pozzan, T., and Lodovichi, C. (2009). Odorant receptors at the growth cone are coupled to localized cAMP and Ca2+ increases. Proc Natl Acad Sci *106*, 3537-3542.

Mombaerts, P. (2006). Axonal wiring in the mouse olfactory system. Annu Rev Cell Dev Biol *22*, 713-737.

Mori, K., and Sakano, H. (2011). How is the olfactory map formed and interpreted in the mammalian brain? Annu Rev Neurosci *34*, 467-499.

Mori, K., Takahashi, Y.K., Igarashi, K.M., and Yamaguchi, M. (2006). Maps of odorant molecular features in the Mammalian olfactory bulb. Physiol Rev *86*, 409-433.

Neuhaus, E., Zhang, W., Gelis, L., Deng, Y., Noldus, J., and Hatt, H. (2009). Activation of an olfactory receptor inhibits proliferation of prostate cancer cells. J Biol Chem *284*, 16218-16225.

Nguyen, M., Zhou, Z., Marks, C., Ryba, N., and Belluscio, L. (2007). Prominent roles for odorant receptor coding sequences in allelic exclusion. Cell *131*, 1009-1017.

Pacifico, R., Dewan, A., Cawley, D., Guo, C., and Bozza, T. (2012). An olfactory subsystem that mediates high-sensitivity detection of volatile amines. Cell Rep *2*, 76-88.

Potter, S., Zheng, C., Koos, D., Feinstein, P., Fraser, S., and Mombaerts, P. (2001). Structure and emergence of specific olfactory glomeruli in the mouse. J Neurosci *21*, 9713-9723.

Rahayel, S., Frasnelli, J., and Joubert, S. (2012). The effect of Alzheimer's disease and Parkinson's disease on olfaction: a meta-analysis. Behav Brain Res *231*, 60-74.

Ressler, K., Sullivan, S., and Buck, L. (1994). Information coding in the olfactory system: evidence for a stereotyped and highly organized epitope map in the olfactory bulb. Cell *79*, 1245-1255.

Schwarting, G.A., Raitcheva, D., Crandall, J.E., Burkhardt, C., and Puschel, A.W. (2004). Semaphorin 3A-mediated axon guidance regulates convergence and targeting of P2 odorant receptor axons. Eur J Neurosci *19*, 1800-1810.

Serizawa, S., Miyamichi, K., Nakatani, H., Suzuki, M., Saito, M., Yoshihara, Y., and H, S. (2003). Negative feedback regulation ensures the one receptor-one olfactory neuron rule in mouse. Science *302*, 2088-2094.

Shykind, B., Rohani, S., O'Donnell, S., Nemes, A., Mendelsohn, M., Sun, Y., Axel, R., and Barnea, G. (2004). Gene switching and the stability of odorant receptor gene choice. Cell *117*, 801-815.

Shykind, B.M. (2005). Regulation of odorant receptors: one allele at a time. Hum Mol Genet *14 Spec No 1*, R33-39.

Simara, P., Motl, J.A., and Kaufman, D.S. (2013). Pluripotent stem cells and gene therapy. Transl Res *161*, 284-292.

Sosulski, D., Bloom, M., Cutforth, T., Axel, R., and Datta, S. (2011). Distinct representations of olfactory information in different cortical centres. Nature *472*, 213-216.

Soucy, E.R., Albeanu, D.F., Fantana, A.L., Murthy, V.N., and Meister, M. (2009). Precision and diversity in an odor map on the olfactory bulb. Nat Neurosci *12*, 210-220.

Spehr, M., Gisselmann, G., Poplawski, A., Riffell, J., Wetzel, C., Zimmer, R., and Hatt, H. (2003). Identification of a testicular odorant receptor mediating human sperm chemotaxis. Science *299*, 2054-2058.

St John, J., Clarris, H., McKeown, S., Royal, S., and Key, B. (2003). Sorting and convergence of primary olfactory axons are independent of the olfactory bulb. J Comp Neurol *464*, 131-140.

Takeuchi, H., Inokuchi, K., Aoki, M., Suto, F., Tsuboi, A., Matsuda, I., Suzuki, M., Aiba, A., Serizawa, S., Yoshihara, Y., *et al.* (2010). Sequential Arrival and Graded Secretion of Sema3F by Olfactory Neuron Axons Specify Map Topography at the Bulb. Cell *141*, 1056-1067.

Treloar, H.B., Purcell, A.L., and Greer, C.A. (1999). Glomerular formation in the developing rat olfactory bulb. J Comp Neurol *413*, 289-304.

Vassar, R., Chao, S., Sitcheran, R., Nuñez, J., Vosshall, L., and Axel, R. (1994). Topographic organization of sensory projections to the olfactory bulb. Cell *79*, 981-991.

Wong, K.K., Muller, M.L., Kuwabara, H., Studenski, S.A., and Bohnen, N.I. (2010). Olfactory loss and nigrostriatal dopaminergic denervation in the elderly. Neurosci Lett *484*, 163-167.

Zou, D.J., Feinstein, P., Rivers, A.L., Mathews, G.A., Kim, A., Greer, C.A., Mombaerts, P., and Firestein, S. (2004). Postnatal refinement of peripheral olfactory projections. Science *304*, 1976-1979.

APPENDIX - GLOSSARY

Accessory olfactory bulb (AOB) – a structure of the brain where glomeruli are formed by the vomeronasal sensory neurons

C6 – an odorant receptor; G. Barnea previously generated an antibody for the receptor protein which allows visualization of the C6 expressing OSNs and their axons

Chemotopy – the representation of the ligand binding properties of different odorant receptors in the spatial organization of the glomeruli dedicated to these odorant receptors. That is, an organizational representation where the olfactory sensory neurons that are activated by chemically similar ligands form neighboring glomeruli in the olfactory bulb.

Class I odorant receptors – a type of odorant receptors whose sequences most resemble the odorant receptors expressed by fish

Class II odorant receptors – a type of odorant receptors whose sequences most resemble the odorant receptors expressed in mammals

Convergence – the phenomenon that olfactory sensory neurons expressing the same olfactory chemoreceptor form a small number of homogeneous glomeruli that do not receive afferents from olfactory sensory neurons expressing other olfactory chemoreceptors, also known as the "one receptor per glomerulus" rule

Doxycycline (dox) – silences the TO28 transgene, an antibiotic administered via supplemented chow provided *ad libitum*

Ectopic glomeruli – glomeruli formed by axons expressing TO28

Endogenous MOR28 axons – the axons of the olfactory sensory neurons that express the endogenous, wildtype allele of MOR28 and not the transgenic allele of MOR28

Extracellular matrix (ECM) – any material part of a tissue that is not part of a cell

Formyl peptide receptor (FPR) – G protein-coupled receptors expressed by vomeronasal sensory neurons which serve as olfactory chemosensors

G protein-coupled receptor (GPCR) – a family of receptors that are classified by their seven transmembrane domain structures and ability to couple with G protein effectors

Glomerular map – the arrangement of glomeruli dedicated to different olfactory chemoreceptors that is spatially conserved between the members of a given species

Glomeruli – neuropil structures formed by the convergence of the axons of olfactory sensory neurons, also contains the dendrites of mitral and tufted cells as well as glia

Green fluorescent protein (GFP) – a protein exogenous to the mouse that is used as a reporter gene, visualized by antibody staining or autofluorescence

Grüneberg ganglion (GG) – a subsystem of the olfactory system, located at the anterior tip of the nose

Guanylyl cyclase D (GC-D) – proteins expressed by olfactory sensory neurons which serve as olfactory chemosensors

Homotypic attraction – a mechanism in which the axons of olfactory sensory neurons expressing the same odorant receptor exhibit an affinity for each other, resulting in co-fasciculation and convergence

Internal ribosome entry site (IRES) – a nucleotide sequence that allows cap-independent protein translation, allowing the construction of bicistronic messages where two proteins are produced from one promoter

M50 – an odorant receptor; G. Barnea previously generated an antibody for the receptor protein which allows visualization of the M50 expressing OSNs and their axons

M71 – an odorant receptor; G. Barnea previously generated an antibody for the receptor protein which allows visualization of the M71 expressing OSNs and their axons

M72 – an odorant receptor

Main olfactory epithelium (MOE) – the sheet of cells that lines the back of the nasal cavity, contains the cell bodies of olfactory sensory neurons and considered the main subsystem of the olfactory system

Monoallelic exclusion – the phenomenon that olfactory sensory neurons normally express one odorant receptor-coding allele, also known as the "one receptor per neuron" rule

MOR23 – an odorant receptor; G. Barnea previously generated an antibody for the receptor protein which allows visualization of the MOR23 expressing OSNs and their axons

MOR256-17 – an odorant receptor

MOR28 – an odorant receptor; G. Barnea previously generated an antibody for the receptor protein which allows visualization of the MOR28 expressing OSNs and their axons. The work in this thesis involves the wildtype MOR28 allele as well as a transgenic MOR28 allele.

Odorant receptor (OR) – G protein-coupled receptors expressed by olfactory sensory neurons, considered as the main olfactory chemoreceptor that mediates the majority of olfactory perception

Olfactory bulb (OB) – a structure of the brain where glomeruli are formed

Olfactory chemoreceptor – receptors expressed by the olfactory sensory neurons throughout the olfactory system that mediate the signal transduction activated by odorants. Includes formyl peptide receptors, guanylyl cyclase D, odorant receptors, trace amine-associated receptors, and the vomeronasal receptors.

Olfactory marker protein (OMP) – a highly expressed, cytoplasmic protein found in all mature olfactory sensory neurons with the exception of the olfactory sensory neurons expressing guanylyl cyclase D

Olfactory sensory neurons (OSNs) – sensory neurons of the olfactory system; they express olfactory chemoreceptors and synapse within glomeruli

"One receptor per glomerulus" – the phenomenon that olfactory sensory neurons expressing the same olfactory chemoreceptor form a small number of homogeneous glomeruli that do not receive afferents from olfactory sensory neurons expressing other olfactory chemoreceptors, also referred to as convergence

"One receptor per neuron" – the phenomenon that olfactory sensory neurons normally express one odorant receptor-coding allele, also known as monoallelic exclusion

P2 – an odorant receptor

Rerouted glomeruli – supernumerary glomeruli formed by axons expressing only the endogenous, wildtype the MOR28. Only formed when TO28 is expressed within the olfactory system during a critical period

Retinal ganglion cells (RGCs) – sensory neurons of the visual system; they express photoreceptors and synapse in the visual cortex

Septal organ (SO) – a subsystem of the olfactory system, located at the opening nasopalatine duct that connects the mouth with the nasal cavity

Superior colliculus (SC) – a structure in the visual cortex of the brain where retinal ganglion cells synapse, the vertebrate analog of the invertebrate optic tectum

TetO::MOR28-IRES-lacZ (TO28) – a transgene consisting of the tetO (tet operon) promoter driving the expression of MOR28 and β-galactosidase, activated by the tetracycline transactivator and silenced by the administration of doxycycline. The founder lines that bear separate integrations of TO28 are called TO28 low (TO28L) and TO28 high (TO28H).

Tetracycline transactivator (tTA) – a transcriptional activator exogenous to mice that will activate transgenes controlled by the tet operon

Trace amine-associated receptor (TAAR) – G protein-coupled receptors expressed by olfactory sensory neurons which serve as olfactory chemosensors

Type I guidance molecules – canonical guidance molecules that are expressed on the axon tips of immature olfactory sensory neurons. Their expression levels are not affected by naris occlusion

Type II guidance molecules – canonical guidance molecules that are expressed on the axon tips of mature olfactory sensory neurons. Their expression levels are affected by naris occlusion

Vomeronasal organ (VNO) - a subsystem of the olfactory system, located above the palate

Vomeronasal sensory neurons (VSNs) – sensory neurons of the olfactory system; they express olfactory chemoreceptors and synapse within glomeruli in the accessory olfactory bulb

Wildtype MOR28 glomeruli – the glomeruli formed by the axons expressing the endogenous, wildtype allele of MOR28. When the TO28 transgene is expressed, these are innervated by TO28 axons and distinguished from rerouted glomeruli by size and location in the OB.

Wildtype MOR28 OSNs – the axons of the olfactory sensory neurons that express the endogenous, wildtype allele of MOR28 and not MOR28-IRES-C6

B-galactosidase (lacZ) – an enzyme exogenous to the mouse that is used as a reporter gene, visualized by antibody staining or colorimetric staining with the X-gal substrate